


2016

# Analyzing Pterosaur Ontogeny and Sexual Dimorphism with Multivariate Allometry

Erick Charles Anderson  
anderson343@marshall.edu

Follow this and additional works at: <http://mds.marshall.edu/etd>

 Part of the [Animal Sciences Commons](#), [Ecology and Evolutionary Biology Commons](#), and the [Paleontology Commons](#)

---

## Recommended Citation

Anderson, Erick Charles, "Analyzing Pterosaur Ontogeny and Sexual Dimorphism with Multivariate Allometry" (2016). *Theses, Dissertations and Capstones*. 1031.  
<http://mds.marshall.edu/etd/1031>

This Thesis is brought to you for free and open access by Marshall Digital Scholar. It has been accepted for inclusion in Theses, Dissertations and Capstones by an authorized administrator of Marshall Digital Scholar. For more information, please contact [zhangj@marshall.edu](mailto:zhangj@marshall.edu), [martj@marshall.edu](mailto:martj@marshall.edu).

ANALYZING PTEROSAUR ONTOGENY AND SEXUAL  
DIMORPHISM WITH MULTIVARIATE ALLOMETRY

A thesis submitted to  
the Graduate College of  
Marshall University  
In partial fulfillment of  
the requirements for the degree of  
Master of Science  
in  
Biological Sciences  
by

Erick Charles Anderson

Approved by

Dr. Frank R. O'Keefe, Committee Chairperson

Dr. Suzanne Strait

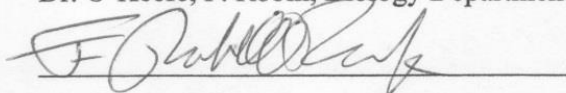
Dr. Andy Grass

Marshall University  
May 2016

## APPROVAL OF THESIS

We, the faculty supervising the work of Erick Charles Anderson, affirm that the thesis, *Analyzing Pterosaur Ontogeny and Sexual Dimorphism with Multivariate Allometry*, meets the high academic standards for original scholarship and creative work established by the Biology Department and the College of Science. This work also conforms to the editorial standards of our discipline and the Graduate College of Marshall University. With our signatures, we approve the manuscript for publication.

Dr. O'Keefe, F. Robin, Biology Department

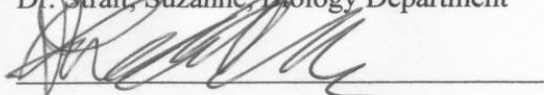


Committee Chairperson

Date

May 6 2016

Dr. Strait, Suzanne, Biology Department



Committee Member

Date

5/6/16

Dr. Grass, Andy, Medical Department

Andy Grass

Committee Member

Date

5/6/16

Erick Charles Anderson  
ALL RIGHTS RESERVED



## **Acknowledgments**

I would like to thank Dr. F. Robin O’Keefe for his guidance and advice during my three years at Marshall University. His past research and experience with reptile evolution made this research possible. I would also like to thank Dr. Andy Grass for his advice during the course of the research. I would like to thank my fellow graduate students Donald Morgan and Tiffany Aeling for their support, encouragement, and advice in the lab and bar during our two years working together. My family was a large part of my success with this research supporting and keeping me on track during my three years at Marshall University. I would like to thank the Biology Department here at Marshall for hiring me as a Teaching Assistant, giving me experience instructing students, and giving me financial support for tuition and monthly costs of living. Finally I would like to thank my family for their long lasting support during my entire academic career.

## CONTENTS

List of Tables -----	viii
List of Figures -----	ix
Abstract -----	x
Chapter One -----	1
Pterosaur Taxonomy and Phylogeny -----	1
Background -----	1
Research Approach -----	3
Phylogenetic Origins -----	6
Diversity -----	8
Non-pterodactyloids -----	9
Dimorphodontidae -----	9
Anurognathidae -----	10
“Campylognathoididae -----	12
Rhamphorhynchidae -----	14
Rhamphorhynchinae -----	15
Scaphognathinae -----	16
Monofenestrians -----	17
Wukongopteridae -----	17
Ornithocheiroidea -----	20
Ornithocheiridae -----	20
Pteranodontia -----	22
Istiodactylidae -----	23
Lophocratia -----	24
Ctenochasmatoidea -----	24
Azhdarchoidea -----	27
Growth of Animals -----	29
Surface Area – Volume Paradox -----	29
Allometry and Isometry -----	30
Conclusion -----	31
Chapter Two -----	32
Ontogenetic Allometry of Skeletal Elements and Surface Area of <i>Pterodactylus antiquus</i> and <i>Aurorazhdarcho micronyx</i> -----	32
Introduction -----	32
Allometry and Isometry -----	33
Growth: Surface Area – Volume Paradox -----	35
Experimental Design -----	36
Materials and Methods -----	37
Principle Component Analysis (PCA) -----	38
Bivariate Linear Regression -----	39
Wing Surface Area Reconstructions -----	40
Results -----	41
Principle Component 1 -----	41

Skull, Mandible, and Cervical Series	41
Humerus, Ulna, Radius, and PCRW	41
IVMc, Phalanges I-IV	44
Femur and Tibia	45
Bivariate Linear Regression	45
Skull, Mandible, and Cervical Series	45
Humerus, Ulna, Radius, and PCRW	46
IVMc, Phalanges I-IV	46
Femur and Tibia	49
Surface Area of Brachiopatagiums	50
<i>Pterodactylus antiquus</i>	50
<i>Aurorazhdarcho micronyx</i>	51
Major Delineating Characters between	
<i>P. antiquus</i> and <i>A. micronyx</i>	52
Skull	52
IVMc and Phalanx I	52
Tibia	53
Discussion	54
Interspecific Comparative Wing Reconstructions	55
Intraspecific Comparative Wing Reconstructions	58
<i>Pterodactylus antiquus</i>	58
<i>Aurorazhdarcho micronyx</i>	61
Possible Effects of Pneumatization on Allometry	61
Conclusion	62
Ontogeny and Sexual Dimorphism	62
<i>Pterodactylus antiquus</i>	62
<i>Aurorazhdarcho micronyx</i>	62
Chapter Three	64
<i>Pteranodon</i> and Sexual Dimorphism in Wing Shape	
and Surface Areas of Pterosaurs, Bats, and Moths	64
Introduction	64
Review of Chapter Two Results	64
Experimental Design	65
Wing Shape in Other Species	67
Materials and Methods	70
Results	72
Bivariate Linear Regression	72
Discussion	73
Bivariate Linear Regression of <i>Pteranodon</i> and Pooled <i>P. antiquus</i> / <i>A. micronyx</i>	75
Phylogenetic Allometry (Pooled Data of All Three Species)	77
Conclusion	79
References	81

Appendix A: Raw Data for All 39 Specimens Used -----	91
Appendix B: Results for all 14 Principle Components-----	92
Appendix C: Bivariate Plots of All 14 ln-lengths vs ln-Geometric Mean -----	93
Appendix D: Standarized Angles Used for Wing Reconstructions-----	94
Appendix E: All 39 Wing Reconstructions-----	95
<i>Pterodactylus antiquus</i> -----	95
<i>Aurorazhdarcho micronyx</i> -----	121
Appendix F: Letter from Institutional Research Board -----	133

**LIST OF TABLES**

1	Principle Components Analysis Results-----	41
2	Bivariate Linear Regression Calculations-----	47
3	Surface Area Calculations-----	50
4	<i>Pteranodon</i> IVMc lengths-----	71
5	<i>Pteranodon</i> Associated Femur and IVMc lengths -----	71

## LIST OF FIGURES

1	Labeled Pterosaur -----	1
2	Sauropsida Phylogeny -----	6
3	Pterosauria Phylogeny -----	8
4	<i>Dimorphodon micronyx</i> -----	9
5	<i>Anurognathus ammoni</i> -----	10
6	<i>Eudimorphodon ranzii</i> -----	12
7	<i>Rhamphorhynchus</i> skull -----	15
8	<i>Scaphognathus</i> skull -----	16
9	<i>Darwinopterus</i> illustration -----	18
10	<i>Pteranodon longiceps</i> skull and cervical series -----	22
11	<i>Nyctosaurus gracilis</i> skull cast -----	22
12	<i>Istiodactylus latidens</i> illustration -----	23
13	<i>Pterodaustro guinazi</i> illustration -----	24
14	<i>Pterodactylus antiquus</i> dorsal/sacral skeletal schematic -----	25
15	<i>Quetzalcoatlus sp.</i> illustration -----	27
16	General depiction of a pterosaur with labeled features and bones -----	35
17	Principle Component One Coefficients -----	42
18	Linear Regression Slopes -----	48
19	Bivariate Plot of the ln-Geometric mean vs ln-Surface Area -----	50
20	Bivariate Plots of the ln-Skull, ln-IVMc, ln-Phalanx I, & ln-Tibia -----	53
21	Allometry Summary Schematic -----	56
22	Interspecific Wing Comparisons -----	57
23	Intraspecific Wing Comparisons: <i>Pterodactylus antiquus</i> -----	59
24	Intraspecific Wing Comparisons: <i>Aurorazhdarcho micronyx</i> -----	60
25	Sexual Dimorphism in Moth Wings -----	68
26	Sexual Dimorphism in Bat Wings -----	69
27	The frequency distribution of the 64 <i>Pteranodon</i> IVMc length measurements ---	72
28	Bivariate Linear Regression of <i>Pteranodon</i> ln-Geometric vs ln-IVMc -----	74
29	Bivariate Linear Regressions of Pooled Specimen Data -----	76
30	Phylogenetic Allometry -----	78

## ABSTRACT

The relationships of pterosaurs have been previously inferred from observed traits, depositional environments, and phylogenetic associations. A great deal of research has begun to analyze pterosaur ontogeny, mass estimates, wing dynamics, and sexual dimorphism in the last two decades. The latter has received the least attention because of the large data set required for statistical analyses. Analyzing pterosaurs using osteological measurements will reveal different aspects of size and shape variation in Pterosauria (in place of character states) and sexual dimorphism when present. Some of these variations, not easily recognized visually, will be observed using multivariate allometry methods including Principle Component Analysis (PCA) and bivariate regression analysis. Using PCA to variance analysis has better visualized ontogeny and sexual dimorphism among *Pterodactylus antiquus*, and *Aurorazhdarcho micronyx*. Each of the 24 (*P. antiquus*) and 15 (*A. micronyx*) specimens had 14 length measurements used to assess isometric and allometric growth. Results for *P. antiquus* analyses show modular isometric growth in the 4<sup>th</sup> metacarpal, phalanges I-II, and the femur. Bivariate plots of the ln-geometric mean vs ln-lengths correlate with the PCA showing graphically the relationship between *P. antiquus* and *A. micronyx* which are argued here to be sexually dimorphic and conspecific. Wing schematic reconstructions of all 39 specimens were done to calculate individual surface areas and scaled to show relative intraspecific wing shape and size. Finally, *Pteranodon*, previously identified having sexually dimorphic groups, was compared with ln-4<sup>th</sup> metacarpal vs ln-femur data, bivariately, revealing differences likely due to the constraints of size (*P. antiquus* and *A. micronyx* = group 1; *Pteranodon* = group 2).

## CHAPTER ONE

### PTEROSAUR TAXONOMY AND PHYLOGENY

#### Background

Between the years of 1767 and 1784 an exquisitely preserved pterosaur specimen was found. This specimen would later become the holotype of *Pterodactylus antiquus*. From that fossil's discovery to the present, about 5,500 specimens of pterosaur have been found ranging from ~220 Ma to 65.5 Ma, giving the clade a known time span of ~154.5 myr (Unwin 2005). They have no extant descendants, going completely extinct at the end of the Cretaceous along with the non-avian dinosaurs and large marine reptiles. Pterosaur anatomy is quite different than that of most other diapsid reptiles. Their basic anatomy was like that of a quadrupedal animal with re-curved claws at the ends of each digit, a long tail (lost in derived species), a long neck,

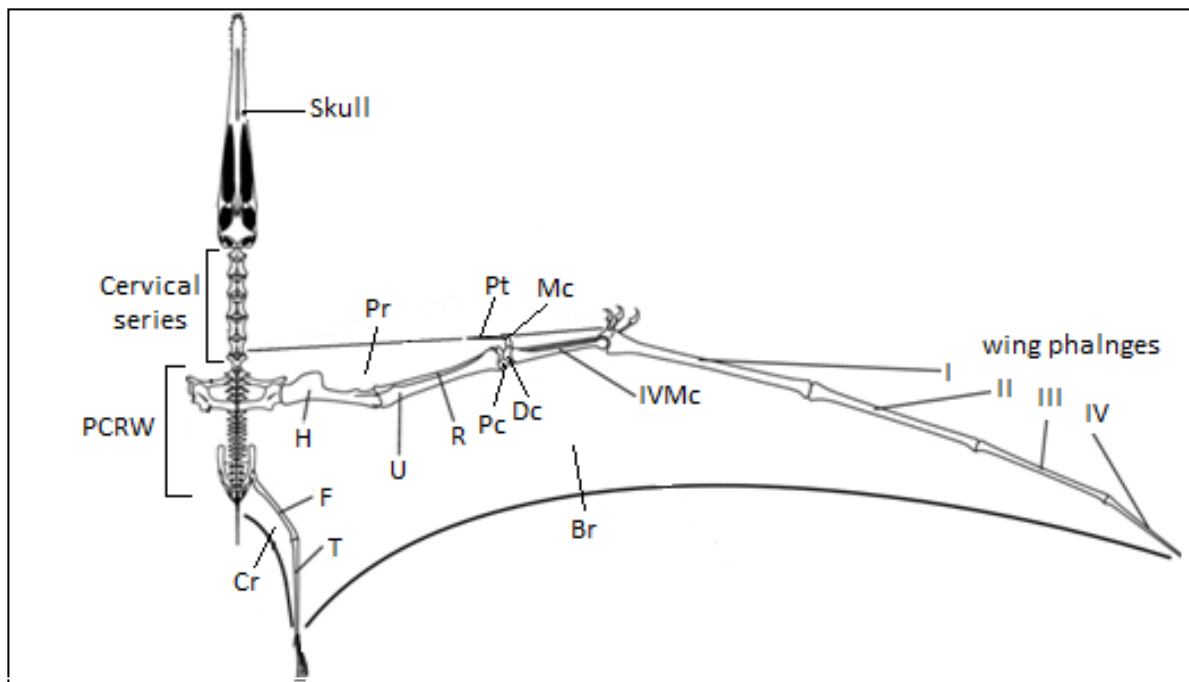


Figure 1 Labeled Pterosaur. Dorsal view, brachioptagium (Br), the unique pteroid bone (Pt) supporting the propatagium (Pr) and the cruroptagium (Cr) medial to the leg. Labels: Dc, distal carpal; F, femur; H, humerus; Mc, medial carpal; Pc, proximal carpal; R, radius; T, tibiotarsus; U, ulna; wing phalanges: I-IV; IVMc, 4th metacarpal. Scale bar = 200mm. Wilkinson, Unwin, and Ellington 2006.

and an elongate skull, with some Cretaceous species losing all their teeth. Characteristic of all



species, however, were the elongated arm elements, with a hyper-elongated 4<sup>th</sup> manus digit that had four phalanges, also hyper-elongated. Like many other reptiles they lost their 5<sup>th</sup> manus digit. This elongated 4<sup>th</sup> digit carrying the wing membrane (brachiopatagium) was attached, running the entire length of the arm/finger and the length of the body and down to the ankle (Figure 1). Along with these specializations, pterosaurs had two neomorphic bones that were autapomorphic to pterosaurs. The first was the pteroid bone, also seen in Figure 1, which attached to their frontal membrane (propatagium) functioning to manipulate this anterior membrane during flight. The second was the pre-pubis. The pre-pubis projected anteriorly from the ilia of the pelvic girdle, and likely served as attachment sites for abdominal muscles used for breathing (Unwin 2005; Claessens, O'Connor, and Unwin 2009).

The rigid thoracic region of all pterosaurs required an alternative mode for breathing relative to more basal reptiles. Their pulmonary system was analogous to birds. The skull, cervical vertebrae, and shoulder girdle in early species and, additionally, the limbs in later species have pneumatic foramina found in characteristic locations, notably in ornithocheiroidea (e.g., *Pteranodon*), for pneumatic tissues that correlate with foramina found in birds (Wedel 2003; O'Connor and Claessens 2005). Pterosaurs' increasing hollow bone space throughout their evolution allowed for expanded air-sacs within their skeleton increasing their respiratory efficiency. This pneumaticity suggests that, like modern birds, they had a unidirectional pulmonary system that was far more efficient than our mammalian bidirectional system. A unidirectional system operates by sucking air in then pushing the deoxygenated air out through the air-sacs rather than exhaling it directly. A unidirectional system would have allowed for a very active lifestyle, giving pterosaurs the freedom to stay in flight for significant periods of time.

## **Research Approach**

Over the past 230 years, beginning in 1784 with the first scientific publication of a pterosaur, the quantity of pterosaur specimens and species described has risen to about 5,500 specimens and about 140 species (Collini 1784). A tremendous amount of research has been done on individual species' anatomies, functional morphology, and phylogeny. Most of this work has been descriptive and phylogenetic in nature.

The concept of allometry was developed by Huxley to examine the relative growth of two or more areas of an organism or multiple organisms (1932). Since then it has become clear that growth is just one source of variation in size and shape. Huxley's original concept is now called ontogenetic allometry, and is one of three. The second is static allometry, which is the study of the variation among individuals of the same population in the same age group. The final is evolutionary allometry concerning phylogenetic variation among taxa (Cock 1966; Gould 1966, 1975; Klingenberg 1996). Evolutionary allometry has not been done comparing the broad range of families and species among pterosaurs which would analyze their shape variation as it changed during their 140 myr existence. Analyses of phylogenetic, ontogenetic, and evolutionary allometry on pterosaur longitudinal morphometrics collected from numerous publications will be the focus of this research.

A recent paper used Principle Coordinate Analysis (PCoA) to assess morphological difference in 53 pterosaur taxa. Prestice, Ruta, and Benton (2011) used 80 skeletal character states, pulled directly from the taxonomic data matrix published in Lü, Ji, Yuan, and Ji's (2006) phylogeny paper, to delineate a morphospace for the taxa present. That research yielded significant results ( $p < 0.05$ ) that the two major taxa of pterosaurs, non-pterodactyloids and pterodactyloids, were different, suggesting that their modes of life were heavily selective towards

these differences (Prestice et al. 2011). That approach handles the statistical problem of species not being independent of each other due to their phylogenetic relations (Klingenberg 1996; Felsenstein 1985; Pagel and Harvey 1988). This phylogenetic method is one way to avoid phylogenetically dependent comparisons, but this requires a high level of understanding of the taxa's phylogeny (Prestice et al. 2011). The alternative method presented here is not as phylogenetically dependent because most of the variation is in one dimension of the PCA analysis (Klingenberg 1996). Doing such an analysis with linear measurements would capture a different aspect of shape variation than was found in the PCoA method, because they record different morphological information. Examining pterosaur morphometrics with multivariate allometry likely hasn't been done because there is not a large published collection of morphometric data compiled from a wide range of families of pterosaurs. The phylogeny have been tested many times by various researchers because a massive data matrix was compiled and has since been built upon and published originally by Lü and Unwin (Lü J., Unwin D. M., Xu L., and Zhang X. 2008; Lü, J., Unwin, D.M., Jin, X., Liu, Y. and Ji, Q. 2010), with alternative phylogeny results by Andres (2010).

A comparably large data set can be built with linear measurements of pterosaur bones. Width measurements likely cannot be used because they would be skewed by the compressional forces of diagenesis and fossilization over tens of millions of years. Over the centuries numerous, nearly complete, specimens have been found with representatives from all the major families of Pterosauria. Such an accumulation of data will allow an interspecific (evolutionary allometry) study that can reveal new pieces of information about the size and shape variation seen throughout pterosaurs and selective pressures they underwent as they adapted to new ecological

niches, and for some families, re-adaptation to terrestrial lifestyles while maintaining aerial ability.

For some species we are fortunate to have more than a few nearly complete specimens, for example *Pterodactylus*, *Aurorazhdarcho*, *Ctenochasma*, *Pteranodon*, *Pterodaustro*, *Darwinopterus* and *Dorygnathus*. The first two, *Pterodactylus* and *Aurorazhdarcho*, have 24 and 15, respectively, nearly complete specimens from the Solnhofen Formation in Germany (Wellnhofer 1970). Unwin published a graph in his 2003 book where he discussed these specimens briefly and showed that *Pterodactylus* appeared to have an isometric growth. However, he did not go into any depth numerically, nor publish the data he used in the graph. Isometry in any pterosaur would be remarkable. With the data from the 24 specimens of *Pterodactylus* we can investigate whether this species does in fact show ontogenetic isometry and its significance down to each skeletal element.

One analysis method that will be used in this study is Principle Component Analysis (PCA). It will break down the data into its underlying structure, thus their size and shape variations into Principle Components (PC). Each PC describes orthogonal axes representing different variations. PC1 will represent the largest variance, being usually interpreted as size. PC2, PC3, etc. are typically interpreted as shape variation scores (Klingenberg 1996). Multivariate allometry will be used to examine Ctenochasmatoidea species growth curves to determine whether they show allometry like the rest of the pterosaurs or if they had a unique modular isometry in their ontogeny relative to other pterosaurs. Correlation of determination ( $R^2$ ) and their standard error (SE) will give us confidence intervals for each bone element.  $R^2$  will give us a value, 0 to 1, that describes how well a cluster of data points fit onto the linear regression (best-fit) line. Zero would mean the line doesn't describe the data at all. An  $R^2$  of 1

means the regression line perfectly describes the data and extrapolating variables outside the cluster would be accurate. Typically, an  $R^2$  above 0.60 of a regression line is worthwhile, meaning the independent variable describes about 60 percent of the dependent variable (Glantz and Slinker 1990). The  $R^2$  is calculated by the software used to plot the data, along the standard error (SE). The standard error is calculated by dividing the sample standard deviation (s) by the square root of the sample size (n):  $[SE = \frac{s}{\sqrt{n}}]$ . The confidence intervals tell us whether the calculations are  $\geq 95$  percent confidence that the slope (x) describes the population  $[CI = x \pm (SE \times 1.96)]$ . A confidence interval  $< 0.05$  gives a 95 percent probability that the sample data set describes the population (Glantz and Slinker 1990).

### Phylogenetic Origins

Like many things regarding pterosaur phylogeny, their ‘home’ on the sauropsida cladistic tree is contentious. The development of their appendicular skeleton and ankles, including the four fossilized soft-shelled eggs, tell us they were amniotes (Witton 2013). Skull characteristics define them further, telling us they were archosauromorph diapsid reptiles. The contention

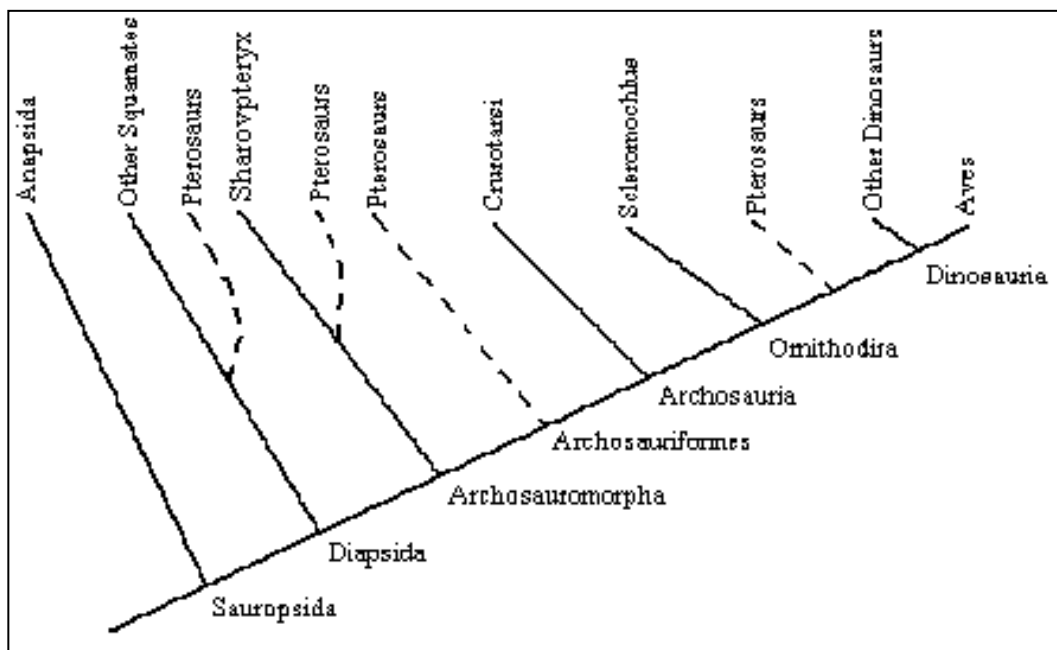


Figure 2 Sauropsida Phylogeny. Shows the four hypothesized locations for the pterosaur divergence within Sauropsida.

begins here. Somewhere in diapsid evolution they diverge. There are four main hypotheses for placement of pterosaurs in Sauropsida phylogenetics (Figure 2). The far left position, with pterosaurs being closely related to squamates, has little following due to the poor techniques used in the analyses by Peters (2008) with critiques by prominent pterosaur researchers Bennett (2005), and Hone and Benton (2007). That position has little support and is the most unlikely. The close relation of the second position with *Sharovpteryx* is also not well supported. At first glance at *Sharovpteryx* would suggest close relation due to similar large wing membranes, although they differ radically from pterosaurs in being hindlimb dominated. Other than that there are no other shared characteristics to support this topology (Sereno 1991; Bennett 1996a; Hone and Benton 2007; Nesbitt and Hone 2010). The third position on the tree, third from left on Figure 2, was published by Bennett (1996a) but was criticized for not using all the morphological data available. Bennett's analysis placed pterosaurs at the base of Archosauriform evolution. Later re-evaluation of his methods using all available morphological data, this time including hindlimb characteristics, placed pterosaurs higher up and into Archosauria becoming a sister group to Dinosauria (Benton 1999; Hone and Benton 2007). This is the last position on the far right of Figure 2 and the current consensus.

During their ~150 myr existence pterosaurs went through a slew of modifications as they went from dominantly arboreal living animals capable of active flight with an insectivorous diet. Over time they became highly agile gliders capable of capturing flying insects in the air, a difficult task to achieve. Their morphology began evolving to enhance gliding abilities which reduced the need for energy during flight. They became large enough to diet on fish and perhaps even small mammals and reptiles. Some unique derived pterosaurs became filter feeders and clam-crushers while some of the largest pterosaurs became amazingly adapted for soaring flight,

needing almost no energy while in air using external sources of lift such as thermals and oceanic winds to maintain lift and thrust. But even the earliest pterosaurs were amazingly evolved, already having all the essentials for flight.

## Diversity

Discussed here are the first major taxa of pterosaurs that will be analyzed, the non-pterodactyloids, wukongopteridae, and pterodactyloids. Non-pterodactyloids comprise the ‘basal’ pterosaurs. The descriptive word ‘basal’ should be used with caution as it refers to

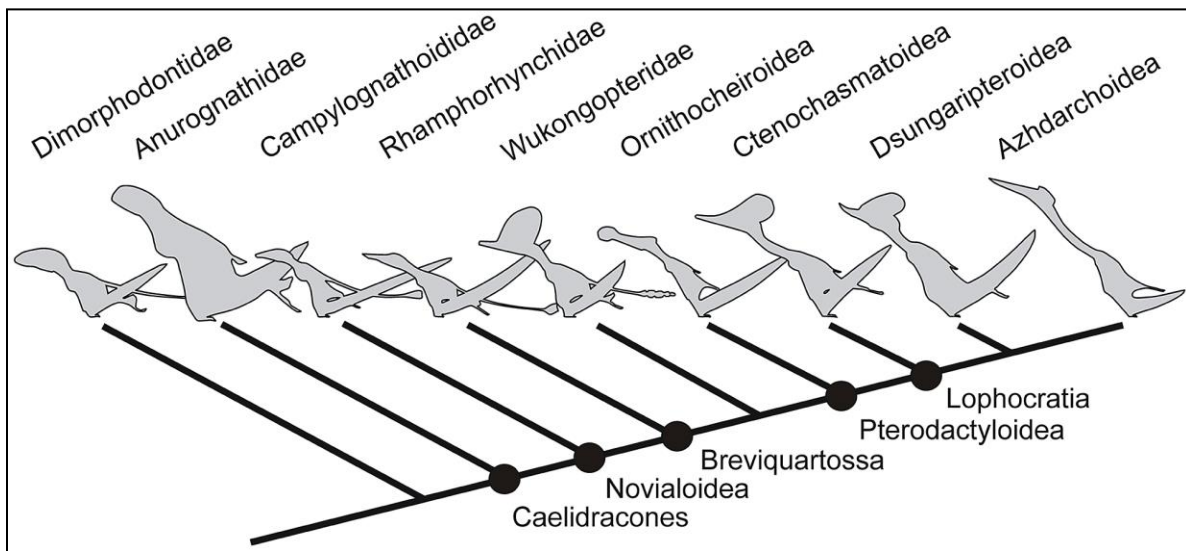


Figure 3 Pterosauria Phylogeny. The nine dominant families and their relative relations and clades. (Naish, Simpson, and Dyke 2013).

pterosaurs more basal than the later, much more derived, pterosaurs. Basal pterosaurs are highly derived reptiles in their own right. The cladistic name ‘Rhamphorhynchoidea’ used to be a taxa that comprised all the basal pterosaurs. ‘Rhamphorhynchoidea’ has since been recognized that its phylogeny is much more complicated and is no longer considered an accepted systematic term. However, the clade that comprises all derived forms, the order Pterodactyloidea, has survived repeated phylogenetic analyses. The term, ‘Non-pterodactyloidea’ is used to refer to the ‘Rhamphorhynchoidea’ group of pterosaurs. Figure 3 shows the relation of the nine families to be discussed.

## Non-pterodactyloids

**Dimorphodontidae.** The earliest pterosaurs have a place within this family, except for *Preondactylus* (Wild 1984). It is considered the node of pterosaur divergence by Unwin in his numerous phylogenetic analyses (Unwin 2003; Lü et al. 2010). It is most closely related to dimorphodontidae. This family of pterosaurs is found in present day New Mexico, England and date back to about 193 Ma in the early Jurassic (Buckland 1829; Clark, Hopson, Hernández, Fastovsky, and Montellano 1998). Their depositional environment was indicative of a coastal area next to ancient seas.

Their anatomy is considered to be the most primitive of all pterosaurs but their flight anatomy was already fully developed, which made them fully capable of aerial mobility (Witton 2013). Figure 4 shows their relatively ‘lizard-like’ anatomy. Their limb proportions have the lowest ratio among all pterosaurs, giving them a somewhat ‘normal’ appearance for a quadruped animal. Despite their large bone volume relative to length and wingspan, they would have been light weight.



Figure 4 *Dimorphodon micronyx*. An example of a dimorphodontidae. Demitry Bogdanov

Their fossilized skeletons suggest that they had a body weight nearly double that of other pterosaur families with similar wingspans, which was about 1.45 meters in adults (Brower and Veinus 1981; Witton 2008a). Another of their primitive characteristics was their short wings relative to their body proportions. This would made them inefficient soarers requiring constant flapping to maintain flight. All pterosaurs share some level of pneumatization within their bones. Pneumatization of bones is the development of open space within the bone that lengthens the bones by re-depositing the bone mass at the opposing ends, thus, lengthening or blowing the



bone up by volume but retaining the same amount of mass. Dimorphodontidae's pneumaticity is limited to their skulls and cervical neck bones (Butler, Barrett, and Gower 2009). Later pterosaur families would evolve a much more pneumatized skeleton allowing for a better distribution of mass relative to surface area via the wings.

Dimorphodontidae hand and claw traits are indicative of living in trees or some other vertical surface such as a cliff, which would serve as safety due to their small size and inability to stay in the air for an extended amount of time. Their jaw and dentition and overall flight abilities would suggest that they were not capable of midair maneuverability needed to catch flying insects (Witton 2013).

**Anurognathidae.** This family of pterosaurs is of great interest because, like the family wukongopteridae, it shares features of both non-pterodactyloids and pterodactyloids. The species that comprise this family were found much sooner than that of wukongopteridae however, starting in 1923 by Ludwig Döderlein. The family's phylogeny is contentious due to its shared features with pterodactyloids (e.g., loss of cervical ribs, short tail, reduced fibula length, conflated nasal and antorbital fenestra: Bennett 1997b; Andres 2010) but the most commonly accepted placement is seen in Figure 2. The specimens of this family are found only on one continent. The rich pterosaur fossil locales in present day Germany, Kazakhstan, and in China have only given us a very small number of preserved specimens for this family, (Döderlein 1923; Wang, Zhou, Zhang and Xu. 2002).



Figure 5 *Anurognathus ammoni*. An example of an anurognathidae. Calyton Mckee

Anurognathidae are characterized by unique and derived traits that set them apart from all other families discussed here. First is their skull; it looks like a frog's. It was broad, short, with

massive orbits relative to the rest of the skull. Like wukongopteridae and all other pterodactyloids, it is thought that their nasal opening and antorbital opening (fenestra in front of the orbital opening) were combined into one opening called a nasoantorbital fenestra (Andres 2010). The facial bones making up the anterior of their skulls are very thin, like rods. All of the jaw mechanics allow for very rapid abduction and adduction of the jaw that gave them very fast ‘snapping’ speed. This skull configuration is a remarkable convergent evolution with modern insect hawkers (Ősi 2010).

Anurognathidae forelimb bones, humeri and ulna/radius, were about 150% as long as their hindlimbs, femora and tibia (Bennett 2007a). This is a drastic difference from dimorphodontidae; this elongation of forelimb bones is only matched by later more derived families of pterosaurs in the Early Cretaceous. The metacarpals in pterosaurs were hyper-elongated in derived families adding a noticeable amount of wing length, but in non-derived families the metacarpals are short, seen in Figure 5 depicting a representative of anurognathidae: *Anurognathus ammoni*. The fourth metacarpal is short in dimorphodontidae, as expected, but it is also very short in anurognathidae being shorter. This family is usually considered the most agile of all pterosaur families. They were compact fliers with wing and body proportions that gave them high aerial maneuverability, added with their skull morphology, making them very competent aerial predators of insects (Bennett 2007a). Some of the species within this family shared a typical pterodactyloid feature, the lack of a long tail, but a very unique feature among this family is their ability to flex their wing-finger bones, curling their wing. This is not seen in any other family nor is its function understood. Anurognathidae showed superiority in aerial agility and were likely the first predators of flying insects. Before this family appeared was

another, the "campylognathoididae," which showed the first elongation of skull length that is a prominent feature in later pterodactyloids.

**“Campylognathoididae.”** The phylogeny of this family with all its species and its relationship with other families is one of the greatest puzzles among pterosaur relations. Most pterosaurologists follow the phylogeny determined by Lü et al. (2010) in regards to its placement with other pterosaur families. Their phylogeny is reflected in Figure 2. The term “campylognathoididae” is used because of the great contention with this family’s phylogeny (Witton 2013). There is no commonly accepted consensus on this family's interrelations, nor its relationship to the other major families of non-pterodactyloids.



Figure 6 *Eudimorphodon ranzii*. A member of “campylognathoididae” showing the multicusped teeth in some genera. *Eudimorphodon ranzii*. (Zambelli 1973)

This family is our first known major radiation of pterosaurs, starting in the Late Triassic about 210 to 204 Ma in the Norian Age ending around 183 to 176 Ma (Dalla Vecchia 2003b; Barrett, Butler, Edwards, and Milner 2008). This family existed for about 40 Myr, undergoing an extensive evolution of genera and species within. Despite their extensive speciation they are all constrained to present day Europe. Most species are from the rocks in Germany and Italy with a species found in Greenland as well. The depositional environment they are found in is coastal or not very far from an ancient body of water.

What has been preserved has given “campylognathoididae” a wingspan range of about 70 centimeters to 1.8 meters (Witton 2013). This family of pterosaurs, apart from the previously discussed families, had some of the earliest low, narrow skulls that would become common but much elongated later in the Cretaceous. They also bore sagittal crests on the dorsal surface of the skull, with a triangular sail. A diagnostic trait of this family is that the most posterior and dorsal opening in the skull (superior temporal fenestra) was characteristically the largest of all the openings in the skull. The enlargement of this opening is likely related to the adaptation of the dentition of this family. This is the only group of pterosaurs that developed multicusped teeth, in particular *Caviramus sp.* and *Eudimorphodon ranzii* (Fröbisch and Fröbisch 2006; Stecher 2008; Zambelli 1973).

Figure 6 shows the multicusped teeth that line the jaws of a *Eudimorphodon ranzii*. How this type of tooth played a part in the change in size of the superior temporal fenestra had to do with oral processing of food. The upper and lower temporal fenestra, the most posterior openings in the skull were locations for muscle attachment for the jaw. In other pterosaurs these openings were smaller. They didn't need large robust muscles since they grabbed their prey and swallowed it whole. So it would be logical and appears in “campylognathoididae” for these openings to enlarge when the animal uses them more for oral processing. This oral processing is indicated by the adaptation of the saw like teeth that were lined and wedged together, being multicusped, like a long continuous blade (Fröbisch and Fröbisch 2006; Stecher 2008). An additional piece of evidence that the teeth were used for processing food was the crown tips showing wear (Ősi 2010).

This family of pterosaurs shared the wing proportions of other early pterosaurs discussed such as *Preondactylus* and *dimorphodontidae*. However their shoulder girdle and forelimbs

became much more robust. The four wing finger bones become very thin and develop a very narrow wing. The robust upper body and narrow wings suggest the ability to generate powerful bursts of speed in flight. These traits are analogous to modern falcons and mastiff birds (Hildebrand 1995). What this family's anatomy tells us is that this family of pterosaurs adapted specifically for aerial predation of small to medium sized prey items in the air and on the ground. Their robust nature and strong biting force with rows of sharp multicusped teeth would have made them aerial hunters. This assortment of characters makes them unique because those adaptations: robust skeletons, strong aerial agility, and oral processing of food, are not seen in any other pterosaur. The fossil record has the last of this remarkable family dying out around 170 Ma, which is the beginning of the temporal range that the last major family of non-pterodactyloids appears in the fossil record.

**Rhamphorhynchidae.** The first members of this family appeared in the Early Jurassic around 180 Ma existing for about 30 Myr until the very Late Jurassic. They are the earliest pterosaurs, according to the fossil record, to have obtained a global distribution. They are found in the Americas, Germany, England, and China. There are two subfamilies within this family, the Rhamphorhynchinae and the Scaphognathinae. These two groups are united by a few features. The first is their simply shaped conical teeth that are low in number (usually about eleven pairs of teeth, Witton 2013). Another is the curved phalanges (digit bones) in the fifth toe that are attached to the membrane between the legs (crurupatagium) and that fifth toe. The other four toes are not attached. The attachment of the crurupatagium to the fifth toe is of functional significance because it probably was used to manipulate the membrane to make adjustments in flight, similar to how an airplane uses a rudder to adjust the pitch or yaw of the craft (Witton 2013). This crurupatagium is only preserved in a handful of specimens, mostly from this family, but the

elongate fifth toe is present in almost all non-pterodactyls which suggests they all had the crurupatagium. No specimen has ever had a claw on the fifth toe, so its functional purpose was not for grasping any surface.

**Rhamphorhynchinae.** This subfamily is very well documented due to a tremendous number of specimens found in Germany. Their abundance has allowed a large amount of research to be done on this group which has made it one of the more famous groups, more specifically the species *Rhamphorhynchus muensteri*. This subfamily was the earlier of the two groups and was also where the largest of all the Jurassic pterosaurs belonged. There are many specimens from young to full sized adults, reaching up to two meter wingspans. Their skulls are very low and narrow with thin openings for the nasal vestibule. The antorbital fenestra (anterior opening of orbit) is also rather small relative to the other

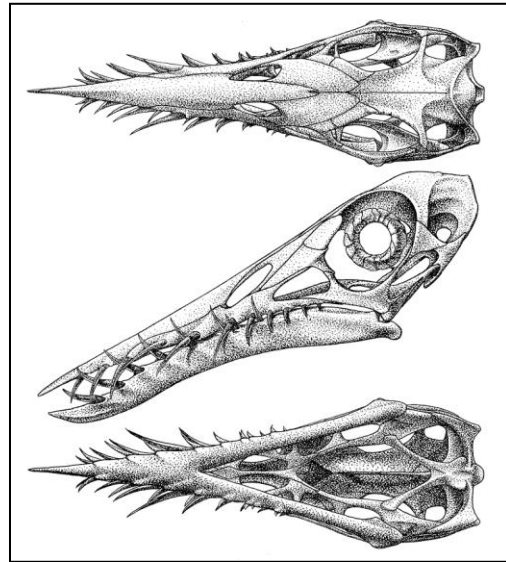


Figure 7 *Rhamphorhynchus* skull. Member of the subfamily Rhamphorhynchinae. *Rhamphorhynchus muensteri*. Hone, Habib, and Lamanna 2013

families of non-pterodactyls. These openings generally serve as muscle attachment sites so their small size indicates small jaw muscles. They are also areas of small stress in the skull, so in this subfamily, at first glance it would imply a lot of stress was present in their skulls due to the small relative openings. The teeth in this subfamily, as seen in Figure 7, are simple, conically shaped, and re-curved, tooth projecting anteriorly. When the jaws are completely adducted they interlock. The function of this forward projection of teeth is universally accepted as being used to capture prey by spearing them initially and swallowing them whole (Cranfield 2000). A primitive condition that this subfamily kept while the other families of non-pterodactyl lost

was their torso being longer than their skull length. This conserved ancestral trait would have been a disadvantage for flight but their long narrow wings versus their estimated mass, a highly contentious topic in pterosaur research, would have still given them excellent gliding ability. Narrowed wings was the change in flight style in non-pterodactyls that would let later pterosaurs use less energy and eventually become more efficient fliers by gliding. Gliding was a major evolutionary step towards what pterosaurs would ultimately be capable of in the air in the Cretaceous. Their forelimbs are the longest of all non-pterodactyls serving to lengthen the wing. This subfamily had a plesiomorphic long tail but in this group they had the most vertebrae producing the longest tail lengths relatively. Their sister subfamily had similar body characteristics but their skulls are what set them apart.

**Scaphognathinae.** This subfamily had a large range in sizes from 0.7 to 2.5m. Figure 8 shows their chunky skulls and perpendicular teeth in the jaws. The teeth are fewer in number, shorter, more robust, and are perpendicular to the surface of the jaws. This would indicate that a

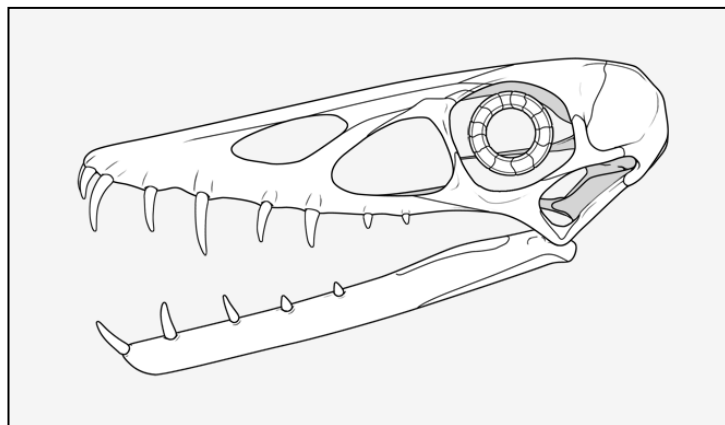


Figure 8 *Scaphognathus* skull. A member of Scaphognathinae. *Scaphognathus crassirostris*. Talkrational.org

different method for capturing prey

was used from their sister subfamily. The increase in robustness would suggest that they preyed upon perhaps larger or prey that put up more of a fight than the prey items that Rhamphorhynchinae dined on. Their neck and shoulder girdle show increased robustness but the proportions in various lengths are almost the same as Rhamphorhynchinae (Cranfield 2000).

## Monofenestrians

**Wukongopteridae.** The first specimen found of this family was named *Darwinopterus modularis*, reflecting the father of evolutionary theory and the modular evolution seen in the animal. Many more specimens of this species and new genera have been described, making it a very well understood animal osteologically (Lü et al. 2011). This family has been recovered from the Tiaojishan Formation in western China dating them to about 158 Ma, although the dating of this site is somewhat contentious. Another locality producing this family is in Britain with specimens dating from about 167 Ma and 154 Ma. This makes all of them late Jurassic animals and existing before any known pterodactyloid. In fact, the Tiaojishan Formation is host to other well-known non-pterodactyloids such as *Pterohynchus*, *Qinglongopterus*, and *Fenghuangopterus* (Witton 2013).

A remarkable discovery found with a *Darwinopterus* specimen was an egg. The embryo was not preserved but it incontrovertibly showed the gender of the animal, and was actually the fourth pterosaur egg found. It is important to note that this family was not a short lived transitional pathway from non-pterodactyloid to pterodactyloid. If all the reports of wukongopteridae individuals are correct then this family existed for roughly ten myr and likely expanded across all of present day Asia (Lü 2010; Lü et al. 2011; Wang et al. 2010).

Despite their importance for showing the transition from non-pterodactyloids to pterodactyloids, known specimens were actually small when compared to pterodactyloids and even non-pterodactyloids. The juveniles found in China range from 0.65 to 0.8 meter wingspans, but one adult specimen, *Cuspicephalus*, has a predicted wingspan of over two meters (Wang, Kellner, Jiang, and Meng 2009; Lü et al. 2010, Martill and Etches 2013). A depiction of a *Darwinopterus modularis* in flight illustrated by Witton, Figure 9. Their skull and neck anatomy



is remarkably similar to pterodactyloids. Their skull was elongated with conical shaped teeth, in some cases triangular, few in number and restricted to about the front half of the jaws. Their quadrate bone angles posteriorly, as seen in pterodactyloids, with the foramen magnum repositioned to the back of the skull, also a very typical pterodactyloid feature.

Minus the elongation of the skull, the most noticeable feature that would normally specify pterodactyloid is the conflation of the nasal opening and antorbital fenestra into one large hole, nasoantorbital fenestra. The dorsal surface of the skull above the nasoantorbital fenestra, orbital, and superior temporal fenestrae has a short fibrous bony crest that very likely had a large soft-tissue crest.

A feature seen in many pterodactyloids is a fused mandibular symphysis (Witton 2013). The cervical vertebrae also show pterodactyloid characteristics such as low neural spines and the lack of cervical ribs. This last feature is not restricted to

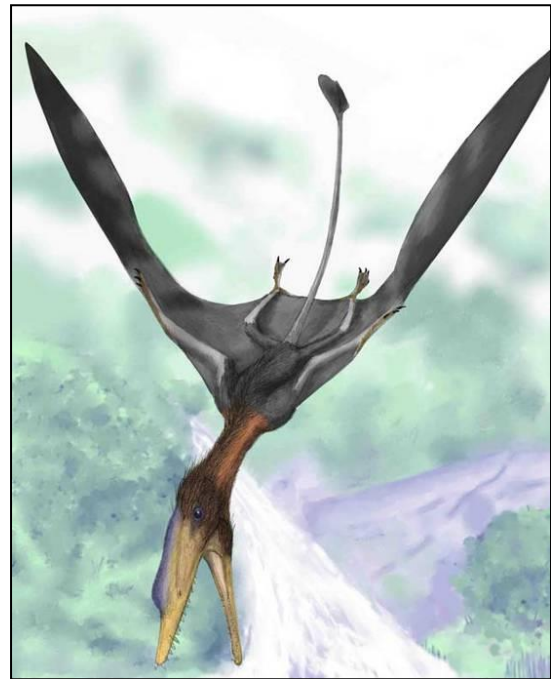


Figure 9 *Darwinopterus* illustration. By Mark Witton.

pterodactyloids and wukongopteridae, but also seen in the frog skull-like *Anurognathus* discussed earlier. There is no question that the skull and cervical vertebrae have a host of pterodactyloid traits and would no doubt be identified as a pterodactyloid with only the skull. However, their post-cervical anatomy is very characteristic of non-pterodactyloids, except for one feature, the elongated pteroid bone, which is relatively short (Lü et al. 2010).

Early pterosaurs had a short pteroid relative to its other wing components, while derived forms shared an elongated pteroid adapted for a longer length likely as part of their adaptation to

gliding and soaring rather than being active fliers. The rest of their post cervical anatomy is very similar to that of rhamphorhynchidae, including the presence of a long tail. They do however have shorter wingfingers than found in rhamphorhynchidae (Witton 2013). In 2009, when the first specimens were described, an initial analysis of their modular evolution was formulated and discussed a two phase evolution from non-pterodactyloid to pterodactyloid bauplans, seen in Figure 2 (Lü, Unwin, Jin, Liu, and Ji 2009). Essentially hypothesizing the change in skull, neck, and pteroid underwent changes during a phase one of adaptation followed by changes in the post cervical anatomy, that then characterize most pterodactyloid taxa.

The flight and terrestrial locomotion of this family has not been formally investigated but their short wings, large pteroid (suggesting a large propatagium), and broad wings would initially infer a reasonably agile flier capable of high angle take-offs and tight turning ability (Lü et al. 2010). This type of flight would be expected in densely vegetated settings, which is the type of flora, characterized by the lacustrine deposits, in the Tiaojishan. Movement on the ground has not been studied either but limb proportions are low compared to pterodactyloids. With their apparent high angle launching ability and their small size, they may have used small bursts of flight to get around like small modern birds. At some point in the middle or late Jurassic, wukongopteridae-like (or closely related) pterosaurs adapted these same traits and additional traits to their post cervical anatomy.

This second major taxa of pterosaurs consists of about two-thirds of all known pterosaur species, most evidently due to their dominance of the skies and global distribution, allowing for a better fossil record than the more ancient and more restricted geographical distributions of non-pterodactyloids. This group is highly diverse with environmental specialists for terrestrial settings and groups highly adapted for aerial lifestyles. The latter group of aerial adapted

pterosaurs are collectively placed in a taxa called ornithocheiroidea, and the terrestrially honed pterosaurs are placed in the taxa lophocratia.

### **Ornithocheiroidea**

**Ornithocheiridae.** Without a doubt the most diverse and abundant of all families of pterodactyloids with a 55 Myr existence was this group of soaring pterosaurs. They are also the best studied morphologically and functionally. They have a global distribution with specimens on every continent except Antarctica. More specifically, specimens have been found in the Cambridge Greensand of England dating to ~110 Ma, the famous Santana Formation in Brazil between 125 and 100 Ma, the Tarrant Formation in Texas dating to ~97 Ma, a species in Morocco found in the Kem Kem Beds dated to ~105 Ma, and specimens found in Australia in the Toolebuc Formation dating to ~110 Ma. See Witton (2013) for a detailed listing of references of genus locales. However, only two localities have produced complete specimens, the Santana and Crato Formations in Brazil.

Specimens from these sites give us wingspans of four to seven meters, although some have estimated some up to nine meters (Dalla Vecchia and Ligabue 1993). Their skulls are very elongate with a long rostrum and a nasoantorbital fenestra taking up only about the second half of the skull. The anterior portions in some species have a rounded crest seen in Figure 5. The anterior crest in species start at the anterior tip of the skull while other species are ten plus millimeters back from the most anterior tip of the rostrum (Witton 2013). Some of these species in this family lack these crests completely. All bear rows of teeth running the anterior two-thirds of the upper jaw and half of the lower. Their teeth increase in size by two or three then begin reducing in size towards the back. This dental pattern is a characteristic fish grabbing dentition, with piscivory likely being their primary diet (Witton 2013). Some species possessed

supraoccipital crests at the posterior end of their skull lacking any observable fibrous bony texture that would indicate the extension of a soft tissue crest (Unwin 2005). Their lower jaws typically have a mandibular symphysis running the anterior 30 percent. A lot is known about ornithocheiridae skulls because some 3D preserved specimens have been found; Witmer CT scanned the braincase and published findings on their brain morphology giving us some detailed neuroanatomy on pterosaurs (Witmer, Chatterjee, Franzosa, and Rowe 2003).

Post-cranial material demonstrates elongated cervical vertebra with tall neural spines. An important trait hypothesized to have allowed pterosaurs to begin to reach larger sizes, is the level of pneumatization in their skeleton. They possessed extensively pneumatized skeletons along with pteranodontia and azhdarchoidea. Their whole vertebral column, trunk components, and forelimbs are filled with space and have pneumatic foramen in specific locations characterizing species (Claessens et al. 2009). Mature individuals have a fused notarium, consisting usually of six dorsal vertebra and seven non-fused dorsals posterior to the notarium. This can vary; some species have dorsal vertebra being 'sacralized' into the pelvic girdle region (Wellnhofer and Kellner 1991; Kellner and Tomida 2000; Veldmeijer 2003).

A notable feature of this family are their forelimbs, which are very long in length in proportion to their body. Their forelimbs were about five times longer than their legs. Their robust pectoral construction, very similar to istiodactylidae, had to be incredibly sturdy to handle the forces generated by the wings and be capable of anchoring the muscles necessary to use the wings in flight (Habib 2008). The deltopectoral crests on the proximal end of the humeri are characteristically warped distally in ornithocheiridae. The wingfinger is the largest seen in pterosaur groups, having reached 60 percent of the entire wing length (Witton 2008a). They have slender femora and tibia were nearly equal length. The femora had a femoral head almost in-line

with the femoral shaft. The small nature of their legs and proportions of their enormous wings, along with the high concentration of their fossils in marine deposits, strongly imply marine soarers (Padian 1983). Their wing shapes are similar to modern oceanic birds that use external sources of lift to remain airborne for extensive amounts of time (Witton 2008a). It is generally accepted that pterosaurs were quadrupedal animals on the ground, but the level of terrestrial ability is variable among families (Habib and Witton 2011; Witton 2013). Being so strongly adapted for flight left ornithocheiridae with disadvantages. Most noticeably is their thin and short legs compared to the length of their forelimbs. The short hindlimbs govern their terrestrial mobility, restricting their pace to the hindlimbs' gait rather than the forelimbs' (Wang, Kellner, Zhou, and Campos 2005). This limb configuration would make them slow and likely very awkward walkers, also implying a very aerial dominated lifestyle.

**Pteranodontia.** Within this family is a very important clade of pterosaurs. Pteranodontia consists of two of the most highly adapted genera for flight in the fossil record. The first to be discussed, *Pteranodon*, is the best recorded and most abundant genus having over 1,100 specimens housed around the world. A skull reconstruction of *Pteranodon longiceps* from the Natural History Museum is shown in Figure 10. Its specimens are restricted to the Late Cretaceous ~86 Ma mostly found in the Americas. The second is *Nyctosaurus* (Figure 11), a very closely related genus that has a



Figure 10 *Pteranodon longiceps* skull and cervical series. Natural History Museum.

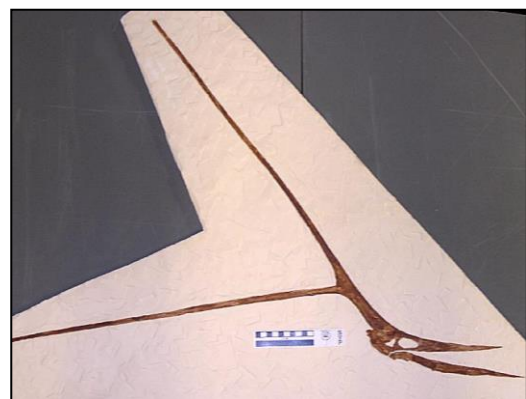


Figure 11 *Nyctosaurus gracilis* skull cast. Sternberg Museum.

similarly fine-tuned anatomy for flight as *Pteranodon*, but with some very discernible differences (Bennett 2003b). The first is the hyper elongated supraoccipital crest that projects posterodorsally that bifurcates forming a massive 'V'. Figure 6 has an illustration of its cranial morphology. A second difference, and characteristic of only two genera including *Anurognathus*, is the lack of a fourth phalanx in the wingfinger. The functional gain, if any, is unknown. The wingspan of species in this clade are two meters to nearly seven meters. All individuals lack any dentition and are some of the derived pterosaurs that became edentulate along with all azhdarchoidea. Despite that fact the two mentioned genera of this clade are the best suited for flight only *Pteranodon's* flight mechanics have been studied extensively (Hankin and Watson 1914; Kripp 1943; Brumwell and Whitfield 1974; Stein 1975; Brower 1983; Hazlehurst and Rayner 1992; Chatterjee and Templin 2004; Elgin et al. 2008; Witton 2008a; Sato et al. 2009; Witton and Habib 2010).

**Istiodactylidae.** This family of pterosaurs were a group of early-cretaceous animals with very long wings with relatively tiny bodies. Their specimens have been found off the coast of England in the Wealden deposits dating to 120 Ma. This family of pterosaurs see a range of wingspan from ~2.4 to 4.3 meters (Wang, Campos, Zhou, and Kellner 2008; Andres and Ji 2008). Istiodactylidae anatomy, particularly the skull, is autapomorphic. The most obvious trait,

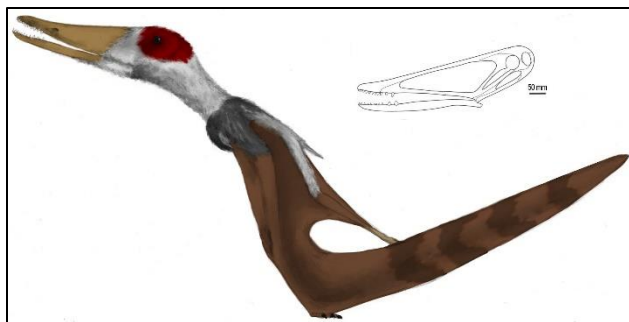


Figure 12 *Istiodactylus latidens* illustration. It had a 4.2 meter wingspan. A drawing by Mark Witton.

seen in Figure 12, is the massive nasoantorbital fenestra. This fenestra is the largest seen in any pterosaur and *Istiodactylus latidens* is the species with the largest in this family. Typically bordering this fenestra, dorsally and ventrally, was thin bone. This

would have made their skulls fairly fragile compared to some other families of pterosaur, suggesting a small prey diet (Witton 2012). Their dentition was restricted to the anterior third of the jaws, and comprised ~12-15 teeth on each side of a jaw. The teeth were short, triangular, and laterally compressed, all of which sat in front of where the nasoantorbital fenestra began nearly forming a continuous cutting surface. The rostrum is rounded in cross section and flattens out at the tip into a blunted end. Their elongate skull is inclined at the posterior end, synapomorphic to all pterodactyloids having the tilted quadrate bone. Their orbital sockets were also lengthened, stretching along the posterior wall of the nasoantorbital fenestra with the eye at the superior portion. Pterodactyloid skulls are characteristically very narrow compared to their length but istiodactylidae are an exception; the *I. latidens* skull is nearly 30 percent its skull length at the jaw joint. A reconstruction of *I. latidens* can be seen in Figure 12.

## Lophocratia

**Ctenochasmatoidea.** This is the first of the pterodactyloids that were more terrestrially adapted rather than being more suited for the air. They generally had more robust limbs, longer hindlimbs, and a deltopectoral crest that was rather simple, inferring less usage (Unwin 2003).

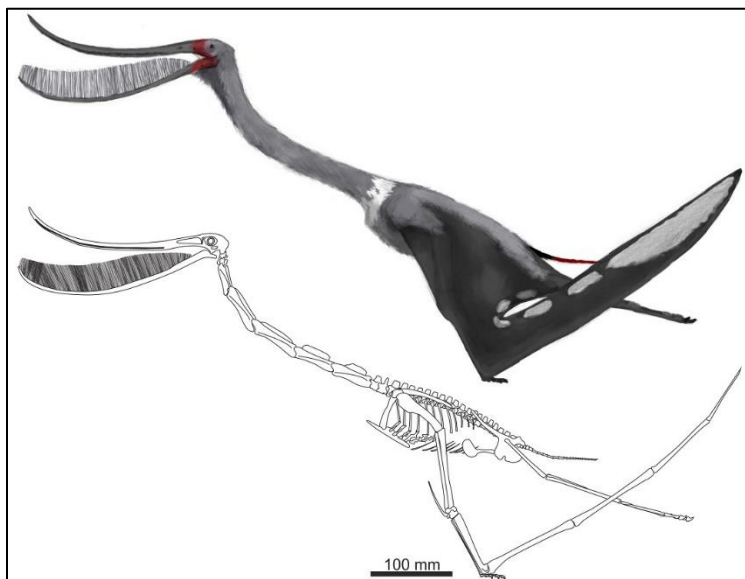


Figure 13 *Pterodaustro guinazi* illustration. Skeletal model and recreation by Mark Witton. Note the row of long and packed teeth that acted as filters.

Their anatomy suggests that they waded in shallow water like shorebirds picking prey items, or in some specialized cases, filter feeding as seen in *Pterodaustro*. Their fossils are mostly found in Late Jurassic to Early Cretaceous deposits in Asia, Europe, South

America, Africa, and North America with special attention in Germany's deposits including the Solnhofen Limestone dating to ~150 Ma. Their entire depositional range is 150 to 105 Ma giving them a very large span.

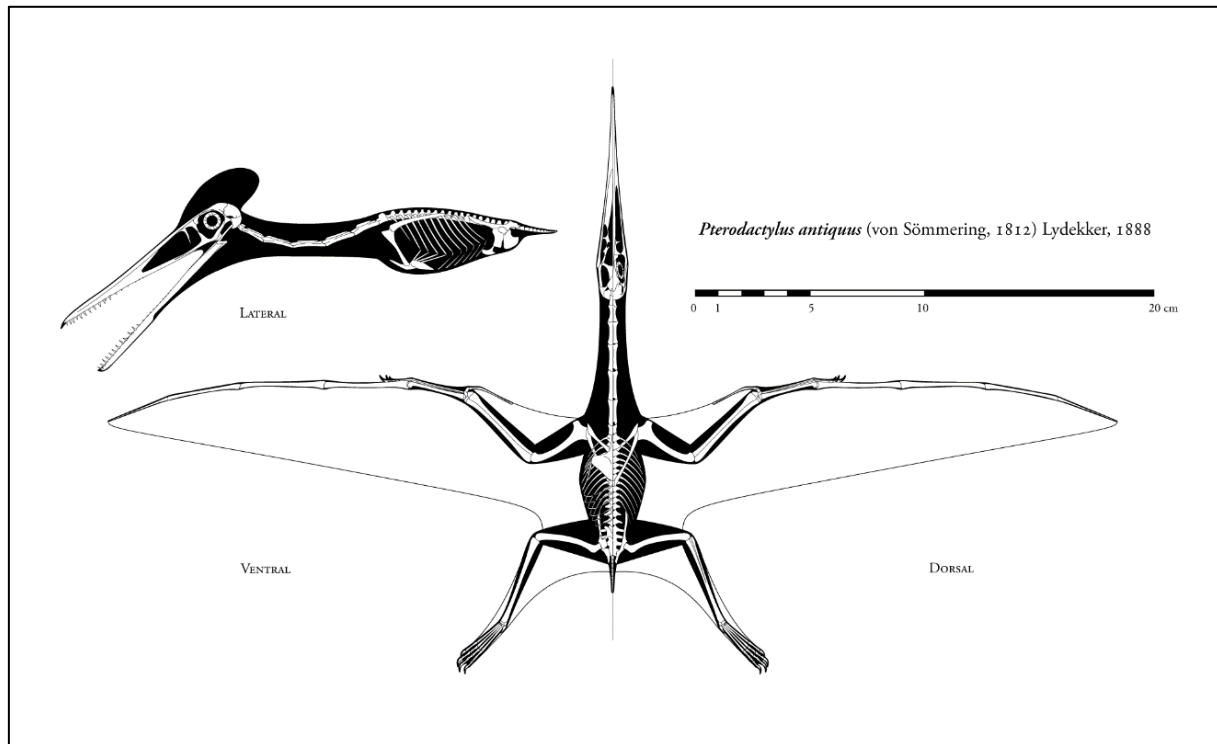


Figure 14 *Pterodactylus antiquus* dorsal/sacral skeletal schematic. Both dorsal and ventral view along with a lateral view. This is the main species that will be analyzed in Chapter 2 of this thesis. Created by Mike Hanson.

Unusual to other pterodactyloids is the restriction of pneumatization to the skull and axial skeleton. This and the lack of the substantial body size that other families reach would initially indicate a correlation (Claessens et al. 2009). Without the expansive network of hollowed bone they could not reach large sizes, but since there are no adults for many of the species in this family may be the reason we don't see any pneumatization in the limbs as seen in other families. Adults may develop expanded pneumatization and larger sizes. The largest known specimen, inferred from skull material, is estimated at 4.2 meters wingspan seen in *Morganopterus* (Lü, Pu, Xu, Wu, and Wei 2012). All other species have wingspans around two meters.



This family of pterosaurs is variable and diverse. They are a very well documented group (Wellnhofer 1970; Fabre 1976; Bennett 1996b; Bennett 2007a; Chiappe, Kellner, Rivaola, Davila, and Fox 2000). The skulls are some of the most variable parts of this family, with a wide variety of quantity and shape of dentition, space between the teeth, and their function. The dental count ranges from 40 in *Pterodactylus* to 260 in *Ctenochasma*, the hallmark species of this family. The former's dentition were typical of grabbing prey items from the water or ground surface and swallowing them whole, while the latter's teeth were recurved and long and likely used to 'comb' out small food items from the water (Unwin 2005). *Pterodaustro* has nearly a thousand teeth with a diameter of 0.3 millimeters and 20mm long that was a filter feeder like modern day flamingos seen in Figure 13 (Chiappe and Chinsamy 1996). The feeding types discussed here led to the selection pressures of their post-cervical adaptations. Their diversity have some typical features that are shared among most species. The first is an expanded neurocranial region posteriorly reclining the back of the skull causing the occipital face to face ventrally (Witton 2013). Most species have cranial crests and although some lack bony projections some specimens show soft-tissue crests without any bony crest supporting it (Tischlinger and Frey 2010).

Ctenochasmatoidea trunk skeletons have some unusual traits that are unique to pterodactyloids (Figure 14). The first is lack of fusion in the dorsal vertebra; there is no notarium in this family. This lack of fusion would have limited their ability to handle the stresses of flight demands. The alternative way they developed to handle the stresses is the long scapula that instead of articulating perpendicularly with the notarium, as in other groups of pterosaurs, ran medially down the length of the vertebra attaching itself to the thoracic region (Bennett 2003a). Their humeri were half the length of their trunks which is a very low ratio among any group with

a simple deltopectoral crest (Bennett 2007a). Entire wings are only known for a few species, but it seems that those preserved had wingfingers comprising of nearly 60 percent of the entire wing. In ctenochasmatoidea we see much longer and robust feet that would have been much more advantageous for terrestrial locomotion, especially for shallow water wading (Witton and Naish 2008). Their similar limb proportions also would have been advantageous giving them greater maneuverability and efficiency on the ground.

**Azhdarchoidea.** Easily the most intriguing family of pterosaurs was this group of the most massive flying reptiles (Figure 15). Standing taller than modern giraffes, they may have eaten small mammals and dinosaurs. They had some of the longest skulls of nonmarine tetrapods, and flight analyses clock them at

reaching speeds in the air at 50 to 60 mph with their nearly 40 foot wingspans (Witton and Habib 2010).

Azhdarchoidea have been found in the Maastrichtian deposits of Jordan, the United States including Montana, New Mexico, Oregon, and Texas, Uzbekistan, Russia, China, and Morocco (Lawson 1975b; Buffetaut, Lauret, Le Loeuff, and Bilotte 1997; Padian and Smith 1992; Godfrey and

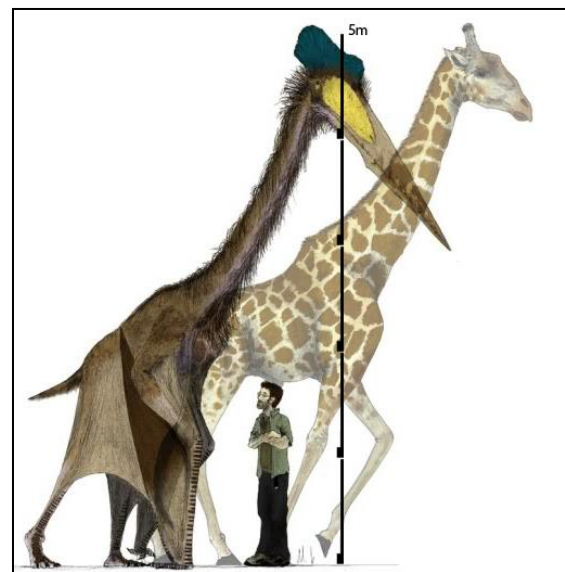


Figure 15 *Quetzalcoatlus* sp. illustration. Mark Witton.

Currie 2005; Nessov 1984; Averianov, Arkhangelsky, and Pervushov 2008; Padian and Smith 1992; McGowen, Padian, De Sosa, and Harmon 2002). They range from ~112 to 65 Ma, being the very last group of pterosaurs.

Unfortunately, azhdarchoidea are also some of the least known due to their highly fragmented fossil record. Their range of wingspan length goes from the smallest at ~2.5 meters

to 13 meters (Frey and Martill 1996). Some species of azhdarchoidea have typically proportioned skulls for pterodactyloids, but some became up to ten times longer than wide as *Zhejiangopterus* and *Quetzalcoatlus sp.* Mostly anterior portions of skulls are known, but they reveal that the eye stays very close to the jaw joint, in a ventral position compared to almost every other pterosaur. The jaw joint itself is interesting because it appears to be very robust. A specimen of *Zhejiangopterus* has a preserved posterior cranial region and shows a rotated occipital face oriented ventrally (Unwin 2003). This rotated facet would indicate that the cervical vertebra would have articulated at a rather sharp angle with the skull (a feature also seen in derived ctenochasmatoidea, Unwin 2003). They had very long mandibular symphysis stretching 60 percent of the lower jaw. Their cervical series still only had seven vertebra, but they were hyper-elongated to such a degree that they nearly surpassed the length of their skulls, which in adults was approaching three meters (Buffetaut et al. 1997).

The azhdarchoidea trunk skeleton was tiny in comparison to their skull and neck at less than a meter long (Witton and Habib 2010). Their bodies were robustly built however. They had large surface areas with enough room to pack on more muscle than what was needed to fly itself and more importantly, take-off and land (Paul 2002). Their humeri and cervical vertebrae are the most common azhdarchoidea remains found. Humeri reached lengths of almost six meters long and 80 centimeters in diameter at the shaft; they were enormous. Witton noted that the diameter was comparable to that of a two tonne hippopotamus indicating the level of stress and compression that this animal put onto the forelimbs (Witton 2013). The wing metacarpals were 2.5 times longer than the humeri, which is the largest ratio of any pterosaur (Witton 2013). Like most other pterosaurs, their wingfinger consisted of about half the entire wing with reducing phalanx lengths more distally. A few crushed specimens show that their pelvis was small and

compact. The hindlimbs were long with the femora 80 percent the length of the tibiotarsus (Unwin 2003). They were actually quite long and gave azhdarchoidea very tall statures comparable to other pterosaurs. Their large aspect ratio would have given them soaring abilities, and statistical analyses with aerodynamic mechanics has shown they were very much capable of launching and maintaining flapping flight for enough time to find external sources of lift (Witton and Habib 2010). It is important to note that this analysis, and all other flight analyses, are based on very contentious mass estimates. Terrestrial locomotion in this family hasn't been given much attention, but with such long extremities it is thought that they may have walked similarly to giraffes moving both left limbs forward at the same time followed by the same with right limbs (Witton and Naish 2008).

### **Growth of Animals**

**Surface Area – Volume Paradox.** During an animal's growth history (ontogeny) it experiences changes in size and shape developmentally. These changes can also be tracked during the evolution of taxa through time. As an individual grows its proportions typically change accounting for what is called the surface area – volume paradox. Simply, the ratios between the surface area (SA) and volume (V) of a growing animal do not increase linearly. Instead, the ratio of the SA and V gets smaller with the SA getting smaller while the V gets larger. For example, consider three cubes; cube A has a length (L) of 2, cube B has a length of 3, and cube C has a length of 7. Cube A will have a SA=24 and V=8; Cube B: SA=54 and V=27; Cube C: SA=294 and V=343. These examples demonstrate how the increase in  $L^2=SA$  and  $L^3=V$  cause rapid changes in V compared to the SA of a cube or an animal.

Typically in animals, you will see 'positive allometry' when lengths and SA increases to compensate for the cubic increase in mass. If a mouse was scaled up 'isometrically' (no change

in proportions or shape) its legs would break just trying to support its weight while standing upright. This is why an elephant has proportionally thicker limb bones to account for the large mass it has at its size. Conversely, 'negative allometry' is also seen where the proportions of a particular area decreases relative to the rest of the body during ontogeny.

**Allometry and Isometry.** The mathematical bases for calculating scaling relationships (allometry and isometry) is described with:  $[y = ax^b] = [\log(y) = \log(a) + (b) \cdot \log(x)]$ , with  $a$  = y-intercept,  $b$  = slope], using the natural log of the data (Huxley 1932; Small 1996). When the slope is equal to 1, the variables are showing isometry with the same proportional changes. When the slope is less than 1 it is showing negative allometry with the 'y' variable having smaller change than the 'x' variable. Positive allometry is seen when the slope is greater than 1 when the 'y' variable has larger change than the 'x' variable. All allometric relationships are due to necessary changes in the body to maintain functional efficiency with increase in size, for example, the limbs of mice and elephants. Another example are the wing elements of a pterosaur compared to its axial skeleton during ontogeny.

Changes would need to occur with the wing elements to increase its brachiopatagium (wing-membrane) SA accounting for their increase in volume (and mass) as they grew and as they evolved into adults and larger, more derived, forms. Since the surface area is squared, isometry for an increase in SA is 2. So as a flying animal grows, its surface area of the wing will need to be greater than 2 to have positive allometry increasing proportionally with the increase in body volume/mass which is increasing cubically. Positive allometry is therefore the expected allometric relationship for increase in body size with wing surface area in pterosaurs.

## Conclusion

Pterosauria is a highly morphologically varied clade of flying reptiles that has not had their variation described on a broad scale quantitatively. Using methods such as PCA and multivariate allometry statistics will give us insight into what was happening to their osteology as selective pressures changed their anatomy for different lifestyles. PCA should be able to break down what the major veritable traits were in pterosaurs apart from size, which will typically always be the first principle component describing any animal's data set. At first glance, Unwin showed that *Pterodactylus* has an isometric ontogeny while other groups are allometric, which is found in most animals (2003). In Chapter 2 the allometry and isometry of *Pterodactylus antiquus* and its close relative *Aurorazhdarcho micronyx* will be investigated and compared.

## CHAPTER TWO

### ONTOGENETIC ALLOMETRY OF SKELETAL ELEMENTS AND SURFACE AREA OF *PTERODACTYLUS ANTIQUUS* AND *AURORAZHDARCHO MICRONYX*

#### Introduction

Since Peter Wellnhofer's 1970 monograph on Solnhofen pterosaurs was published, the data collected has been used to test hypotheses for validity of taxonomy, conspecific or congeneric relationships, and studies of ontogeny (Mateer 1976, Bennet 1996b, Jouve 2004, Bennett 2013). The continued contention of generic relationships and possible sexual dimorphism of the species *Pterodactylus antiquus* and *Aurorazhdarcho micronyx* are examined in this study. The longitudinal length data published by Wellnhofer and corrected by Bennett (2013) are used in a Principal Component Analysis, linear regression with calculated geometric mean, and for the schematic reconstructions of their wings to calculate surface areas for an additional linear regression analysis and layered schematic analysis.

A typical problem with fossil collections is the quantity of individuals of a species. To compound the problem is the lack of completeness of the individuals within a species that have been found. This problem has mostly precluded intraspecific analyses of species variation in the fossil record, including pterosaurs. However, because of their abundance in the Solnhofen Limestone of Germany, *Pterodactylus antiquus* (first described by Collini in 1784) is one of the largest collection of individuals within the same species with specimens nearly complete (Wellnhofer 1970). Also included in this monograph was *Aurorazhdarcho micronyx* (formally *Pterodactylus micronyx*; Jouve 2004; Bennet 2013) in similar abundance and completeness from the same horizon and

locality; being found in Lower Tithonian, Solnhofen LS, Malm Zeta 2, of Eichstätt, Bavaria, Germany.

Studying these specimens quantitatively using multivariate methods is not new, but better software and understanding of the mathematics is allowing further and more detailed interpretations to be made on Wellnhofer's data. Mateer used the same dataset for *Pterodactylus antiquus* (and formerly *P. kochi*) to assess possible intraspecific and interspecific relations among species that are now considered conspecific to *P. antiquus* (1976). Jouve used tooth count and skull length to propose that *P. kochi* was conspecific and a junior synonym of *P. antiquus* (2004). Bennet used the length data of *Pterodactylus* to bolster the synonymy of *P. kochi* with *P. antiquus* and re-diagnosed the Solnhofen Pterodactyloid fauna. In the studies by Mateer (1976) and Bennet (2013) Principle Component Analysis was used to make interpretations and develop hypotheses for the relationships of the Pterodactyloid fauna from the Solnhofen beds. While both of these studies used the same data and multivariate method (PCA) as the analysis presented here, the present study is more detailed and has a more complete experimental design. Further interpretations will be made that reveal new and interesting results regarding the ontogeny, shape, and relative size of *Pterodactylus antiquus* and *Aurorazhdarcho micronyx* wing surface area.

### **Allometry and Isometry**

The size variation in morphometric variables is usually associated with variations in shape due to metric characters being heavily correlated to other characters. There are then three levels of allometry that can be distinguished: static allometry, ontogenic allometry, and evolutionary allometry.



Static allometry is the variation that can be found among the individuals of the same population and age class (Gould 1975). This allometry can be easy to study in a species with discrete growth stages and with determinate growth. The second, ontogenetic allometry, calculates the variation of characters of a species during growth. Isometry (simple allometry) occurs with the ratio of two variables staying constant (Huxley 1932, Shae 1985). Positive allometry occurs when the dependent variable increases in size faster than the independent variable while negative allometry has the dependent decreasing in size relative to the independent variable. There are three types of data typically used with ontogenetic allometry: longitudinal data, cross-sectional length data with known growth stages, and cross-sectional data with no known growth stages (Cock 1966). *Evolutionary allometry* analyzes the change in characters among species with a common ancestor or a known evolutionary lineage and is a tool to analyze changes at a phylogenetic level. With this level of allometry it is important to use specimens of the same ontogenetic stage to avoid confounding evolutionary change due to heterochrony.

All levels of allometry are empirical based using measurement data in its analyses. When bivariate plots are produced it was realized early on (Huxley 1932) that the growth of an organism typically follows a curved line. When the data is logarithmically transformed the trend becomes more linear. The power function that describes allometry [ $y = ax^b$ ] when log-transformed [ $\log(y) = \log(a) + (b) \log(x)$ ] where x and y are the character measurements, a = y-intercept, and b = slope, will be the mathematical basis used in this study (Huxley 1932). The special case of isometry [b = 1], describes proportional increase in both characters considered. Positive allometry [b >

1] describes  $(\log y)$  scaling faster than  $(\log x)$ . Negative allometry describes  $(\log x)$  scaling faster than  $(\log y)$  (Klingenberg 1996).

### Growth: Surface Area – Volume Paradox

As an individual grows it experiences changes in size and shape. This is partially due to the different scaling of the surface area with the volume during growth. The area ( $sa^2$ ) increases squared compared to the cubic ( $v^3$ ) increase in volume making them non-linear and is known as the surface area – volume paradox (Schmidt-Nelson 1984). A simple example would be a cube increasing in size. Starting at a length of  $[x = 2]$ , the initial [surface area = 24] squared units while the [volume = 8] cubic units. If length increases to  $[x = 4]$ , the new [surface area = 96] squared units and [volume = 64] cubic units. Just by doubling in length, the ratio of volume to surface area went from  $[1/3]$  to  $[2/3]$ . As an animal grows it will have a positive allometry in surface area, and volume will always have a positive allometry with surface area. The volume

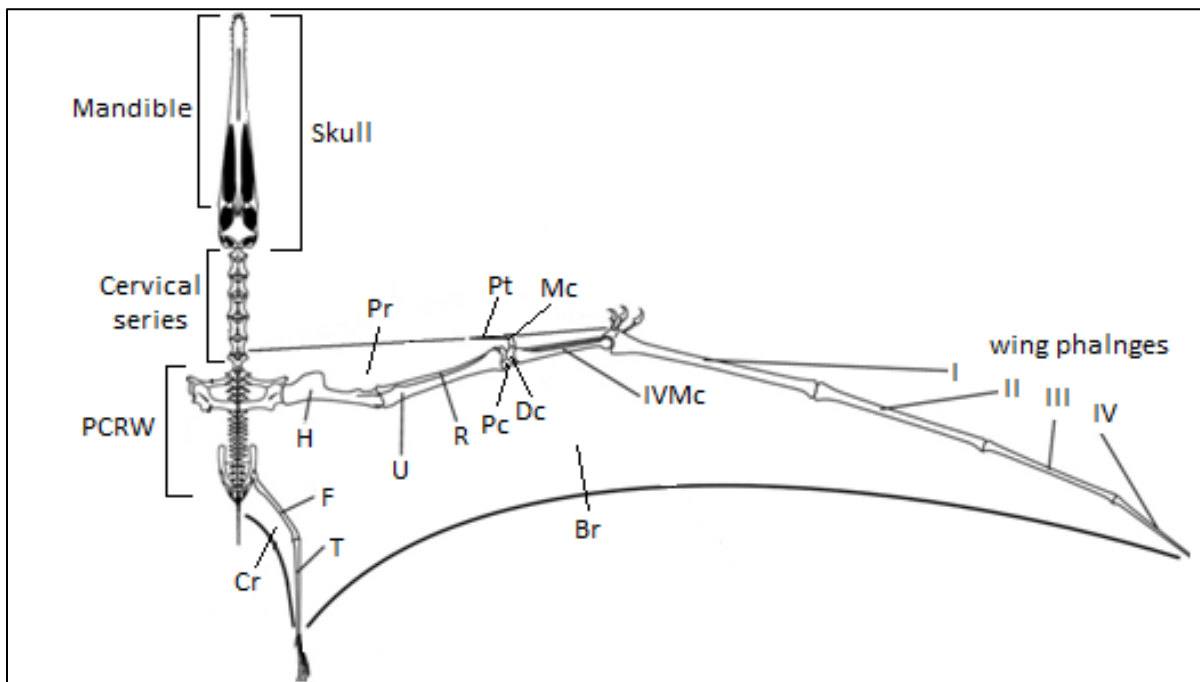


Figure 16 General depiction of a pterosaur with labeled features and bones. Elements used in the evolutionary allometry analysis are bolded ( $n = 14$ ). **Skull**; **Mandible**; **Cervical series**; **PCRW**: dorsal/sacral series; **H**: humerus; **U**: ulna; **R**: radius; **IVMc**: 4<sup>th</sup> metacarpal; **Wing phalanges I-IV** **F**: femur; **T**: tibia; **Pr**: Propatagium; **Pt**: pteroid; **Mc**: metacarpal; **Pc**: proximal carpal; **Dc**: distal carpal; **Br**: brachioptagium. Wilkinson et al. 2006.

increases much more rapidly than the surface area of the cube and the same effect is seen in organisms increasing in size.

### **Experimental Design**

Positive allometry would be expected for any ontogenetic analysis of surface area (or regional surface area) or volume for any species. When this is applied to pterosaurs, specifically the surface area of their main wing membrane, the brachiopatagium (Figure 16: Br), should have a clear positive allometry seen in the membrane relative to the growth of the animal as a whole. Pterosaurs will experience the same increase of squared surface area versus cubic volume increase as any growing animal. Its increase in volume is going to be correlated with its increase in mass. **The null hypotheses for this study: the increase in mass during growth negatively effects the wing carrying capacity by adding load (per squared unit) and must be compensated by a proportional increase in the wing membrane's surface area to account for redistribution of the added mass. Positive allometry will be seen in the forelimb and distal wing elements along with the hindlimb elements accounting for the breadth of the brachiopatagium length.** Without a live pterosaur we cannot get accurate volume/mass measurements, so another proxy for size increase is necessary. In this study, the ln-geometric mean (ln-GM) of each individual will be calculated from 14 longitudinal measurements representative of the whole animal [ $GM = \sqrt[n]{x^1 \cdot x^2 \cdot \dots \cdot x^n}$ ],  $n = 14$ ]. The ln-GM is an indicator of isometry. When other variables are compared to it, levels of positive and negative allometry can be assessed (O'Keefe, Meachen, Fet, Brannick 2013).

This study concerns the allometric growth of *Pterodactylus antiquus* and *Aurorazhdarcho micronyx* using 14 longitudinal measurements to analyze their

ontogenies and serves as a comparative study of the two species to investigate long standing contentions about their relationships. Each of the 14 variables for all 39 specimens will be assessed with a multivariate analysis and bivariate linear regression using ln-GM. These analyses will calculate the allometry for each of the 14 length measurements with the null hypothesis of positive allometry. Reconstructions of brachiopatagium flight membranes are used to preliminarily investigate the expectation of positive allometry in wing surface area against the overall growth of the two species intraspecifically. This bivariate linear regression will also use respective ln-GMs as a proxy for increased size for the calculated surface area.

## **Materials and Methods**

All of the data collected for this study came from Wellnhofer's 1970 monograph and Bennet's 2013 article detailing corrections to measurements of the *P. antiquus* specimen: TM 10341. The species *Pterodactylus antiquus* has 24 nearly complete specimens used here, and *Aurorazhdarcho micronyx* has 15 (raw data can be found in Appendix A). All the individuals from both species used are from Tithonian, Solnhofen LS, Malm Zeta 2 & 3, of Eichstätt, Bavaria, Germany. They are both within the Family ctenochasmatidae, within the Superfamily ctenochasmatoidea (Unwin 2003). Each of the 39 specimens have longitudinal measurements of 14 elements of its axial and appendicular skeleton with 0.93 percent missing data (4/429). Missing data was estimated from the complete data of the specimens of the same species. The 14 lengths used are: skull, mandible, cervical series, PCRW, humerus, radius, ulna, IVMc, phalanges I-IV, femur, and tibia; and are all labeled in Figure 16 (PCRW; praecaudale Rumpfwirbelsäule = combined dorsal and sacral vertebrae). A Mac OS X version 10.6.8 ran Jmp software version 6.0.3 for all analyses.

## **Principle Component Analysis (PCA)**

This multivariate analysis was first proposed by Jolicoeur (1963a) as means to make multivariate (4+ dimensional) plots more interpretable for three-dimensional minds. This analysis is the multivariate version of the allometry equation described previously. PCA is used to pull out the underlining structure within the multidimensional data cloud produced by four or more characters; in this study 14 variables are used. This process ultimately reduces the number of variables to be interpreted within its covariance matrix. It is done by geometrically finding the linear combination with the longest axis of variation in the data cloud, this new axis is called Principle Component 1 (PC1) and describes the largest amount of variation in the covariance matrix (Bookstein et al. 1985). PC1 can be described as the least-squares fit of the straight line to data points of log-transformed, bivariate, and multivariate data (Jolicoeur 1963a; Jolicoeur 1963b).

Multivariate analyses typically find that one dimension of the data contains about 99 percent of the variation: PC1. The reason for this high percentage is nearly all the variation is due to variation in size (Klingenberg 1996). For this reason, only PC1 will be analyzed in this study. All 14 PCs generated in the PCA can be found in Appendix B. Each PC generates a coefficient for each variable and represents the cosine of the angle between the PC (1, 2, etc.) 'axis' and original axis of the respective variable. The coefficients of PC1 represent the increase in each variable relative to size which makes them the coefficients of the multivariate allometry equation (Jolicoeur 1963a; Jolicoeur 1963b; Klingenberg and Zimmermann 1992; Pimentel 1979) and was termed the allometry vector by Shea (1985).

The following PCs are orthogonal to the former with decreasing size in variation and labeled PC2, PC3, etc., until 100 percent of the variation is described. The total number of dimensions (PCs) equals the number of variables used (Klingenberg 1996). PCA will take these (PCs) and rotate the coordinate system fitting the PCs as the new axes of interpretation.

The ln-GM is not used in the PCA. However, a weighted GM of all variables could be calculated by multiplying the PC1 coefficients by the square root of n, (in this study [n = 14]). This calculated GM would compare the variables to a measure of overall size, similar to the bivariate linear regression described previously (Klingenberg 1996). This approach is not used, instead, the number of variables used here [n = 14] will be used to calculate isometry =  $[\sqrt{1/14}]$  so,  $[\sqrt{1/14} = 0.26726]$  (O’Keefe et al. 2013). Each PC1 coefficient is standardized by dividing them all by isometric value for 14 variables, 0.26726. Standardization makes interpretations for allometry easier.

### **Bivariate Linear Regression**

The second analysis tool used in this study uses the ln-GM, previously discussed, as an indicator for relative size growth, thus, an indicator of isometry (O’Keefe et al. 2013). Each of the 14 ln-length measurements were plotted against the ln-GM, serving as the independent variable in each case. The least-squares fit line (trend line) was calculated generating a linear equation for each of the 14 bivariate plots with both *P. antiquus* and *A. micronyx* side-by-side. The slope of these linear equations revealed the relative degree of allometry. The slopes were standardized to 1 by dividing them by 1 for relative comparison to the PCA coefficients of each variable. Coefficients of determination ( $R^2$ ) were calculated for each linear best-fit line along with standard error (SE) to the sample mean. Confidence intervals are calculated for *P. antiquus* and *A. Micronyx* with: [slope  $\pm$  2 x SE].

### **Wing Surface Area Reconstructions.**

Using a schematic from Wilkinson, Unwin, and Ellington (2006) angles between each element were measured and used as a standard to draw the elements of each of the 39 specimens with their relative lengths (Appendix D). Then a straight line was drawn from the articulation points to the knee. The distal end of the fourth phalanx was connected to the distal end of the tibia with a straight line. The areas of the nine non-right triangles was calculated by hand measuring each of the three sides. All nine areas were added together for the total surface area. The ankle is the current accepted posterior end attachment of the brachiopatagium (Elgin, Hone, and Frey 2011). A straight line as the trailing edge was first proposed by Marsh (1882) and since then eight other trailing edge curves have been proposed (Elgin et al. 2011). No favored trailing edge configuration is currently accepted and cannot be integrated into this analysis.

Acknowledging that pterosaur brachiopatagiums did likely have some level of concavity in the trailing edge because of the aerodynamic advantages, reconstructions generated for this analysis used straight trailing edges (Palmer and Dyke 2009). The calculations and interpretations will not give inaccurate conclusions if the degree of concavity stays consistent during the ontogeny within each species. This implies the over calculations for the surface area will also be consistent giving an accurate reflection of relative surface area estimates. Note: for a squared unit area, isometry = 2 due to the two dimensional area the variables are expanding in. All 39 specimen brachiopatagium reconstructions can be seen in Appendix E.

## Results

### Principle Component 1

The coefficients of PC1 are reported in Table 1. It is easier to make interpretations with the PC1 coefficients graphically and standardized to an isometry of 1 (Figure 17). In Table 1, the total amount of variation in PC1 for *P. antiquus* accounts for 98.376 percent of the variation of the data. The variation in PC1 for *A. micronyx* accounts for 92.397 percent. PC2, PC3, etc., account for < 3 and < 8 percent, respectively, of the data variation. They describe variability of shape change and will not be investigated here. All 14 PCs can be found in Appendix B.

**Skull, Mandible, and Cervical Series.** It is well-known that derived pterosaurs had a heterochronous pattern where the skull, mandible, and length of the cervical series elongated. The expectation of high positive allometry of all three lengths, within both species, is evident in their high coefficients revealing positive allometry. *P. antiquus* had the coefficients: skull (1.095), mandible (1.189), and cervical series (1.240). *A. micronyx* had the coefficients: skull (1.221), mandible (1.393), and cervical series (1.137) (Figure 17). This would be contrasted with non-pterodactyloids (more basal pterosaurs) who had relatively shorter skulls, mandibles, and cervical series lengths. They would likely display positive allometry but at a lower rate.

**Humerus, Ulna, Radius, and PCRW.** With the expectations of the wing elements having positive allometry, it was surprising that all three forelimb bones were negatively

	<i>P.</i> <i>antiquus</i>	<i>A.</i> <i>micronyx</i>
Eigenvalue	2.3463	0.9697
Percent	98.376	92.397
Eigenvectors		
In(Skull)	0.29263	0.32643
In(Mandible)	0.31765	0.37226
In(Cervical)	0.33151	0.30377
In(PCRW)	0.25204	0.22226
In(Humerus)	0.22346	0.19743
In(Radius)	0.24498	0.21895
In(Ulna)	0.24498	0.21895
In(IVMc)	0.2677	0.33896
In(I)	0.26319	0.29107
In(II)	0.23336	0.22737
In(III)	0.23791	0.16173
In(IV)	0.23523	0.11961
In(Femur)	0.26394	0.28076
In(Tibia)	0.27962	0.32821

Table 1 Principle Components Analysis Results. *P. antiquus* (P:) n=24 and *A. micronyx* (A:) n=15 showing only PC1. P: Allometry vectors showing variation in size and indicates isometry in dorsal/sacral series (PCRW), IVMc, phalanges I and II, and the femur. A: Allometry vectors is an indicator of size as well, showing that there was no isometry in this close relative of *P. antiquus*. Instead the skull, mandible, IVMc, and tibia show high positive allometry while the rest, particularly wing phalanx 4, have low loadings. Isometry=0.26726 for 14 variables.



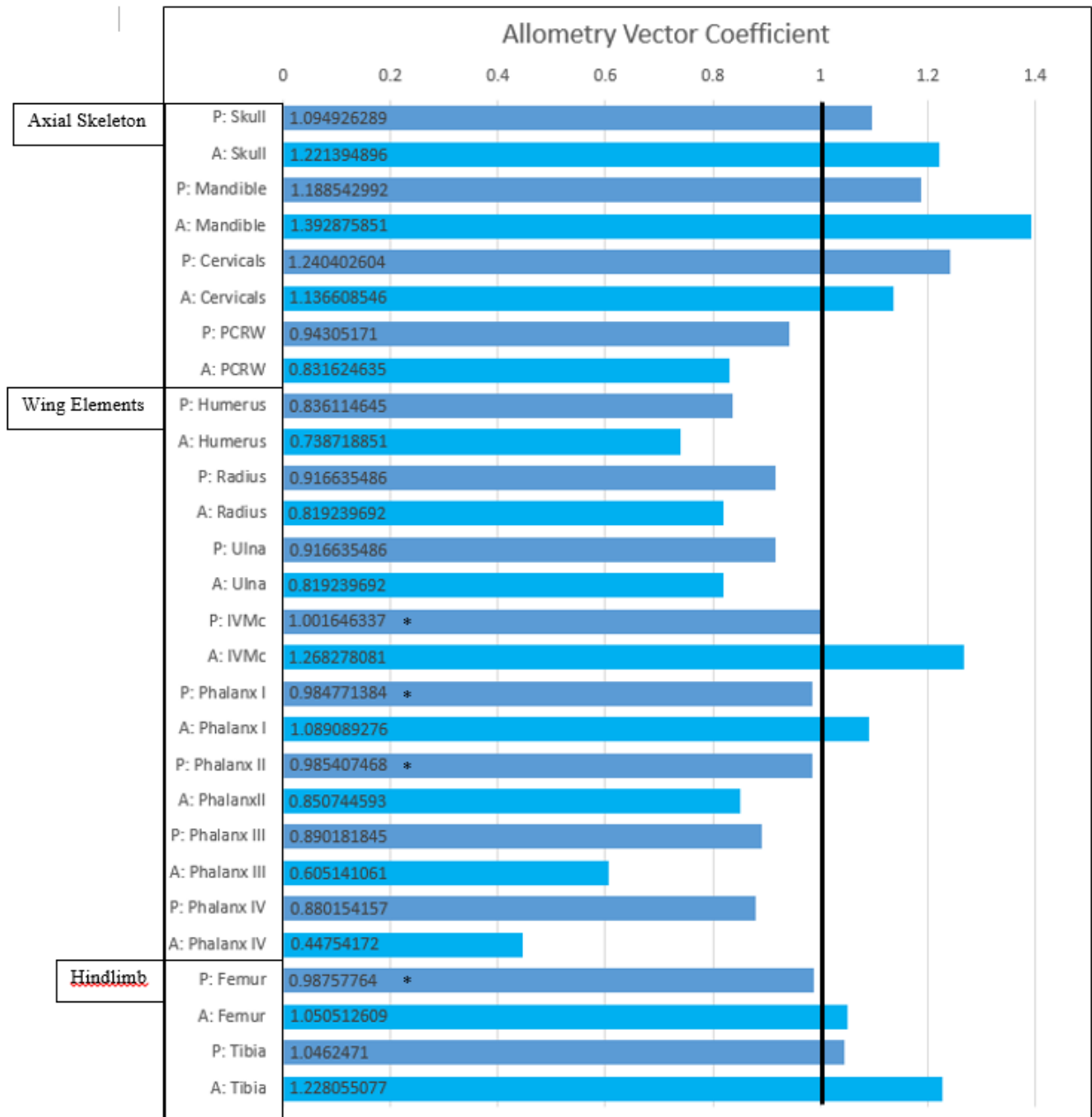


Figure 17 Principle Component One Coefficients. All PC1 coefficients are scaled to 1 by dividing each eigenvalue coefficient by isometry, 0.26726 P. antiquus and A. micronyx. The elements are side-by-side with a green bar representing isometry (= 1). The skulls, mandibles, and cervical series' show positive allometry for both species. The forearms display negative allometry for both species. The hindlimbs for A. micronyx are positively allometric while Pterodactylus show isometry for the femur and slight positive allometry in the tibia. The wing finger phalanges are very variable between the two species, the isometry found in the phalanx I and II in Pterodactylus are noteworthy. The greatest variation in growth is the 4<sup>th</sup> metacarpal (IVMc). P. antiquus displays isometry while A. micronyx has very strong positive allometry. Linear regression isometry with CI<0.05 is indicated by \*

allometric for both species. Recent allometry work of non-avian dinosaurs and American alligators has seen a similar pattern of negative allometry in the forelimbs (Reisz, Scott, Sues, Evans, and Raath 2005; Livingston, Bonnan, Elsey, Sandrik, and Wilhite 2009). Plesiosaurs, an extinct clade of marine reptiles, also show this negatively allometric trend in the forelimb elements (O'Keefe and Carrano 2005). Now, it is apparent in pterosaurs, and would suggest it as a plesiomorphic trait in Sauropsida. The reduction in size of the forelimb elements in *P. antiquus* and *A. micronyx* brings up the contentious debate of quadrupedal re-adaptation seen in derived pterosaurs. Recently investigated was the relationship of the evolution of bipedalism and negative allometry in the forelimbs (Livingston et al. 2009). It is likely that there is a strong correlation of pterosaur flight, their terrestrial locomotion, and the observed allometry found here that requires further analysis. For *P. antiquus* and *A. micronyx*, this means that as the individuals grew, their forelimbs counteracted the positive allometry expected in the wing length and wing surface area. *P. antiquus* had the coefficients: humerus (0.836), ulna (0.917), and radius (0.917). *A. micronyx* had the coefficients: humerus (0.739), ulna (0.819), and radius (0.819) (Figure 17).

The combined length of the dorsal and sacral vertebral series, PCRW, shows negative allometry in both species: *P. antiquus* (0.943), *A. micronyx* (0.832) (Figure 17). Relative to basal pterosaurs, derived pterosaurs' trunk became more compact and fused. This rigid structure gave their wings a stronger frame that muscles could mount onto for use during flight. So the negative allometry found in these two derived pterosaurs is not unexpected. However, the negative allometry does play against the positive allometry expected in the breadth of the brachioptagium. Numerous other flight aerodynamic variables are likely involved with the trunk length that are not considered here.

**IVMc, Phalanges I-IV.** Coefficients from PC1 for the IVMc are both very different between the two species and begin to reveal an interesting phenomenon in their distal wings. *P. antiquus* has a coefficient of 1.002 while *A. micronyx* has a coefficient of 1.268, isometry and positive allometry, respectively with isometry = 1. This variable separates both species drastically. The growth of *P. antiquus*' IVMc is static during growth while *A. micronyx* has high positive allometry in its IVMc. This element in *A. micronyx* follows the null hypothesis but the more distal elements beyond phalanx I do not.

These elements also give marked delineations between both species. *P. antiquus* shows isometry in phalanges I-II (0.985, 0.985). This combined isometry forms an ontogenetic modular isometry within the distal wing of this species. Phalanges III-IV are negatively allometric (0.890, 0.880) at about the same degree as the forelimb elements. This overall isometry and negative allometry indicates that the entire wing length of *P. antiquus* had an overall negative allometry with modular isometry.

The ontogeny in *A. micronyx*'s distal wing is totally different than *P. antiquus*. Phalanx I in *A. micronyx* does have a positive allometry (1.089) but is noticeably smaller than its IVMc. The coefficient of phalanx II gets even smaller (0.851) moving into negative allometry and a pattern can begin to be seen with a similar decrease in coefficient size for phalanges III and IV (0.605, 0.448). This pattern found in *A. micronyx* and the overall negative allometry will be examined further in the bivariate linear regression analyses.

**Femur and Tibia.** For both elements of the hindlimb in *P. antiquus*, an isometric coefficient is calculated in the femur (0.988) and positive allometry in the tibia (1.046) (Figure 17). This isometry gives a nearly static growth rate in the hindlimbs. Allometry in

the tibia would logically have most effect of brachiopatagium's breadth. Unlike the rest of the calculated elements, the tibia in *P. antiquus* seems to display a small degree of positive allometry. The hindlimbs in *A. micronyx* show different ontogenies in both elements. The femur's coefficient displays small positive allometry (1.051) while the tibia has very high positive allometry (1.228) (Figure 17). These differences are another major character between both species. Most noticeably in the tibia, *A. micronyx* has enormous positive allometry in the lower leg which would likely have a big effect on the allometry in the breadth of the brachiopatagium.

### **Bivariate Linear Regression**

Each of the 14 bivariate linear regression statistics are listed in Table 2. For *P. antiquus*, all the R<sup>2</sup>-values are >0.962 reflecting a great approximation of the linear slope to data points. Likely due to the smaller data set in *A. micronyx*, the wing phalanges III (0.741) and IV (0.681) had low R<sup>2</sup>-values while the rest of the elements were >0.884. The results of the PCA and bivariate linear regression can easily be compared having standardized each of the calculated values to 1. The overall pattern and sizes of the standardized values correlate well, affirming that the coefficients in PC1 are representative of variation in size. The confidence intervals for each slope are bracketed in Figure 18.

**Skull, Mandible, and Cervical Series.** The findings of the bivariate linear regression are similar to the PCA. Again, positive allometry is calculated in the skull, mandible, and cervical length which are expected results for species of derived pterosaurs (Figure 18). However, the confidence intervals are the largest in this region for both species with large standard errors (Table 2). These large intervals allow for vague interpretations of the population mean for these

elements. Larger sample sizes of both species are necessary for a more accurate SE to be calculated.

**Humerus, Ulna, Radius, and PCRW.** The slopes of the forelimb elements and their confidence intervals are listed in Table 2. All the elements again reveal negative allometry with confidence intervals  $>0.05$ . So there are two analyses that show negative allometry in the forelimbs correlating with previous research of terrestrial and marine reptiles discussed in the PCA results (Figure 18). There is likely something more complex occurring with these two species and pterosaurs in general with these elements involving terrestrial and aerodynamic constraints that are keeping these bones from lengthening.

The combined dorsal and sacral series mirror the PCA analysis with negative allometry. This result was unexpected because of the increased compactness of derived pterosaur trunks but it is still a bizarre phenomenon in an animal that should be doing everything possible to increase surface area of the brachiopatagium. The negative allometry found in the forelimbs and PCRW both show that there are some other constraints within pterosaurs that had them work against their increasing mass during growth.

**IVMc, Phalanges I-IV.** The linear regression for this element is remarkably isometric with a slope of  $1.008 \pm 0.042$  (Table 2). In Figure 18, isometry is marked by a solid black line that the *P. antiquus* IVMc bar is resting on. This element has a  $>95$  percent confidence making it very interesting. In derived pterosaurs it is known that the IVMc hyper-elongates but in this species it had static growth selected for after previously undergoing levels of positive allometry in its evolutionary lineage. *A. micronyx* has a completely different ontogeny occurring in this element. Having a slope of  $1.311 \pm 0.160$ , it is well into positive allometry (Table 2). You can see the drastic difference in Figure 18

Element	Sp.	R <sup>2</sup>	Slope	SE	Lower SE	Upper SE
Skull	P	0.979459	1.1011493	0.033998	1.0331533	1.1691453
	A	0.936018	1.2603173	0.091389	1.0775393	1.4430953
Mandible	P	0.967101	1.1946134	0.046976	1.1006614	1.2885654
	A	0.884408	1.436756	0.144062	1.148632	1.72488
Cervical	P	0.981066	1.247455	0.036948	1.173559	1.321351
	A	0.884666	1.1722674	0.117393	0.9374814	1.4070534
PCRW	P	0.982427	0.9488681	0.027056	0.8947561	1.0029801
	A	0.973735	0.8604818	0.039195	0.7820918	0.9388718
Humerus	P	0.984034	0.841838	0.022862	0.796114	0.887562
	A	0.963933	0.7661577	0.041103	0.6839517	0.8483637
Radius	P	0.988982	0.9228635	0.020768	0.8813275	0.9643995
	A	0.975065	0.8513524	0.037759	0.7758344	0.9268704
Ulna	P	0.988982	0.9228635	0.020768	0.8813275	0.9643995
	A	1.975065	0.8513524	0.037759	0.7758344	0.9268704
IVMc	<b>P</b>	<b>0.99046</b>	<b>1.008042</b>	<b>0.0211</b>	<b>0.965852</b>	<b>1.0502319</b>
	A	0.953381	1.3106513	0.080383	1.1498853	1.4714173
W-Phalanx I	<b>P</b>	<b>0.98951</b>	<b>0.99126</b>	<b>0.02177</b>	<b>0.94773</b>	<b>1.0347897</b>
	A	0.962147	1.1296361	0.062144	1.0053481	1.2539241
W-Phalanx II	<b>P</b>	<b>0.9943</b>	<b>0.991756</b>	<b>0.016</b>	<b>0.959748</b>	<b>1.0237635</b>
	A	0.929013	0.8879604	0.068077	0.7518064	1.0241144
W-Phalanx III	P	0.984418	0.8962019	0.024039	0.8481239	0.9442799
	A	0.741139	0.6371579	0.104438	0.4282819	0.8460339
W-Phalanx IV	P	0.962838	0.8862051	0.037119	0.8119671	0.9604431
	A	0.681869	0.4709355	0.089216	0.2925035	0.6493675
Femur	<b>P</b>	<b>0.9886</b>	<b>0.993972</b>	<b>0.02276</b>	<b>0.948456</b>	<b>1.0394882</b>
	A	0.891712	1.092139	0.105556	0.881027	1.303251
Tibia	P	0.996408	1.0528923	0.013478	1.0259363	1.0798483
	A	0.980464	1.2728348	0.049832	1.1731708	1.3724988
					0	0
Wing SA	P	0.99282	1.8512465	0.033564	1.7841185	1.9183745
	A	0.990075	2.0102437	0.055821	1.8986017	2.1218857

Table 2 Bivariate Linear Regression Calculations. Calculations of the In-transformed data in the linear regression analysis for principle component 1 for *P. antiquus* and *A. micronyx*. **P** and **A** are bold for elements that display isometry and CI<0.05.

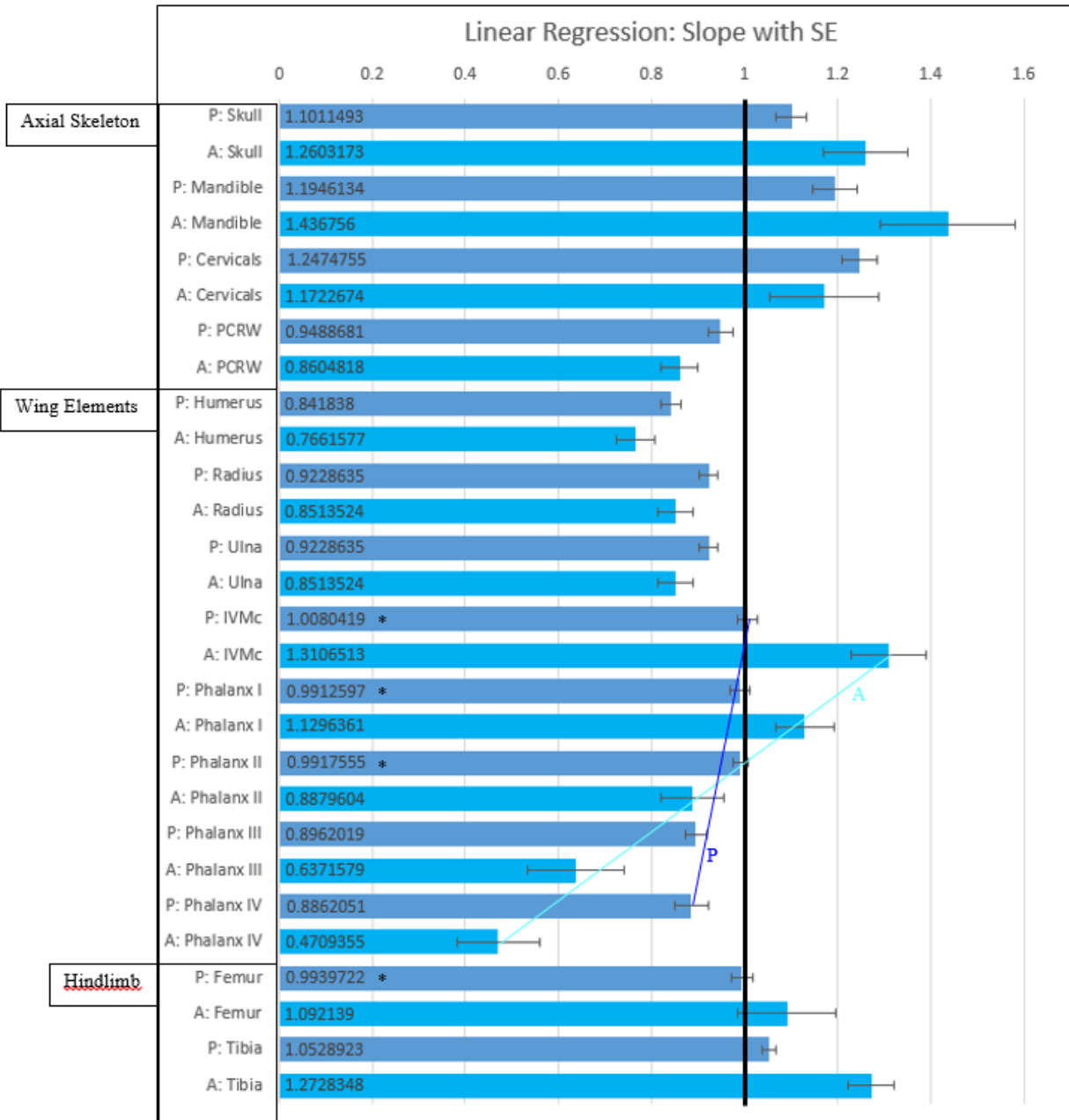


Figure 18 Linear Regression Slopes. All slopes for *P. antiquus* and *A. micronyx* with error bars. The skulls, mandibles, and cervical series' show positive allometry for both species. The forearms display negative allometry for both species. The hindlimbs for *A. micronyx* are positively allometric while *P. antiquus* show isometry for the femur and show positive allometry in the tibia. The wing finger phalanges are very variable between the two species; the isometry found in the phalanx I and II in *P. antiquus* are noteworthy. The greatest variation in growth is the 4<sup>th</sup> metacarpal (IVMc). *P. antiquus* displays isometry while *A. micronyx* has very strong positive allometry. Line P: *P. antiquus*; Line A: *A. micronyx*. Linear regression isometry with  $CI < 0.05$  is indicated by \*

graphically between the IVMc ontogenies. The slope of *A. micronyx*'s IVMc was expected by the null hypothesis for this analysis but the degree of positive allometry is still quite extreme.

Phalanges I-II in *P. antiquus* have slopes and standard errors that give these elements statistically significant isometric values:  $0.991 \pm 0.042$ ,  $0.992 \pm 0.032$ , respectively. What this does, as discussed briefly in the PCA results, is give *P. antiquus* ontogenetic modular isometry in its distal wing. All three elements (including the IVMc) in this modular segment have >95 confidence for isometry, revealing a novel observation in pterosaurs. Phalanges III-IV in *P. antiquus* have a negatively allometric slope of  $0.896 \pm 0.048$  and  $0.886 \pm 0.074$ , respectively. These elements are going against the null hypothesis and working to decrease the size of the brachiopatagium's surface area.

Phalanx I of the *A. micronyx* has a slope of  $1.130 \pm 0.124$  (Table 2). It is the last element in the distal wing to show positive allometry. As seen in the PCA results, the slopes decrease in size from the IVMc to phalanx IV. Phalanges II, III, and IV have respective slopes of:  $0.888 \pm 0.136$ ,  $0.637 \pm 0.208$ , and  $0.471 \pm 0.178$  (Table 2). Although no isometry is found in *A. micronyx*, it has its own interesting ontogenetic pattern seen in Figure 18.

**Femur and Tibia.** The femur in *P. antiquus* is another element that reveals an isometric ontogeny with a slope of  $0.994 \pm 0.045$ . The tibia is positively allometric having a slope of  $1.053 \pm 0.026$  (Table 2). Both of these slopes have >95 percent confidence. Although there is positive allometry in the tibia, it is small. So during its ontogeny there was not much relative length being added, so their effect on the breadth of the brachiopatagium was small. There is a different ontogeny occurring in the hindlimbs of *A. micronyx*. The femur has a slope of  $1.092 \pm 0.210$ . Although the confidence interval brackets it into isometry, a larger data set would likely tighten the SE revealing it to be positively allometric. The tibia, however, has a very large slope of 1.273



$\pm 0.100$  (Table 2). Unlike *P. antiquus*, the tibia of *A. micronyx* has a noticeable effect on the breadth of the brachiopatagium. In Figure 18, it is obvious to see the extreme positive allometry in the IVMc and tibia of *A. micronyx*, which is drastically different from *P. antiquus*.

### Surface Area of Brachiopatagiums

At the bottom of Table 2 are the calculated statistics of the two bivariate linear regressions of the surface areas for each species against their ln-geometric mean (n=24 for *P. antiquus*; n=15 for *A. micronyx*). The calculated surface areas for each of the 39 specimens are listed in Table 3. The

<i>P. antiquus</i>				<i>A. micronyx</i>	
#	SA	#	SA	#	SA
1	4506.95	15	15744.4375	26	4219.0469
2	20958.5	16	17694.0625	27	4815.25
3	22656.625	17	19164.0625	28	5610.15624
4	24000.5	18	20047.1111	29	6968.725
5	40436	19	20044.7222	30	6420.875
6	2490.90625	20	21247.5556	31	8577.3125
7	2918.46875	21	22067.6667	32	7093.375
8	4791.125	22	33175	33	12581.125
9	4013.742188	23	17995.625	34	14551.125
10	9065.9375	24	11826	35	17763.875
11	12260.5			36	20646.5625
12	13087.625			37	7626.375
13	18328.9357			38	9739.0625
14	16994.5			39	13066.59375

Table 3 Surface Area Calculations. Calculations of the surface areas for each of 39 specimens. Scaled drawings are in Appendix C.

surface areas were ln-transformed and plotted against the ln-GM. The R<sup>2</sup>-values for both species were nearly 1 (>0.99) (Table 2). The R<sup>2</sup> describes the variance of the SA being nearly 100 percent predictable by the ln-GM for the brachiopatagium.

*Pterodactylus antiquus*. As discussed in the Introduction, isometry with a squared unit area equals a slope of 2. The slope of *P. antiquus* reveals a negative allometry slope of  $1.85 \pm 0.0670$  (Table 2). This slope shows that as they grew, their brachiopatagiums were growing slower than the rest of

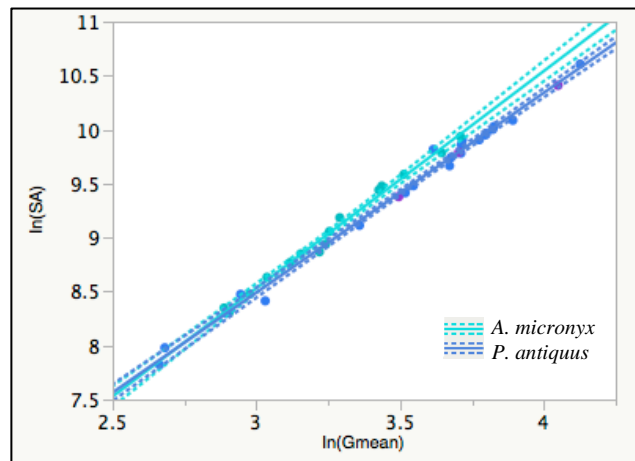


Figure 19 Bivariate Plot of the ln-Geometric mean vs ln-Surface Area. *P. antiquus*' slope is negatively allometric [ $\ln(\text{SA}) = 2.935 + 1.851 * \ln(\text{Gmean})$ ] with a SE = 0.0336. *A. micronyx* has an isometric slope [ $\ln(\text{SA}) = 2.501 + 2.010 * \ln(\text{Gmean})$ ] with a SE = 0.0558.

their body proportionally. Figure 19 shows the slopes of both species. It appears that the slopes describe similar growth but they reveal different trajectories of ontogeny. *P. antiquus*' membrane growth goes against the null hypothesis that the membrane surface area would have a distinct positive allometry with relative growth of the animal. This result may mean that the increased mass during growth was not having such a negative effect on its aerodynamics requiring positive allometry, or even isometry.

The role of the hindlimbs is not apparent at first until it is understood that the brachioptagium membrane runs the length of the trunk and down the legs to the ankle, that these elements did play a role in the breadth of the main wing membrane (Elgin et al. 2011). The exact amount of effect this linear direction had on the overall squared area is unknown.

*Aurorazhdarcho micronyx*. An unexpected slope was calculated for *A. micronyx* brachioptagium at  $2.010 \pm 0.110$  (Table 2). These two slopes can be seen plotted against each other for both species in Figure 19. Despite the large standard error, it can be suggested that this species had a main membrane growth near isometry during its ontogeny. What is seen in *A. micronyx* is more complex. With the initially high positive allometry in IVMc at a slope of 1.31, the following wing phalanx slopes scale down in size: P-I (1.130), P-II (0.888), P-III (0.637), and P-IV (0.471) by about 0.21. So it is very interesting to find the membrane slope near isometry. These values would suggest that the allometry in the lengths of the distal wing was heavily constrained to maintain the membrane isometry, likely for aerodynamic requirements. With the growth of the wing in the lateral direction appearing to be more strongly influenced by negative allometry in *A. micronyx*, and for the surface area of the wing to be sustained at near isometry, the legs would need to have a positive allometry. In the tibia of *A. micronyx*, that is exactly what seems to be occurring. The same assumptions can be made for *P. antiquus* except the constraints

would have been for the negative allometry of the surface area with the femur and tibia staying near isometry.

### **Major Delineating Characters between *P. antiquus* and *A. micronyx***

Each of the 14 characters had bivariate plots generated that compared each element and their ln-GM. All 14 plots can be seen in Appendix C. Only four will be discussed here: skull, IVMc, phalanx I, and the tibia (Figure 20). These four plots highlight some of the major differences between the two species. The other ten plots have a large amount of overlap with the two species' slopes and do not reveal differences.

**Skull.** In Figure 20A, the slopes of the wings appear to run nearly parallel with no confidence interval overlap. What is interesting to consider here, when looking for differences between species, is if *A. micronyx* is scaled up in size to match *P. antiquus*, its skull length would still not match the size of *P. antiquus* based on these results. These two species have different constraints for the skull size relative to their overall size. Both show positive allometry in the PCA and linear regression but *A. micronyx* shows much more extreme positive allometry. Despite the allometry, its skull is still relatively smaller than *P. antiquus*.

**IVMc and Phalanx I.** The IVMc is an element of great interest throughout this study. In both animals it is showing drastically different but independently interesting ontogenies. *P. antiquus* has >95 percent isometry, forming modular isometry with the following wing phalanges I and II. *A. micronyx* has a very high positive allometry, the highest of all wing elements among both species. The drastic differences in slopes can be seen in Figure 20B. A similar difference in ontogenies is occurring in phalanx I (Figure

20C). While *P. antiquus* has a slope near 1, *A. micronyx* is still positively allometric with zero overlap in the confidence intervals.

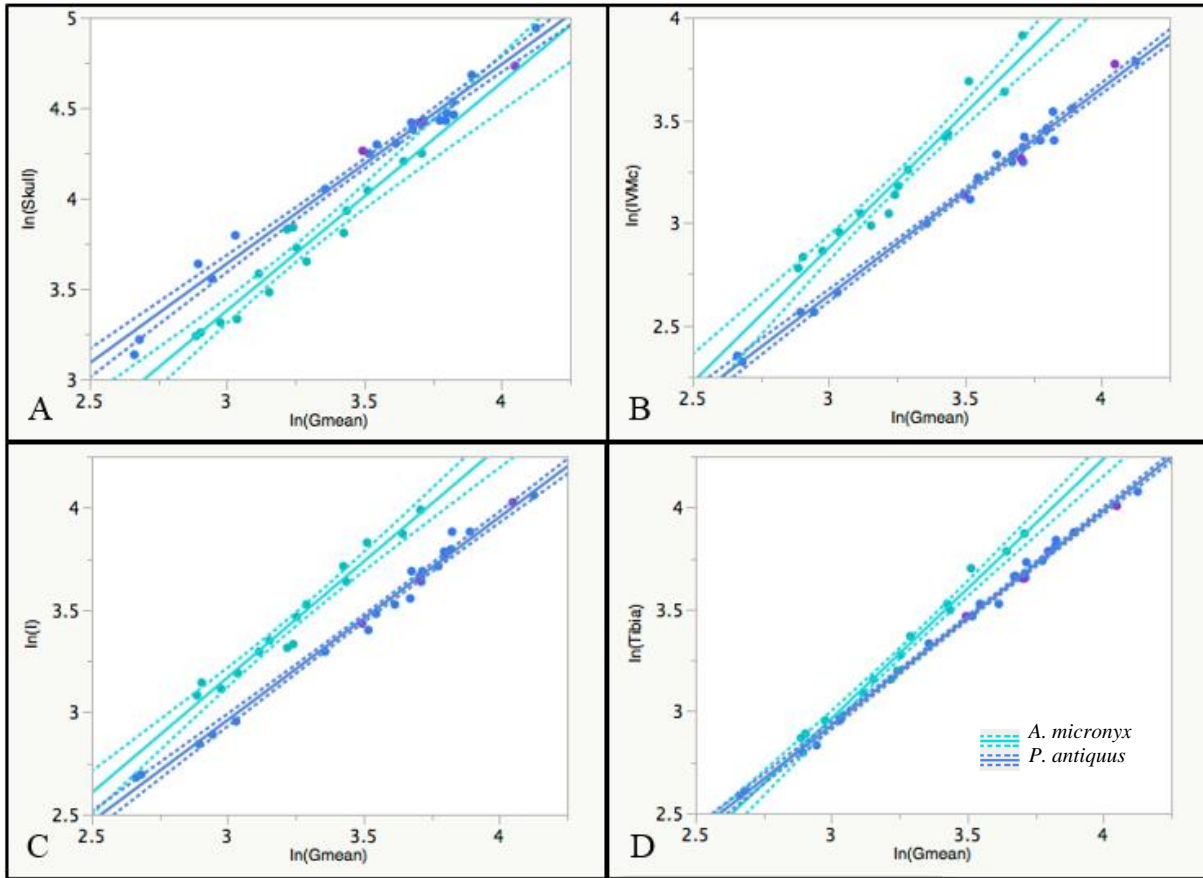


Figure 20 Bivariate Plots of the ln-Skull, ln-IVMc, ln-Phalanx I, & ln-Tibia. *P. antiquus* is plotted alongside *A. micronyx* in each graph A, B, C, and D. **A:** [ $\ln(\text{Skull } P) = 0.335385 + 1.1011493 \ln(\text{GM})$ ]; [ $\ln(\text{Skull } A) = -0.401962 + 1.2603173 \ln(\text{GM})$ ]. **B:** [ $\ln(\text{IVMc } P) = -0.37792 + 1.0080419 \ln(\text{GM})$ ]; [ $\text{IVMc } A = -1.053996 + 1.3106513 \ln(\text{GM})$ ]; **C:** [ $\ln(\text{Phalanx I } P) = -0.012429 + 0.9912597 \ln(\text{GM})$ ]; [ $\ln(\text{Phalanx I } A) = -0.219043 + 1.1296361 \ln(\text{GM})$ ]. **D:** [ $\ln(\text{Tibia } P) = -0.22844 + 1.0528923 \ln(\text{GM})$ ]; [ $\ln(\text{Tibia } A) = -0.854563 + 1.2728348 \ln(\text{GM})$ ]. See Table 2 for additional statistics for each graph.

**Tibia.** When comparing the slopes graphically in Figure 20D, the initial sizes of the tibia were the same sizes. During their ontogenies however, they grew at different trajectories with *P. antiquus* having small positive allometry while *A. micronyx* had very high positive allometry. This extreme positive allometry would not have only effected the brachiopatagium breadth, but also the uropatagium (Figure 16), the membrane between hindlimbs, possibly giving some level of positive allometry to that membrane as well.

## Discussion

It is clear that there are some distinct dissimilarities between *P. antiquus* and *A. micronyx*. Those differences are most noticeable with Figure 18 observing Line P and Line A showing the patterns that can be seen with the wing elements during ontogeny. These lines represent the different ontogenetic patterns among these two species. Along with the different patterns of growth in the distal wing, there are the previously discussed differences in the skull, tibia, and the brachioptagium surface area ontogenies that separate these two species very well. The results show isolated trajectories for the individual elements, observed ontogenetic modular isometry in *P. antiquus*, and isolated ontogenies in the brachioptagium surface area. With these results alone it can be argued further that these are in fact two different groups of pterosaurs. However, the large amount of morphological similarities cannot be ignored. *A. micronyx*' recent placement into *Aurorazhdarcho* (Jouve 2004) was based hastily on a poor analysis. Jouve's work was recently agreed with by Bennett (2013) but contention of its placement remains.

There are two ideas that have been suggested ever since the data for both of these two species was published by Wellnhofer (1970). The first, which has not received much attention, is sexual dimorphism originally suggested by Wellnhofer (1970) and again by Mateer (1976). Recently, however, the second and favored explanation was examined by Bennett (2013) who has strongly suggested that they are not conspecific and *A. micronyx* are likely juveniles of *Gnathosaurus subulatus* (see also Bennett 1996a). This assessment is made despite lacking an associated skull and postcranial skeleton for the *G. subulatus* (only one known specimen) to compare it to *A. micronyx*. It was also in Bennett's 2013 article that he reaffirmed *A. micronyx* to the genus *Aurorazhdarcho* from the genus

*Pterodactylus* after Jouve (2004) reassigned them. Bennett gave new diagnoses believing characters 1,3-6, 10 would not be present in larger individuals (more mature) and did little to little to distinguish them from other Solnhofen pterodactyloids (See Bennett 2013 for details of new descriptions). Due to larger individuals of *A. micronyx* not available, it is difficult to justify whether they are two species. With lacking evidence conclusively justifying *A. micronyx* to another genus or otherwise, other ideas still have merit. With distinct differences between the two species statistically observable, summarized in Figure 21, their allometries could be used for this conclusion. However, determining whether differences among two closely morphological and temporal species are due to speciation or sexual dimorphism is difficult.

### **Interspecific Comparative Wing Reconstructions**

There are, however, some interesting conclusions that can be assessed from some of the layered reconstructions of their wings. These differences can be, in part, interpreted as sexual dimorphic constraints. The largest of each species used in this comparative analysis (RM St. 18184 = *P. antiquus* (dark blue) (PCRW length = 90mm); CM 11426 = *A. micronyx* (light blue)(PCRW length = 58mm) were layered and scaled to size with the distance from the shoulder to the knee (Figure 22). Despite *P. antiquus* being known to be a larger animal, *A. micronyx* has a relatively larger wing span and wing breadth. The wing reconstructions have a straight trailing edge from the ankle to the wing-distal tip for simplicity; the reason for this is explained in detail in the Methods. It is odd that there would be such a relationship between *P. antiquus* and *A. micronyx*. They could have evolved their unique wing ontogenies separately or, if conspecific, evolved intraspecifically meeting differential sexually dimorphic constraints in the distal wing elements. The proposed sexually dimorphic constraints, themselves, required negative allometry in the membrane of *P. antiquus* and isometry in *A. micronyx*. This suggestion is based on

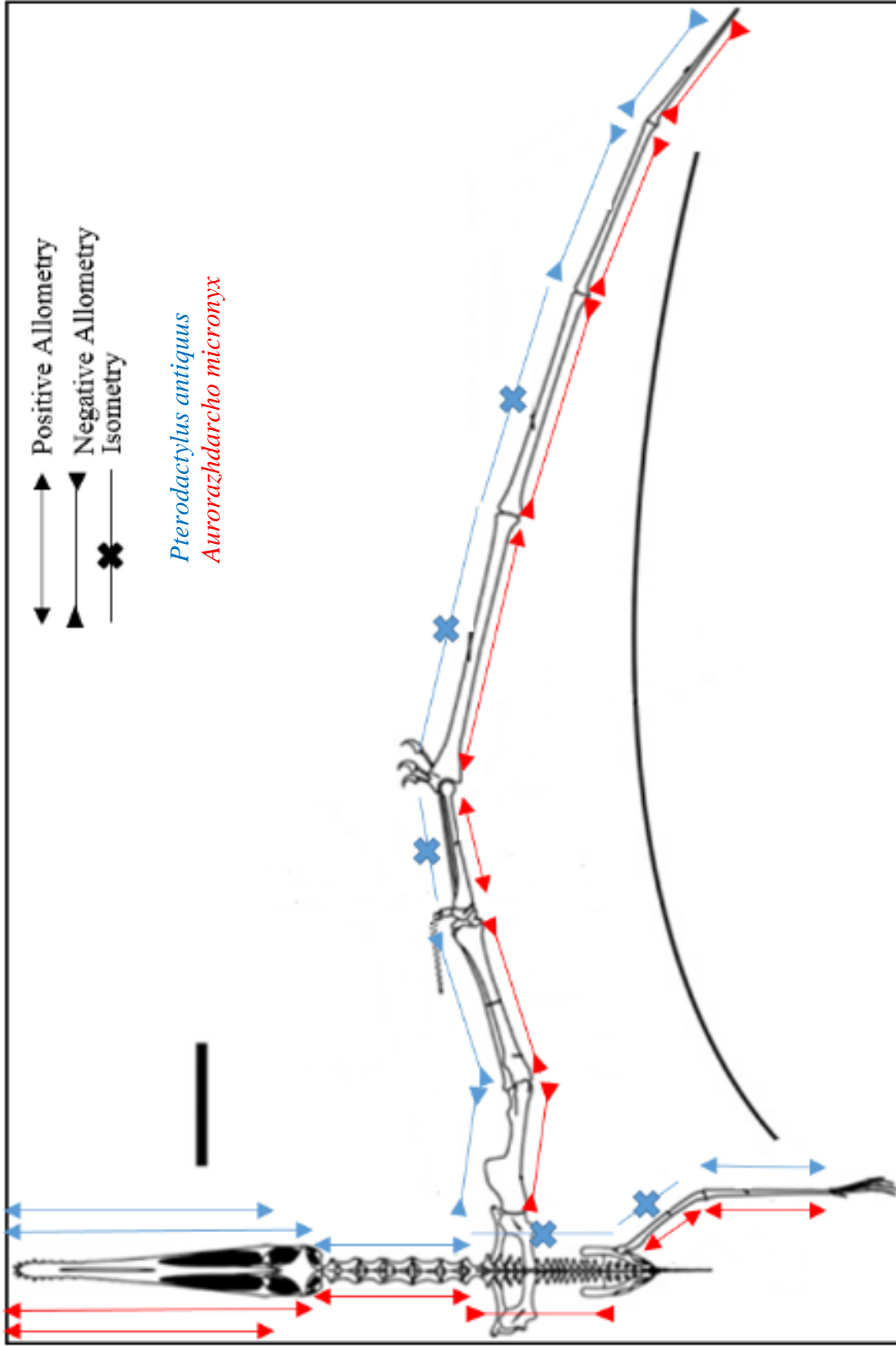


Figure 21 Allometry Summary Schematic. *P. antiquus* in blue and *A. micronyx* in red, positive/negative allometries and isometries are shown side-by-side to show the differences in growth rates in the wing elements between the two species. Despite these differences, both species show similar surface area results with *P. antiquus* having a slightly negative allometry ( $<0.05$ ) in its wing-membrane SA and *A. micronyx* having an isometric growth ( $>0.05$ ) in the wing-membrane SA. Note: *P. antiquus* shows isometry in PCRW but above the alpha value  $>0.05$ . General depiction of a derived pterosaur. Scale bar = 200mm.

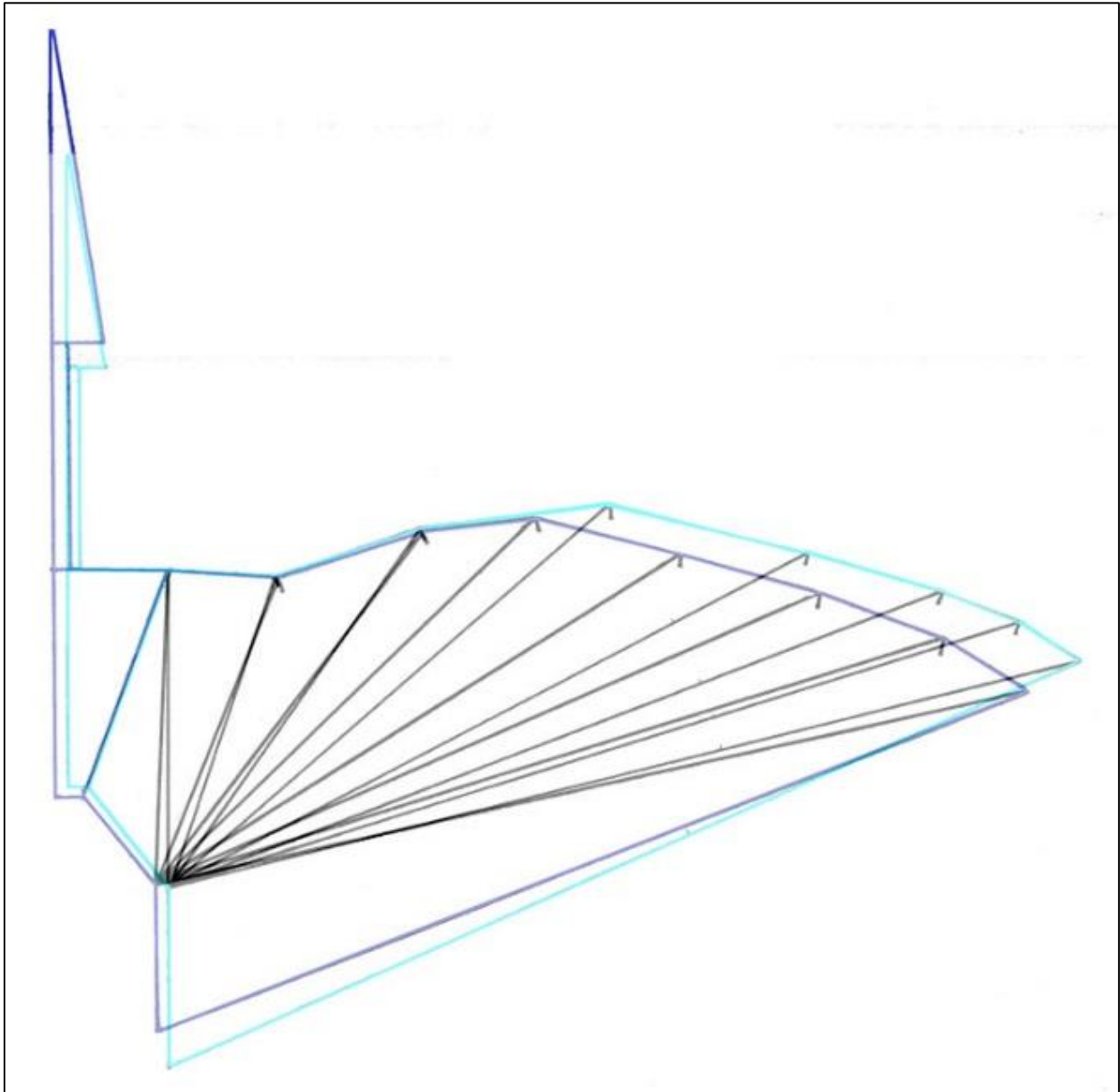


Figure 22 Interspecific Wing Comparisons. Largest adult *P. antiquus* is dark blue; Largest *A. micronyx* is light blue. Scaled with the breadth of the wing from the shoulder joint to the knee joint length so the relative sizes of the wing length and wing-membrane surface area can be seen. Shown here are adults of both species depicting the variation in size of the wing-membrane surface area. Although *P. antiquus* is a larger animal on average, *A. micronyx*'s wing surface area is larger giving it better lift and thrust potential. Its large positive allometric tibia also plays a part in the larger wing surface area giving it more breadth overall.



research on sexual dimorphism in the wings of other flying animals with the female having a relatively larger wing surface area than the male (Camargo and Oliveira 2012; Camargo, Camargo, Corrêa, Camargo, and Diniz 2015). That research suggests that since the female needed more carrying capacity for flight due to increased load during reproduction, they had larger relative surface areas than the males, who could afford less surface area in the wings. These relative sizes would imply that *P. antiquus* would have been male and *A. micronyx* would be female.

### **Intraspecific Comparative Wing Reconstructions**

*Pterodactylus antiquus*. The largest *P. antiquus* (RM St. 18184 (dark blue) (PCRW length = 90mm) is layered with the smallest (BSP 1967 I 276 (red)(PCRW = 20mm) in Figure 23. The negative allometry in the wing surface area calculated in the linear regression  $1.85 \pm 0.066$  (Table 2) can be schematically observed (Figure 23). When scaled for distance between the shoulder and knee, the smaller specimen (red) has a larger surface area relative to body size compared to the largest (dark blue). This visually suggests that as *P. antiquus* individuals grew, their wing surface area was growing slower than their overall size. The only positive allometry associated with the brachiopatagium is in the tibia. The small degree of positive allometry associated with tibia does not seem to have increased the breadth any noticeable amount (Figure 23).

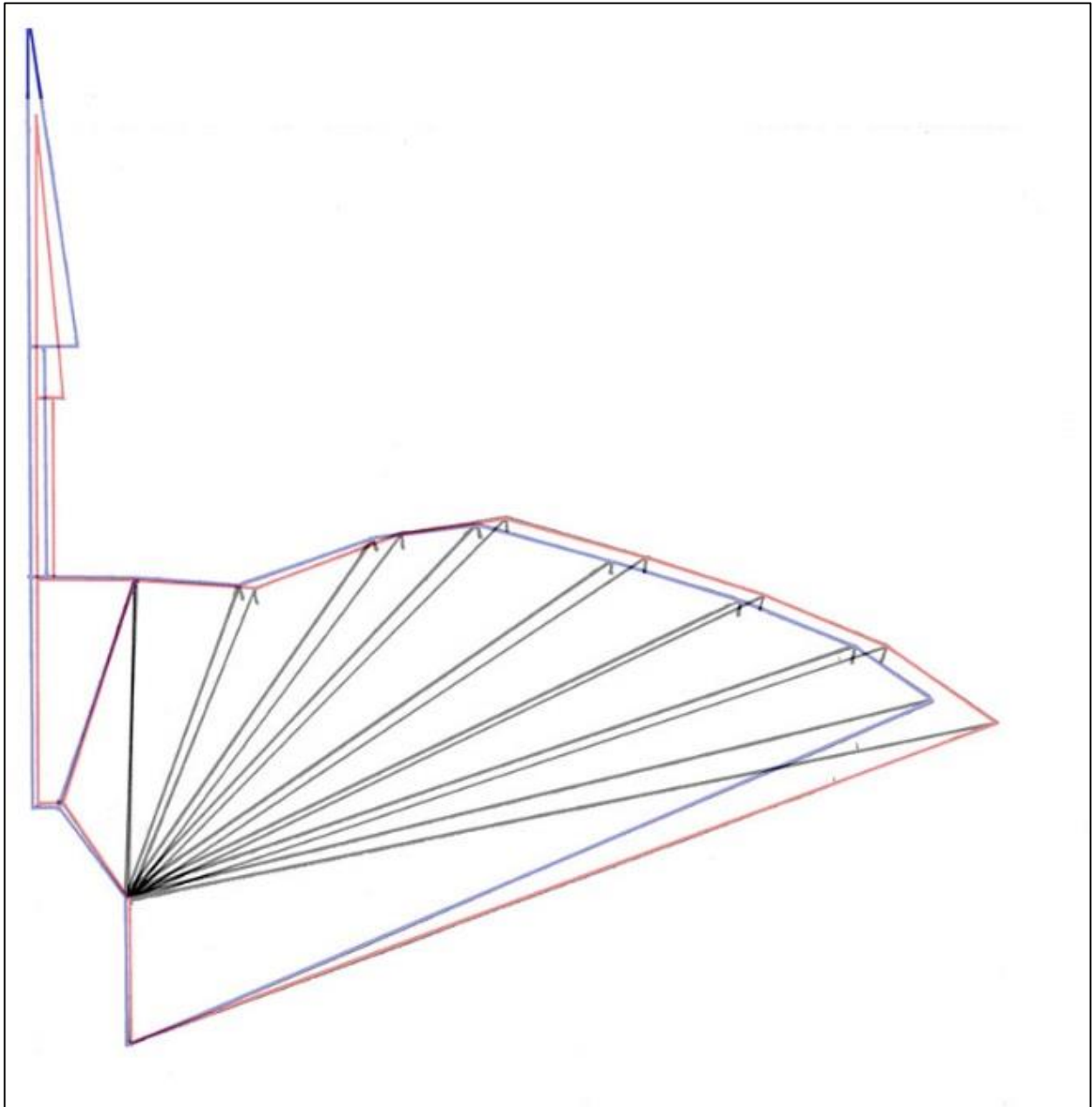


Figure 23 Intraspecific Wing Comparisons: *Pterodactylus antiquus*. Largest adult *P. antiquus* is dark blue; smallest juvenile *P. antiquus* is red. Scaled with the breadth of the wing from the shoulder joint to the knee joint length so the relative sizes of the wing length and wing-membrane surface area can be seen. *P. antiquus* has a negatively allometric wing surface area (1.856, <0.05) that scaled adult and juvenile schematics also show. It is clear here that the wingspan and wing-membrane surface area gets smaller as the animal ages.

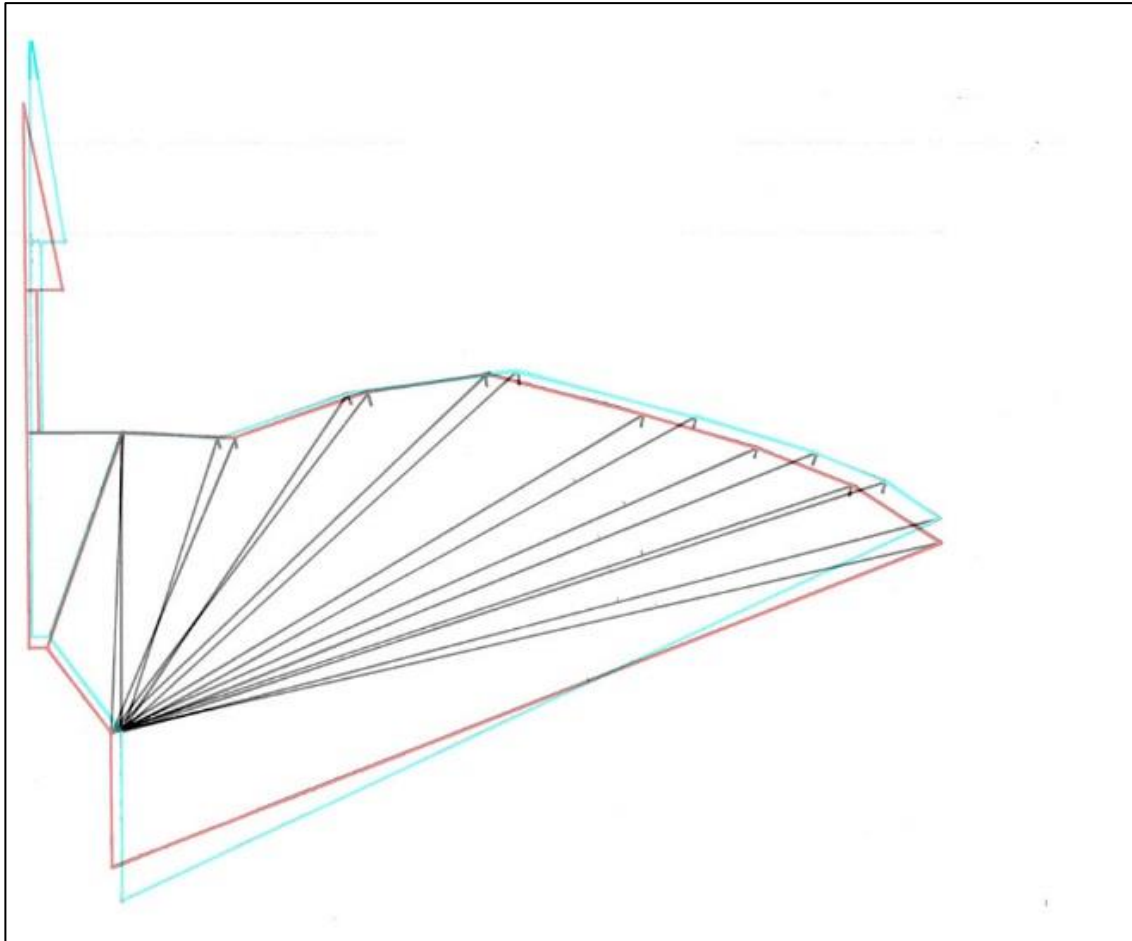


Figure 24 Intraspecific Wing Comparisons: *Aurorazhdarcho micronyx*. Largest *A. micronyx* is light blue; smallest *A. micronyx* is red. Scaled with the breadth of the wing from the shoulder joint to the knee joint length so the relative sizes of the wing length and wing-membrane SA can be seen. *Aurorazhdarcho* has an isometric wing surface area (2.010, >0.05). The scaled juveniles, the largest and smallest in this analysis, also show the apparent isometry in the schematics. This preliminary study shows that the wingspan and wing-membrane surface area stay nearly the same size as the species ages.

*Aurorazhdarcho micronyx*. The largest *A. micronyx* (CM 11426 (light blue)(PCRW length = 58mm) specimen layered over the smallest (BSP 1936 I 50 (red)(PCRW length = 28mm) is seen in Figure 24. Just as with the negatively allometric slope of *P. antiquus*, the isometric slope of *A. micronyx* ( $2.010 \pm 0.110$ ) is observed schematically. The effects of the high positive allometry in the IVMc, and scaled decreasing slope size into negative allometry, are observed with the change in wing shape from the smallest to the largest specimens. The effects of the tibia on the breadth of the brachioptagium are visible in Figure 24. The larger of the *A. micronyx* specimens in Figure 24 is more than twice the size of the smaller. Although all *A. micronyx* specimens known are considered immature, the animal more than doubles in size and maintains nearly isometric growth in its wing surface area with a large amount of differential growth in all of its wing elements including the tibia.

### **Possible Effects of Pneumatization on Allometry**

A well-studied plesiomorphic character of pterosaurs is the pneumaticity in their skeleton. However, the degree of pneumaticity in both species studied here is unknown and unstudied. They would have certainly had at least some in the skull and cervical vertebrae that is found in early, more basal, pterosaurs (Bonde and Christiansen 2003; Butler, Barrett, and Gower 2009). More derived and larger species of pterosaurs have been studied showing that the level of pneumatization increases into the dorsal/sacral vertebrae, limb bones, pectoral girdle, and elements of the hindlimbs (Claessens et al. 2009; Elgin and Hone 2013). *P. antiquus* and *A. micronyx* were both early derived pterosaurs of the late Jurassic and likely did not have as advanced levels of pneumatization as the later derived species in the Cretaceous. Their levels of pneumatization and small size, reaching just over a meter in wing span in both species, may have been what allowed them to get away with their respective ontogenies in their skeletal elements

without increasing in relative brachiopatagium surface area. The ballooning effect of pneumatization distributes bone mass to the proximal and distal tips, increasing in length limb bones and volume while increasing minimally in mass is an interesting characteristic in pterosaurs that may have led to very unique allometries in many other derived pterosaur species (Wedel 2005; Witton 2008a; Elgin and Hone 2013).

## **Conclusion**

### **Ontogeny and Sexual Dimorphism**

*Pterodactylus antiquus*. This species displays ontogenetic modular isometry in the consecutive distal wing elements: IVMc, Phalanx I, and Phalanx II. Additionally, the femur revealed strong isometry in the hindlimb (Figure 21). All four of these elements have >95 percent confidence (Table 2). It is important to note that none of the wing elements in *P. antiquus* had any level of positive allometry in the PCA and bivariate linear regression analyses. The wing reconstructions of the brachiopatagium surface area calculate for a negative allometry in this species and may suggest a possible sexual dimorphic relationship with *A. micronyx*. The results found here are unexpected and on all accounts for this species, rejects the null hypothesis with the expectation of positive allometry in the wing elements.

*Aurorazhdarcho micronyx*. The characteristic reverse down-stepping allometry in its distal wing elements is the most extreme difference between these two species (Figure 18, Line A). With the IVMc, there is high positive allometry. The consecutive phalanges (I-IV) decrease in slope and coefficient size distally reaching high negative allometry. The tibia has a high positive allometry compared to *P. antiquus*, representing a major delineation among the species and has observable effects on the breadth of *A. micronyx* brachiopatagium. The wing reconstructions of the brachiopatagium surface area calculations revealed near isometric

ontogenetic growth. With the results of the allometries of the wing and leg elements, heavy evolutionary constraint on these skeletal components was occurring to maintain the brachiopatagium ontogenic surface area isometry. Apart from the IVMc, phalanx I, and tibia, all other elements and surface area analysis reject the null hypothesis of expected positive allometry throughout the pterosaur anatomy.

This study reveals that pterosaurs had an even more complex evolution than previously known. Holding to the claim that they are different species, it is clear that *P. antiquus* and *A. micronyx* require further investigation in light of the dramatic difference in ontogeny within their distal wing elements and brachiopatagium ontogenies. The approach Bennett had for *Pteranodon* when analyzing sexual dimorphism was measuring the dimensions of the pelvic girdle (1992). Further analysis would involve adding pelvic data of both species to the analysis. Bennett found ‘male’ specimens had narrower widths than the ‘females’ who had wider widths. This concept makes logical sense because pterosaurs are known to be oviparous (Ji, Ji, and Cheng 2004; Lü et al. 2011; Wang et al. 2014). Another issue to be investigated is how *P. antiquus* and *A. micronyx* brachiopatagiums surface areas were able to remain isometric during growth. Although no conclusions can be made whether these two species are conspecific displaying sexual dimorphism or speciation as a result of niching, novel observations of the complexity of pterosaur evolution and ontogeny are observed.

## CHAPTER THREE

### ***PTERANODON* AND SEXUAL DIMORPHISM IN WING SHAPE AND SURFACE AREAS OF PTEROSAURS, BATS, AND MOTHS**

#### **Introduction**

One of the difficulties of the fossil record is the lack of soft tissue and the important distinctions between not only species but of males and females within a species. It is well understood that the vast variations found in individuals within a species have an important role in the process of natural selection acting within a species, on the individuals. It is also well understood that the large variations, not only in size, but other attributes among males and females within a species, are the result of intraspecific selection (Huxley 1860). These ideas are the focus of this chapter and the conclusion of this thesis for *Pterodactylus antiquus* and *Aurorazhdarcho micronyx*.

Despite any large abundance of soft tissue in pterosaur fossils, it's still possible to observe sexual dimorphism in a species using the fossilized bones themselves. However, this requires a high number of not just fossil elements, but a high number of relatively complete individuals preserved of the same species. Fortunately, a high number of nearly complete specimens of *P. antiquus* and *A. micronyx* are known (Wellnhofer 1970).

#### **Review of Chapter Two Results**

Chapter two analyzed the ln-longitudinal data measurements of those species using Principle Component Analysis (PCA) and ran a bivariate linear regression with each of the 14 measurements against the ln-geometric mean (ln-GM) serving as the independent variable. The results of that analysis shows two distinct ontogenetic patterns between the two closely related species, particularly in the distal wing elements. Finally,

because of those differences, each of the 24 *P. antiquus* and 15 *A. micronyx* wings were reconstructed schematically and their surface areas calculated using hand measurements.

An unexpected and interesting result of this was found when the larger of the two species was scaled (from shoulder to knee) and over-lapped (Figure 22: Chapter 2).

Although *P. antiquus* is a larger on average species, *A. micronyx* had a relatively larger wing length and surface area. Similarly, the largest and smallest wing schematics of each species was over-lapped (Figure 23 & 24: Chapter 2) and revealed negative allometry in the growth of *P. antiquus* wing surface area and isometry in the surface area of *A. micronyx*. If these two species were one and the same species, conspecific, it's logical that the male, who is not carrying an extra load such as eggs, would be able to grow into relatively smaller wings. This would imply *P. antiquus* as the proposed male. The female, *A. micronyx*, would require isometry or positive allometry to maintain flight while eggs were developing. The scaled schematics of the largest specimens of both species show a relatively larger wing in *A. micronyx* than *P. antiquus*. For an oviparous flying animal, this makes biologically adaptive sense. So the variation in ontogeny of the wing bone elements would then be expected between males and females.

### **Experimental Design**

One method to test this idea is to look at the data of another species of pterosaur who has had sexual dimorphism already established in another way. Luckily, there is one: *Pteranodon longiceps*. Of the estimated 5,500 fossil fragments of pterosaurs, there are approximately 1,100 individuals of *P. longiceps* identified, by far the most of any species (Miller 1971; Bennett 1992). The issue of course is the lack of completeness of nearly every individual. Bennett has made a career out of analyzing the huge abundance of



*Pteranodon* specimens and fragments (Bennett 1990; 1992; 1993; 2001a; 2001b). His research has clearly established sexual dimorphism in *P. longiceps* using bimodal distributions of various measurements, the clear distinction in crest sizes in the two groups with smaller crests in females and larger in males, and the relative dimensions of the pelvises in the two groups with wider dimensions in females and narrower in males (Bennett 1992; 2001a; 2001b). Using the results and interpretations of Chapter 2, the abundant data of *Pteranodon* longitudinal data measurements can be used to look for allometry in particular elements of interest with expectations derived from Chapter 2 results. This would indirectly show allometry outside of a PCA which requires abundant complete specimens.

In both *P. antiquus* and *A. micronyx* the femur had isometric growth during its ontogeny. Since a geometric mean (an isometric indicator) cannot be calculated for *Pteranodon*, the femur is the best independent variable that can be ideally used against the other variables of *Pteranodon* when interpreting allometry because in both *P. antiquus* and *A. micronyx*, the femur was or very near isometry (Chapter 2: Table 2). It is obvious the issue this may bring knowing the distance in relation of *P. antiquus*/*A. micronyx* and *P. longiceps*. They belong to different superfamilies, ctenochasmatoidea and ornithocheiroidea, respectively. The species are separated by ~65 million years, the same length of time from when the dinosaurs and pterosaurs went extinct to the present. This means using the femur in *Pteranodon* as a proxy for size will have its errors, but until there is an abundant amount of *P. longiceps* specimens with near completeness, those errors cannot be investigated and the assessment for the use of the femur as a size proxy will be assumed.

The wing element with the highest degree of variability among *P. antiquus* and *A. micronyx* is the 4<sup>th</sup> metacarpal (IVMc)(Figure 3 & 4: Chapter 2). **For the hypothesis that *P. antiquus* and *A. micronyx* are male and female there should be a strong bimodal distribution among the males and females of *Pteranodon longiceps*. Additionally, the relationship between the femur and IVMc in *Pteranodon* should show either isometry in females and negative allometry in males. Alternatively, because of their enormous size compared to *P. antiquus* and *A. micronyx*, positive allometry may be more extreme in female *Pteranodon*.** While *P. antiquus*' and *A. micronyx*' small size would allow them to grow relatively isometric wing surface areas, *Pteranodon* is well known for its large size with the largest wingspan reaching ~seven meters (*P. antiquus* and *A. micronyx* both had ~1 meter wingspans) and may need to have had positive allometry in the wing surface area in order to maintain proper lift and thrust ability. This increase is due to the cubic increase in volume (affecting mass as well) compared to squared increase in wing surface area.

### **Wing Shape in Other Species**

There is another group of flying animals that have had a similar wing shape analysis, the moth species in the family sphingidae (Camargo et al 2015). Seven species' wings, of which they have two sets, fore- and hindwings, were analyzed using geometric morphometrics. In the study all the species' females had larger wing surface areas than the males (Figure 25)(Camargo et al 2015). This study also argues that this observation in females is due to the need to reduce the wing loading for reproductive mass increase. Although two sets of wings is quite different to pterosaurs, the same effect of selection appears to occur across several animal phylums.

Specific adaptations of wing shape, total surface area, and even increase of surface areas of particular regions of wings are also seen in bats (Camargo and Oliveira 2012). In Chapter 2 of this study it was found that *Aurorazhdarcho micronyx* had a relatively larger wing (length and width) and surface area compared to *Pterodactylus antiquus*. The proposal in Chapter 2 and 3 is that these two species of pterosaurs are conspecific and represent male and female, *P. antiquus* and *A. micronyx*,

respectively. A major factor in this argument is the analogous nature of similar relative wing size and shape of male and females of other and very distant related flying species. A study on the bat species *Sturnira lilium* used geometric morphometrics to study the shape and surface area of 30 males and 42 females (Camargo and Oliveira

2012). Before this, no intraspecific study had been done with the wing shape of bats. The

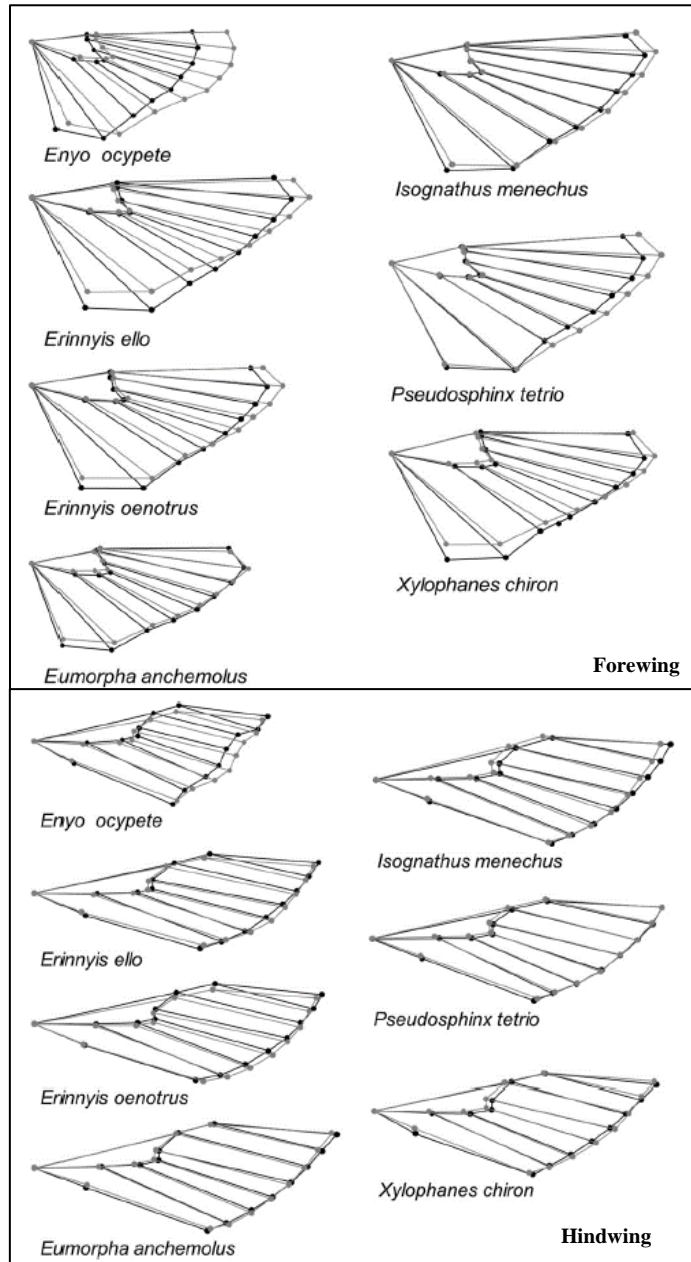


Figure 25 Sexual Dimorphism in Moth Wings. Canonical Variates (CV) analysis of seven Sphingidae species of moths, forewings and hindwings. Black represents males, gray represents females. As in the bat wing analysis. Camargo et al 2015

results of this study found that females had larger surface areas than males (Figure 3). More so, the wing lengths and breadths were also longer. Aspect ratios of wings affect flight speed and in-flight maneuverability, with one counter-acting the other. A high aspect ratio involves a long wingspan with a shorter breadth giving it high speed but lower in-flight maneuverability. High aspect is relative to a low aspect ratio with shorter wingspans and longer breadth giving it less speed and better in-flight maneuverability (Clancy 1975). In the Camargo and Oliveira 2012 paper, they argue that the larger

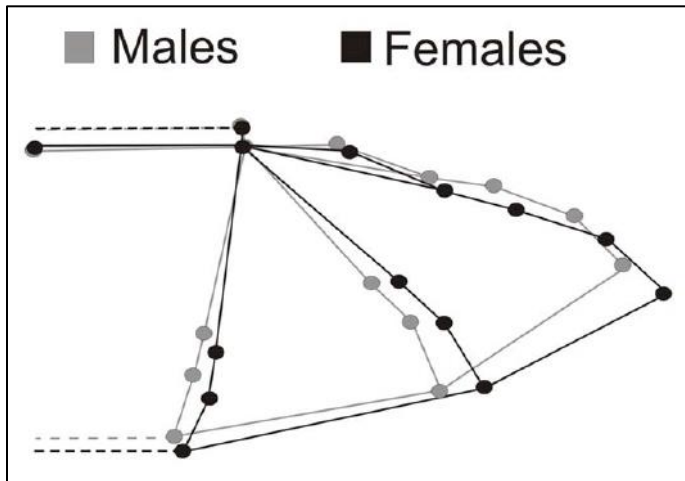


Figure 26 Sexual Dimorphism in Bat Wings. In the study by Camargo and Oliveira 2012, this is the results of the Canonical Variate (CV) analysis of wing shape variables of males and females of the bat species *Sturnia lilium*. These results are significant to the surface area analysis of *Pterodactylus antiquus* and *Aurorazhdarcho micronyx* because it shows a very similar pattern with male and female wing shape and relative size. Bats are the closest analogs to pterosaur in regards to their wings. The similar pattern suggests the same evolutionary constraints for females and males of bats and the small derived pterosaurs, *P. antiquus* and *A. micronyx* which are argued to be conspecific here, male and female, respectively.

wingspan is selected due to the increased weight they carry during pregnancy. With the increased surface areas, the wing loading (weight distribution per squared area of the wing) would be lower (Clancy 1975). A larger surface area would let them carry the extra weight and still maintain proper lift and thrust for flight. This trait is analogous to the relationship observed in the wing layered schematics in Figures 17 and 18 in Chapter 2. They also suggest, as an alternative hypothesis, that the differences in the male and female wing shapes are related to their different diet and life styles. Male *Sturnira lilium* bats have a shorter wingspan and shorter wing breadth while females had longer wingspans and longer wing breadths. What is likely occurring here is both the female's wing loading and the differential lifestyles/diets are affecting their wing shapes via the

limb and manus elements. These interpretations of extant flying animals with analogous wing structures and membranes shed light on and credit the proposal sexual dimorphism between these two species of pterosaurs suggested here to be sexual dimorphs.

## **Materials and Methods**

All of the data used in the *Pteranodon* analysis done here was taken directly from the data table published in Bennett's 2001b article. Despite the large abundance of *P. longiceps* specimens only about 450 were used in his study of the species. Further, just a fragment of those specimens were able to be used in this study. Of the 450 specimens there were sixty-four 4<sup>th</sup> metacarpal (IVMc) length measurements (Table 4). The frequency distribution of those 64 IVMc lengths are shown in Figure 27. An even smaller amount of specimens (n = 17) (Table 5) were used to produce the bivariate plot with the femur data (independent variable) and the IVMc data (dependent variable) using the femur as a proxy for size, an isometric indicator to determine the level of allometry in the IVMc of *Pteranodon longiceps* (Figure 2). A Mac OS X version 10.6.8 ran Jmp software version 6.0.3 for all analyses.

A frequency distribution of the IVMc data was generated to show the bimodal distribution of the element in *Pteranodon longiceps*. It is known, as discussed in the Introduction, that there is sexual dimorphism within this species. So there should be two size classes within the data. The second was a bivariate linear regression of the ln-femur and the ln-IVMc associated data with the ln-femur serving as the independent variable and a size proxy. Finally, the *Pteranodon longiceps*, *P. antiquus*, and *A. micronyx* data was pooled and a phylogenetic trend-line was calculated to show the change in the relationship of the femur and IVMc among these three species.

<i>P. longiceps</i>	mm	Total=64	
Specimen	4th Mc	Specimen	4th Mc
ANMH 4908	294	UM 12404 "A"	408
YPM 1181	295	YPM 1160	410
YPM 2345	308	YPM 2712	412
YPM 2490	308	YPM 2799	412
UALVP 24239	315	LACM 51136	414
MCZ 3815 "A"	333	UM 12401	414
MCZ 3815	336	YPM 2480	419
BMNH 4006	340	FHSM 4526	427
FMNH PR 494	349	YPM 2560	428
KUVP 975	350	FHSM 2120	459
FHSM 2119	352	ROM 26105	484
BMNH 3299	361	AMNH 6158	510
CM 11400	361	YPM 2493	517
YPM 2425	365	NMC 8167	535
UUPI R.197	366	YPM 2452	543
KUVP 977	370	BMNH 2959	552.5
BMNH4542	373	CM 11416	561
YPM 2733	374	YPM 2834	568
YPM 2520	381	YPM 2414	570
YPM 2451	382	KUVP 967	572
CM 1539	384	CM "UNC C"	575
KUVP 85460	386	KUVP 1952	578
YPM 2472	388	FHSM 184	583
USNM 12167	388.5	KUVP 961	589
UM 12404 "B"	389	KUVP "UNC A"	589
LACM "UNC A"	391	YPM 2473	599
KUVP 954	394	YPM 2734	601
LACM 50926	394	YPM 2833	601
YPM 2767	399	BHI "UNC E"	613
YPM 42819	400	SMNS "UNC A"	614
CU 45062	400	USNM 6075	617
UALVP 24238	405	UNSM 50130	620

Table 4 *Pteranodon* IVMc lengths. The 64 *Pteranodon* specimens used in this study from Bennett's 2001b sexual dimorphic analysis.

n=17, mm

<i>P. longiceps</i>	Femur	IVMc	ln(Femur)	ln(IVMc)
AMNH 4908	139	294	4.93447393	5.68357977
AMNH 6158	250	510	5.52146092	6.23441073
BMNH 3299	165	361	5.10594547	5.88887796
BMNH 4006	158	340	5.06259503	5.82894562
CM 11400	168	361	5.12396398	5.88887796
CU 45062	158.5	400	5.06575459	5.99146455
FHSM 184	278	583	5.62762111	6.36818719
KUVP 967	255	572	5.54126355	6.34913899
LACM 50926	186.5	394	5.22843124	5.97635091
MCZ 3815	168	336	5.12396398	5.81711116
ROM 26105	222	484	5.40267738	6.18208491
UALVP 24238	187.5	405	5.23377885	6.00388707
UM 12404 "A"	176	408	5.170484	6.01126717
UUPI R.197	170.5	366	5.1387353	5.90263333
YPM 2451	154	382	5.0369526	5.94542061
YPM 2493	193	517	5.26269019	6.24804287
YPM 2767	178	399	5.18178355	5.98896142

Table 5 *Pteranodon* Associated Femur and IVMc lengths. The 17 length measurements of the *Pteranodon* specimens from Bennett's 2001b analysis that had both a femur and IVMc preserved. Those measurements were then logged and plotted (Figure 28).

## Results

The frequency distribution seen in Figure 27 clearly shows a strong bimodal distribution in the IVMc *P. longiceps* data. This observation corresponds with Bennett's

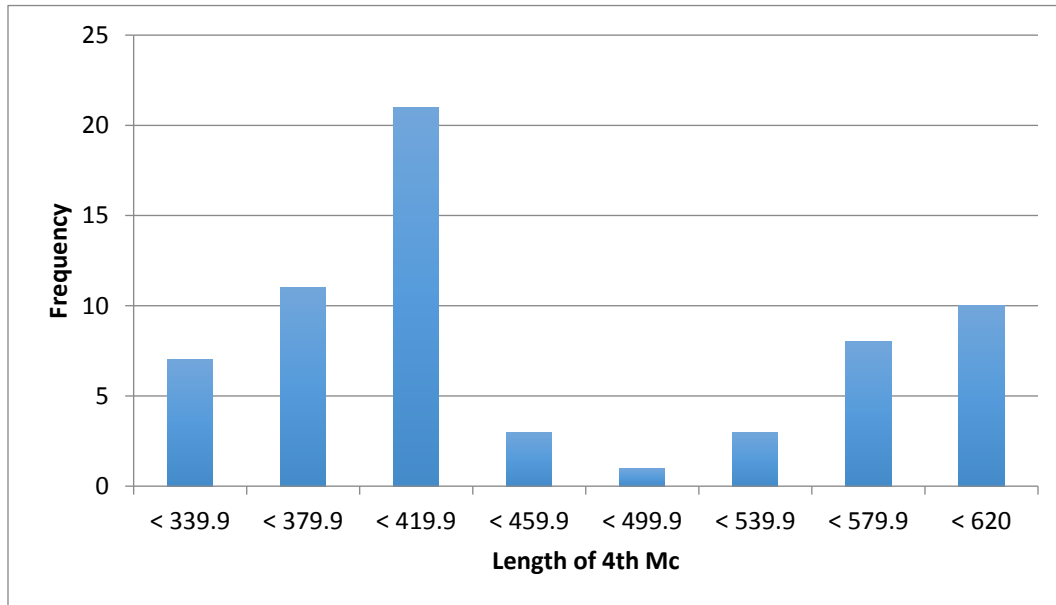


Figure 27 The frequency distribution of the 64 *Pteranodon* IVMc length measurements. A bimodal distribution is present as expected for a species with known sexual dimorphism (Bennett 1992; 2001a; 2001b).

findings in his sexual dimorphism research. It suggests a clear size range for males and females of *Pteranodon* within the data used here (Bennett 2001b). Associating this bimodal distribution with sexual dimorphism can only be applied to *Pteranodon* because of the other characters in that taxa that have been found to correspond with extant animals. Those same characters cannot be investigated with *P. antiquus* or *A. micronyx* because there are too few in specimen count. However, comparing statistical patterns with bivariate linear regressions may reveal similarities.

### Bivariate Linear Regression

Figure 28 shows the bivariate plot of the ln-femur and ln-IVMc data for *Pteranodon*. All of data has the linear equation  $[y = 0.9206x + 1.2117]$  with an  $R^2 = 0.8459$ . Initial observations do not show any clear delineations of two groups in the data.

This is either due to the small sample set ( $n = 17$ ) or there is not clear distinction in the population of the species. The three individuals of interest in Figure 28 are red and appear to be outliers in the data. They also seem to form a straight trajectory; however, being only three data points, any real conclusion is only speculation. These three specimens and their apparent trajectory would form a higher slope, thus, larger positive allometry than the other 14 specimens that otherwise appear to follow the regression line in Figure 28. What can be observed is that there is no positive allometry or isometry of the IVMc in this sample of *Pteranodon* individuals. With Bennett's 1992, 2001a, 2001b findings and conclusions of sexual dimorphism in mind, these 17 specimens have no associated skull or a preserved pelvis to make any clear distinction which specimens are male and female using his accepted features of sex.

The other noticeable two groups have a blue and green ellipsoid around them and appear to be separated by a large gap either in the data, or it represents the boundaries of two possible size classes of *Pteranodon longiceps*. With 17 specimens with associated femur and IVMc, no discernable patterns can be interpreted from this data set.

## **Discussion**

The small sample size available (with both a femur and IVMc) in the data presented in Bennett's 2001b does not give us any clear distinctions between possible allometry trajectories for males and females in the bivariate plot (Figure 28). That portion of the hypothesis presented here remains inconclusive. Further digging into *Pteranodon* collections may reveal additional specimens that can be included in this analysis to better reveal what is occurring intraspecifically. What is conclusive is the negative allometry of the IVMc compared to the femur. We see that when *P. antiquus*



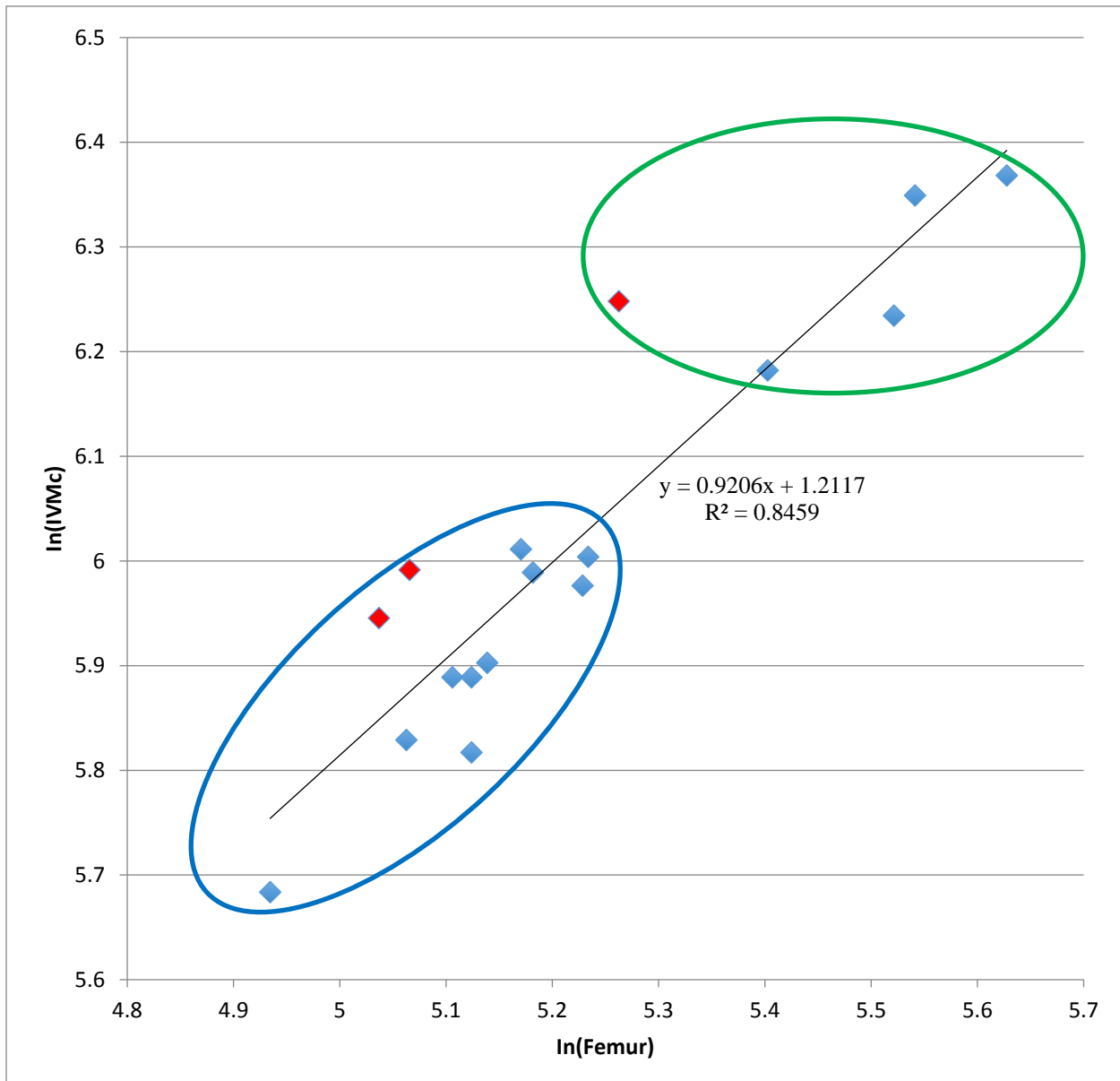


Figure 28 Bivariate Linear Regression of *Pteranodon* ln-Geometric vs ln-IVMc. With a slope  $< 1$ , it reveals, in this sample of *Pteranodon*, that the IVMc is growing slower than the femur. In this study the femur is used as an isometric growth proxy and would then suggest that the IVMc has negative allometry relative to the femur. The three red diamonds appear to be outliers and are suggested to be females of this sample. These are likely females because the conclusions of Chapter 2 have females with larger positive allometry in the IVMc. The occasional increased mass in females during pregnancy requires larger carrying capacity during flight, thus, larger wings would be needed relative to size. Blue and green ellipsoids represent possible size classes. Data from Bennett 2001b. Red dashed line represents a slope of  $= 1$ .

and *A. micronyx* are plotted together the slope drops to 0.945 (Figure 29). When plotted separate *P. antiquus* has a slope of 1.004 and *A. micronyx* has a slope of 1.119. The same net effect may be occurring with the combined male and female *Pteranodon*, but without

being able to conclusively assign male and female to these 17 specimens we cannot test this.

### **Bivariate Linear Regression of *Pteranodon* and Pooled *P. antiquus*/*A. micronyx***

The three dark green diamonds in Figures 29 and 30 (red diamonds in Figure 28) are visual outliers relative to the other 14 specimens and fit the pattern seen between *P. antiquus* and *A. micronyx* as separate groups/trajectories. *Pteranodon* in particular would have had perhaps some of the most extreme selection for lengthening of the wingspan enhancing its soaring ability, which it is thought to have been the most well adapted for during flight (Witton and Habib 2010).

The sexual dimorphism found between *P. antiquus* and *A. micronyx* compared with the *Pteranodon* data reveals the pattern of a larger IVMc in *A. micronyx* relative to *P. antiquus*. This figure treats *P. antiquus* and *A. micronyx* as one data set (Figure 29 & 30). The slope of *P. antiquus*/*A. micronyx* ( $0.9445 \pm 0.116$ ) is nearly parallel with the slope of *Pteranodon* ( $0.9206 \pm 0.202$ ). These seemingly similar patterns are interesting and suggest that a similar ontogeny is occurring between the two species' femur and IVMc despite the large gap in relative sizes of *P. antiquus*/*A. micronyx* and *Pteranodon* indicated by the larger y-intercept of *Pteranodon*, which is a result of their massive size difference. Another characteristic that appears is the linear regression dividing both 'species' within their data-point cluster. The proposed females, *A. micronyx*, are above the plotted regression line due to their relatively larger IVMc with the proposed males, *P. antiquus*. The same characteristic of the linear regression appears to occur in *Pteranodon*. The individuals with relatively larger IVMc's, three in particular (dark green diamonds)

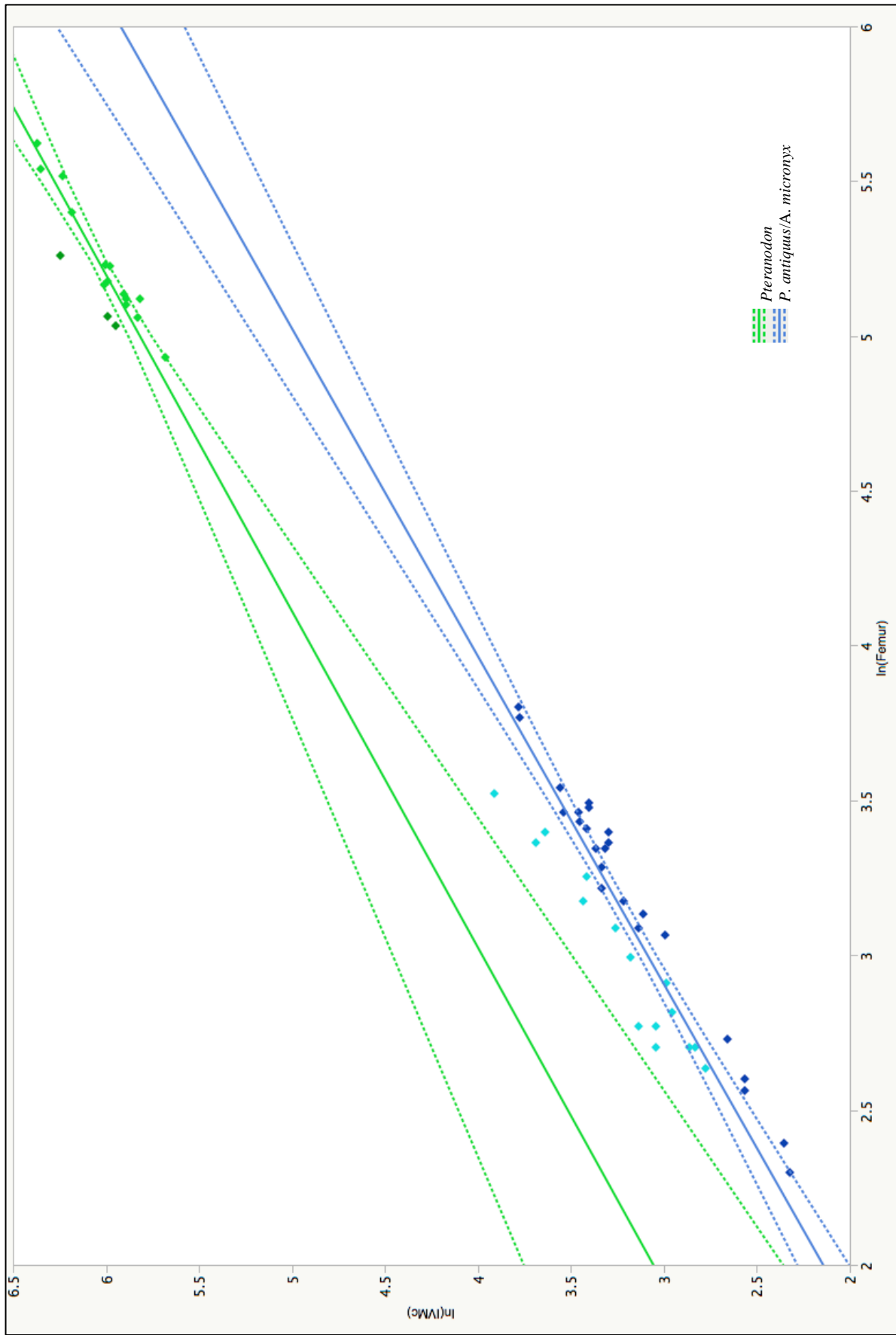


Figure 29 Bivariate Linear Regressions of Pooled Specimen Data. Bivariate plot of the ln-femur and ln-IVMc data of *Pieranodon* (green diamonds) and *P. antiquus* (dark blue diamonds) /*A. micronyx* (light blue diamonds). This shows what may be sexual dimorphic relationships between *P. antiquus* and *A. micronyx* and identifies three (dark green diamonds) *Pieranodon* that may be females. Confidence intervals are also plotted. Linear regressions: *Pieranodon*  $[\ln(\text{IVMc}) = 1.211 + 0.921 * \ln(\text{Femur})]$  (SE = 0.101); *P. antiquus/A. micronyx*  $[\ln(\text{IVMc}) = 0.251 + 0.945 * \ln(\text{Femur})]$  (SE = 0.058).

(CU 45062, YPM 2451, & YPM 2493), plot well above the regression line (Figure 29 & 30). Despite the lack of an associated skull and pelvic girdle for all 17 *Pteranodon* specimens, those three specimens may be females because of their femur and IVMc relationship.

Nothing conclusive can be suggested with the *Pteranodon* data. There appears to be three strong outliers (red diamonds) and two size classes (blue & green ellipsoids) that cannot be interpreted properly because of the lack of data. The null hypothesis presented for the part of the study remains inconclusive due to no proper comparisons of the three species can be made regarding possible sexual dimorphism.

### **Phylogenetic Allometry (Pooled Data of All Three Species)**

When a trend-line is calculated for the pooled data sets in Figure 29, the change in femur and IVMc ontogenic relationship between *Pteranodon* and *P. antiquus/A. micronyx* is observed and calculated (Figure 30). This (red) line represents the positive allometry associated with the increase in size of *Pteranodon* compared to *P. antiquus/A. micronyx*. The original null hypothesis of Chapter 2 was finding positive allometry in the wing components of *P. antiquus/A. micronyx*. That null hypothesis was rejected by these two species. *Pteranodon* obtained massive sizes and observed here is negative allometry in their IVMc relative to their IVMc. The phylogenetic allometry regression line, however,  $(1.301 \pm 0.044)$  shows that during the course of pterosaur evolution in terms of size, there is positive allometry with the IVMc and femur in pterosaurs. The null hypothesis of Chapter 2 is accepted when making interspecific comparisons between these three distantly related and different sized pterosaurs.

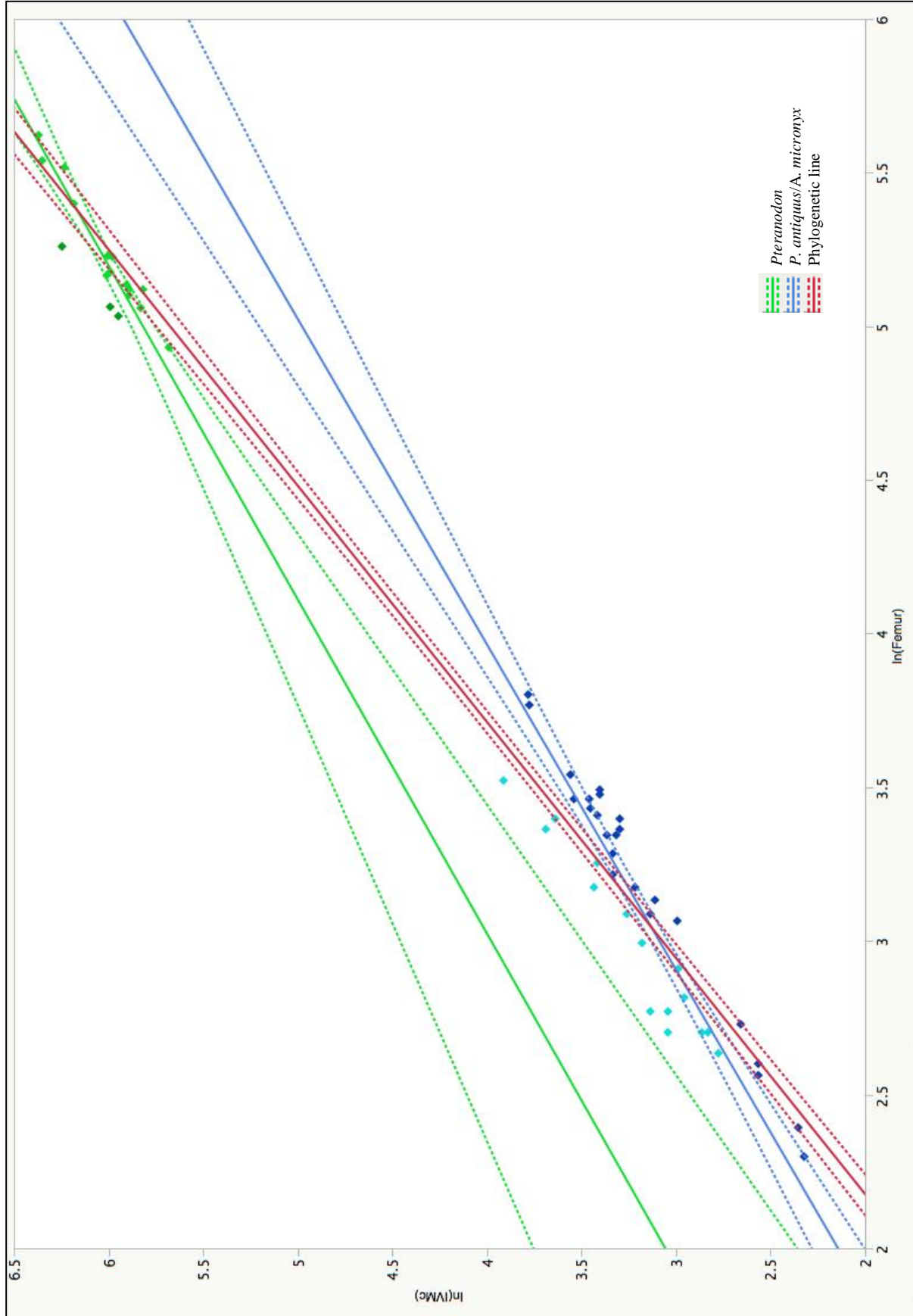


Figure 30 Phylogenetic Allometry. The regression line plotted with the ln-femur and ln-IVMc data of *Pteranodon* (green diamonds) and *P. antitiquus* (dark blue diamonds) / *A. micronyx* (light blue diamonds). Shown is the sexual dimorphic relationships between *P. antitiquus* and *A. micronyx* and identifies three (dark green diamonds) female *Pteranodon*. The females have relatively larger IVMc's than the males and plot above the regression lines. Confidence intervals are also plotted. Linear regressions: *Pteranodon* [ $\ln(\text{IVMc}) = 1.211 + 0.921 * \ln(\text{Femur})$ ] (SE = 0.101); *P. antitiquus/A. micronyx* [ $\ln(\text{IVMc}) = 0.251 + 0.945 * \ln(\text{Femur})$ ] (SE = 0.058); Phylogenetic line [ $\ln(\text{IVMc}) = -0.836 + 1.301 * \ln(\text{Femur})$ ] (SE = 0.023).

## Conclusion

The two pterosaur species *P. antiquus* and *A. micronyx* cannot be concluded to be sexual dimorphs of the same species. They coexisted, being found in the same fossil bed and locale, Lower Tithonian, Solnhofen LS, Malm Zeta 2, of Eichstätt, Bavaria, Germany. They have been suggested to be sexual dimorphs since Wellnhofer's (1970) publication but this was not investigated further. *P. antiquus* has a generally larger body size than *A. micronyx*, even if larger specimens of *A. micronyx* are found; the relative proportions would still be smaller, such as the skull length, due to its small positive allometry found in the PCA of Chapter 2 (Figure 17: Chapter 2). The results of the surface area linear regression analysis and wing schematics of the largest specimens of the two species show that *A. micronyx* had a larger surface area and longer wingspan/breadth relative to *P. antiquus* (Figure 22: Chapter 2). The expected increase in weight during pregnancy would put selective pressure for a larger surface area to reduce wing loading during flight on *A. micronyx*. The isometry found in *P. antiquus*' distal wing elements and brachiopatagium surface area had evolutionary constraints that selected for isometry and negative allometry throughout their wing elements, legs, and brachiopatagium. In *Pteranodon*, however, it's much larger size likely makes positive allometry in the IVMc critical, and likely the rest of the elements of the wing finger would have seen the same effect.

Sexual dimorphism is not a novel observation in pterosaurs but this method using PCA, bivariate linear regression, basic wing reconstructions, and wing surface area calculations along with extant species sexual dimorph analogous (bats and moths) is a new approach to the expanding research in pterosaur paleobiology. Examination of the

pelvises of *P. antiquus* and *A. micronyx* is the next step to test sexual dimorphic characteristics in both species, if preserved orientations allow.

## REFERENCES

- Andres, B. and Ji, Q. 2008. A new pterosaur from the Liaoning Province of China, the phylogeny of the pterodactyloidea, and convergence in their cervical vertebrae. 51: 453–469.
- Andres, B. 2010. Systematics of the Pterosauria. Yale University. p. 366. Dissertation.
- Averianov, A.O., Arkhangelsky, M. S., and Pervushov, E.M. 2008. A new late Cretaceous azhdarchid (Pterosauria, Azhdarchidae) from the Volga Region. *Paleontological Journal*, 42(6), 634-642.
- Barrett, P.M., Butler, R.J., Edwards, N.P., and Milner, A.R. 2008. Pterosaur distribution in the space and time: An atlas. *Zittleiana*. B28: 61-107.
- Bennett, S.C. 1990. A pterodactyloid pterosaur pelvis from the Santana Formation of Brazil: implications for terrestrial locomotion. *Journal of Vertebrate Paleontology* 10.1: 80-85.
- Bennett, S.C. 1992. Sexual dimorphism of Pteranodon and other pterosaurs, with comments on cranial crests. *Journal of Vertebrate Paleontology*, 12(4), 422-434.
- Bennett, S.C. 1993. The Ontogeny of *Pteranodon* and other pterosaurs. *Paleobiology* 19: 92-106.
- Bennett, S.C. 1996a. The Phylogenetic Position of the Pterosauria within the Archosauromorpha. *Zoological Journal of the Linnaean Society* 118: 261-308.
- Bennett, S.C. 1996b. Year-classes of pterosaurs from the Solnhofen Limestone of Germany: taxonomic and systematic implications. *Journal of Vertebrate Paleontology*, 16(3), 432-444.
- Bennett, S.C. 1997b. A second specimen of the pterosaur *Anurognathus ammoni*. *Paläeitschrift*. 81, 376-398.
- Bennett, S.C. 2001a. The osteology and functional morphology of the Late Cretaceous pterosaur *Pteranodon*. *Palaeontographic Abteilung A* 260: 1-112.
- Bennett, S.C. 2001b. The osteology and functional morphology of the Late Cretaceous pterosaur *Pteranodon*. *Palaeontographic Abteilung A* 260: 113-153.
- Bennett, S.C. 2003a. Morphological evolution of the pectoral girdle of pterosaurs: myology and function. *Geological Society, London, Special Publications*, 217(1), 191-215.
- Bennett, S.C. 2003b. New crested specimens of the Late Cretaceous pterosaur *Nyctosaurus*. *Paläontologische Zeitschrift* 77.1: 61-75.



- Bennett, S.C. 2005. Pterosaur science or pterosaur fantasy? *Prehistoric Times* 70: 21-23.
- Bennett, S.C. 2007a. A review of the pterosaur *Ctenochasma*: taxonomy and ontogeny. *Neues Jahrbuch für Geologie und Paläontologie - Abhandlungen*, 245(1): 23-31.
- Bennett, S.C. 2013. New information on body size and cranial display structures of *Pterodactylus antiquus*, with a revision of the genus. *Paläontologische Zeitschrift*, 87(2), 269-289.
- Benton, M.J. 1999. *Scleromochulus taylori* and the origin of dinosaurs and pterosaurs. *Philosophical Transactions of the Royal Society.*, London B 354: 1423-1446.
- Bonde, N. and Christiansen, P. 2003. The detailed anatomy of *Rhamphorhynchus*: axial pneumaticity and its implications. *Geological Society, London, Special Publications*, 217(1), 217-232.
- Bookstein, F., Chernoff, B., Elder, R. L., Humphries, J. M., Smith, G. R., and Strauss, R. E. 1985. Morphometrics in evolutionary biology. *Academy of Natural Sciences of Philadelphia Special Publication* 15.
- Brower, J.C. and Veinus, J. 1981. Allometry in pterosaurs. *Univeristy of Kansas Paleontological Contributions* 105: 1-32.
- Brower, J.C. 1983. The aerodynamics of *Pteranodon* and *Nyctosaurus*, two large pterosaurs from the upper Cretaceous of Kansas. *Journal of Vertebrate Paleontology* 3: 84–124.
- Brumwell, C.D. and Whitfield, G.R. 1974. Biomechanics of *Pteranodon*. *Philosophical Transactions of the Royal Society of London* 267: 503-581.
- Buckland, W. 1829. *Proceedings of the Geological Society London*, 1: 127
- Buffetaut, E., Laurent, Y., Le Loeuff, J.E.A.N., and Bilotte, M. 1997. A terminal Cretaceous giant pterosaur from the French Pyrenees. *Geological Magazine*, 134(04), 553-556.
- Butler, R.J., Barret, P.M., and Gower, D.J. 2009. Postcranial skeleton pneumaticity and air-sacs in the earliest pterosaurs. *Biological Letters* 5: 557-560.
- Camargo, N.F. and Oliveira, H.F.M. 2012. Sexual Dimorphism in *Sturnira lilium* (Chiroptera, Phyllostomidae): Can Pregnancy and Pup Carrying Be Responsible for Differences in Wing Shape?. *Plos ONE* 7(11): e49734. Doi:101371/journal.pone.0048734
- Camargo, W.R.F., Camargo, N.F., Corrêa, D.C.V., Camargo, A.A., and Diniz, I.R. 2015. Sexual Dimorphism and Allometric Effects Associated With the Wing Shape of Seven Moth Species of Sphingidae (Lepidoptera: Bombycoidea). *Journal of Insect Science* 15(1): 107.

- Chatterjee, S. and Templin, R.J. 2004. Posture, locomotion, and paleoecology of pterosaurs. Vol. 376. Geological Society of America.
- Chiappe, L.M. and Chinsamy, A. 1996. *Pterodaustro*'s true teeth. *Nature*. 379:211-212.
- Chiappe, L.M., Kellner, A.W.A., Rivarola, D., Davila, S., and Fox, M. 2000. Cranial morphology of *Pterodaustro guinazui* (Pterosauria: Pterodactyloidea) from the lower Cretaceous of Argentina. *Contributions in Science*. 483: 1-19.
- Claessens, L.P.A.M., O'Connor, P.M., and Unwin, D.M. 2009. Respiratory evolution facilitated the origin of pterosaur flight and aerial gigantism. *PLoS One*. 2009;4(2):e4497. doi: 10.1371/journal.pone.0004497. Epub 2009 Feb 18.
- Clark, J.M., Hopson, J.A., Hernández, R.R., Fastovsky, D.E., and Montellano, M. 1998. Foot posture in a primitive pterosaur. *Nature* 391:886-889
- Clancy, L.J. 1975. *Aerodynamics*. Pitman: 1-610.
- Cock, A.G. 1966. Genetical aspects of metrical growth and form in animals. *Quarterly Review of Biology* 41:131-190.
- Collini, C.A. 1784. Sur quelques zoolithes du cabinet d'histoire naturelle de S.A.S.E. palatine et de Baviere, à Mannheim. In: Acta Academiae Theodoro-Palatinae, vol. 5 Phys., Mannheim 1784, pp 58-71.
- Cranfield, I. 2000. *The Illustrated Directory of Dinosaurs and Other Prehistoric Creatures*. London: Salamander Books, Ltd. Pp. 302-305.
- Dalla Vecchia, F.M. and Ligabue, G. 1993. On the presence of a giant pterosaur in the Lower Cretaceous (Aptian) of Chapada do Araripe (Northeastern Brasil). *Bollettino della Società Paleontologica Italiana* 32: 1. 131- 136
- Dalla Vecchia, F.M. 2003b. New morphological observations on Triassic pterosaurs. *Geological Society of London Special Publication* 217:23-44.
- Döderlein, L. 1923. "Anurognathus Ammoni, ein neuer Flugsaurier." Sitzungsberichte der Mathematisch-Naturwissenschaftlichen Abteilung der Bayerischen Akademie der Wissenschaften zu München, 1923, 306-307.
- Elgin, R.A., Grau, C.A., Palmer, C., Hone, D.W., Greenwell, D., and Benton, M.J. 2008. Aerodynamic characters of the cranial crest in Pteranodon. *Zitteliana* B28: 167-174.
- Elgin, R.A., Hone, D.W., and Frey, E. 2011. The extent of the pterosaur flight membrane. *Acta Palaeontologica Polonica*, 56(1), 99-111.

- Elgin, R.A. and Hone, D.W. 2013. Pneumatization of an immature azhdarchoid pterosaur. *Cretaceous Research*, 45, 16-24.
- Fabre, J.A. 1976. Un nouveau Pterodactylidae du gisement de Canjuers (Var): *Gallodactylus canjuersensis* nov. gen., nov. sp. *Comptes Rendus de l'Academie des Sciences* 279: 2011-2014.
- Felsenstein, J. 1985. Phylogenies and the comparative method. *American Naturalist* 125: 1-15.
- Frey, E. and Martill, D.M. 1996. A reappraisal of *Arambourgiania* (Pterosauria, pterodactyloidea): one of the world's largest flying animals. *Neues Jahrbuch für Geologie und Paläontologie, Abhandlungen* 199: 221-247.
- Fröbisch, N.B. and Fröbisch, J. 2006. A new basal pterosaur genus from the upper Triassic of the northern Calcareous Alps of Switzerland. *Palaeontology* 49: 1081-1090.
- Glantz, S.A. and Slinker, B. K. 1990. *Primer of Applied Regression and Analysis of Variance*. McGraw-Hill. ISBN 0-07-023407-8.
- Godfrey, S.J. and Currie, P.J. 2005. Pterosaurs. In *Dinosaur Provincial Park: A Spectacular Ancient Ecosystem Revealed*, 1, 292.
- Gould, S.J. 1966. Allometry and size in ontogeny and phylogeny. *Biological Reviews* 41:587-440.
- Gould, S.J. 1975. Allometry in primates, with emphasis on scaling and the evolution of the brain. *Contributions to Primatology* 5:244-292.
- Habib, M.B. and Witton, M. 2011. Functional Morphology of Anurognathid Pterosaurs. In *GSA Northeast Regional Conference, Pittsburgh, PA*.
- Habib, M.B. 2008. Comparative evidence for the quadrupedal launch in pterosaurs. *Zitteliana* B28: 161-168.
- Hankin, E.H. and Watson, D.M.S. 1914. On the flight of pterodactylus. *Aeronautical Journal*. 18: 324-335.
- Hazlehurst, G.A. and Rayner, J. 1992. Flight characteristics of Triassic and Jurassic Pterosauria: an appraisal based on wing shape. *Paleobiology* 18: 447-463.
- Hildebrand, M. 1995. *Analysis of Vertebrate Structure*, 4th ed. New York, John Wiley and Sons.
- Hone, D.W. and Benton, M.J. 2007. An evaluation of the phylogenetic relationships of the pterosaurs among archosauromorph reptiles. *Journal of Systematic Palaeontology* 5:465-469.

- Hone, D.W., Habib M.B., and Lamanna M.C. 2013. An annotated and illustrated catalogue of Solnhofen (Upper Jurassic, Germany) pterosaur specimens at Carnegie Museum of Natural History. *Annals of Carnegie Museum* 82:165-191
- Huxley, T.H. 1860. "ART. VIII.—Darwin on the Origin of Species." *Westminster Review* (Book review) London: Baldwin, Cradock, and Joy 17: 541–570.
- Huxley, J.S. 1932. Problems of relative growth. Methuen: London. Reprinted 1972, Dover Publications: New York.
- Ji, Q., Ji, S.A., and Cheng, Y. N. 2004. "Palaeontology: pterosaur egg with a leathery shell." *Nature* 432 (7017): 572.
- Jolicoeur, P. 1963a. The multivariate generalization of the allometry equation. *Biometrics* 19: 497-499.
- Jolicoeur, P. 1963b. The degree of generality of robustness in *Martes Americana*. *Growth* 27: 1-27.
- Jouve, S. 2004. Description of the skull of a *Ctenochasma* (Pterosauria) from the latest Jurassic of eastern France, with a taxonomic revision of European Tithonian Pterodactyloidea. *Journal of Vertebrate Paleontology*, 24(3), 542-554.
- Kellner, A.W.A. and Tomida, Y. 2000. Description of a New Species of Anhangueridae (Pterodactyloidea) with Comments on the Pterosaur Fauna from the Santana Formation (Aptian - Albian), Northeastern Brazil. *National Science Museum, Tokyo, Monographs* 17:1-135.
- Klingenberg, C.P. and Zimmermann, M. 1992. Static, ontogenetic, and evolutionary allometry: a multivariate comparison in nine species of water striders. *American Naturalist*, 601-620. Marcus et al. Blenum Press, New York.
- Klingenberg, C.P. 1996. Multivariate Allometry. *Advances in Morphometrics*, Edited by L. F. Marcus et al. Blenum Press, New York.
- Kripp, D. 1943. Ein Lebensbild von *Pterodaon ingens* auf flugtechnischer Grundlage. *Luftwissen* 8: 217-246.
- Lawson, D.A. 1975b. Could pterosaurs fly? *Science* 188: 676.
- Livingston, V.J., Bonnan, M.F., Elsey, R.M., Sandrik, J.L., and Wilhite, D. 2009. Differential limb scaling in the American alligator (*Alligator mississippiensis*) and its implications for archosaur locomotor evolution. *The Anatomical Record*, 292(6), 787-797.

- Lü, J. 2010. An overview of the pterosaur fossil record in China. Abstract. *Acta Geoscientia Sinica* 31 (1): 49-51.
- Lü, J., Ji, S., Yuan, C., and Ji, Q. 2006. *Pterosaurs from China*. Beijing, Geological Publishing House.
- Lü, J., Pu H., Xu, L., Wu, Y., and Wei, X., 2012. Largest toothed pterosaur skull from the Early Cretaceous Yixian Formation of Western Liaoning, China, with comments on the family Boreopteridae. *Acta Geologica Sinica (English Edition)* 86.2 86: 287-293.
- Lü, J., Unwin, D.M., Deeming, D.C., Jin, X., Liu, Y., and Ji Q. 2011. An Egg-Adult Association, Gender, and Reproduction in Pterosaurs. *Science* 21 January 2011: 331 (6015), 321-324.
- Lü, J., Unwin, D.M., Jin X., Liu, Y., and Ji, Q. 2009. Evidence for modular evolution in a long-tailed pterosaur with a pterodactyloid skull. *Proceedings of the Royal Society of London B: Biological Sciences* 2009 -; DOI: 10.1098/rspb.2009.1603. Published 14 October 2009
- Lü, J., Unwin, D.M., Xu, L., and Zhang, X. 2008. A new azhdarchoid pterosaur from the Lower Cretaceous of China and its implications for pterosaur phylogeny and evolution. *Naturwissenschaften* 95: 891-897.
- Marsh, O.C. 1882. The wings of pterodactyls. *American Journal of Science* 23: 251-256.
- Martill, D.M., and Etches, S. 2013. A monofenestratan pterosaur from the Kimmeridge Clay Formation (Upper Jurassic, Kimmeridgian) of Dorset, England. *Acta Palaeontologica Polonica*.
- Mateer, N.J. 1976. A statistical study of the genus *Pterodactylus*. *Bulletin of the Geological Institutions of the University of Uppsala, ns, 6*, 97-105.
- McGowen, M.R., Padian, K., De Sosa, M.A., and Harmon, R.J. 2002. Description of *Montanazhdarcho minor*, an azhdarchid pterosaur from the Two Medicine Formation (Campanian) of Montana. *PaleoBios*, 22(1), 1-9.
- Miller, H.W. 1971. The taxonomy of the *Pteranodon* species from Kansas. *Transactions of the Kansas Academy of Science (1903)*: 1-19.
- Naish, D., Simpson, M., and Dyke, G. 2013. A new small-bodied azhdarchoid pterosaur from the Lower Cretaceous of England and its implications for pterosaur anatomy, diversity and phylogeny. *PloS one*, 8(3), e58451.
- Nesbitt, S.J. and Hone, D. 2010. An external mandibular fenestra and other archosauriform character states in basal pterosaurs. *Palaeontology* 3: 223-231.
- Nessov, L.A. 1984. Pterosaurs and birds of the Late Cretaceous of Central Asia. *Paläontologische Zeitschrift*, 1, 47-57.

- O'Connor, P.M. and Claessens, L.P.A.M. 2005. Basic avian pulmonary design and flow-through ventilation in non-avian theropod dinosaurs. *Nature* 436:253–256.
- O'Keefe, F.R. and Carrano, M.T. 2005. Correlated trends in the evolution of the plesiosaur locomotor system. *Paleobiology* 31(4): 656-675.
- O'Keefe, F.R., Meachen, J., Fet, E.V., and Brannick, A. 2013. Ecological determinants of clinal morphological variation in the cranium of the North American gray wolf. *J Mammal* 94 (6): 1223–1236. doi: 10.1644/13-mamm-a-069
- Ósi, A. 2010. Feeding-related characters in basal pterosaurs: Implications for jaw mechanism, dental function and diet. *Lethaia* 44: 136-152.
- Padian, K. 1983. A functional analysis of flying and walking in pterosaurs. *Palaeontology* 9: 218-239.
- Padian, K. and Smith, M. 1992. New light on Late Cretaceous pterosaur material from Montana. *Journal of Vertebrate Paleontology*, 12(1), 87-92.
- Pagel, M. D. and Harvey, P. H. 1988. Recent developments in the analysis of comparative data. *Quarterly Review of Biology* 63:4 1H40
- Palmer, C. and Dyke, G. J. 2009. Biomechanics of the unique pterosaur pteroid. *Proceedings of the Royal Society of London B: Biological Sciences*, rspb20091899.
- Paul, G.S. 2002. *Dinosaurs of the air: the evolution and loss of flight in dinosaurs and birds*. JHU Press.
- Peters, D. 2008. The origin and radiation of the Pterosauria. In *Flugsaurier: The Wellnhofer Pterosaur Meeting, Munich, Abstract Volume* edited by D. Hone, 27-28. Munich, Bavarian State Collection for Palaeontology.
- Pimentel, R.A. 1979. *Morphometrics, the multivariate analysis of biological data*. Kendall/Hunt Pub. Co.
- Prestice, K., Ruta, M., and Benton, M.J. 2011. Evolution of morphological disparity in pterosaurs. *Journal of Systematics Palaeontology* 9: 337-353.
- Quenstedt, F.A. 1855. *Über Pterodactylus suevicus im lithographischen Schiefer Wuffenberg*. Tübingen, Universität Tübingen.
- Reisz, R.R., Scott, D., Sues, H.D., Evans, D.C., and Raath, M.A. 2005. Embryos of an Early Jurassic prosauropod dinosaur and their evolutionary significance. *Science*, 309(5735), 761-764.

- Sato, K., Sakamoto, K., Watanuki, Y., Takahashi, A., Katsumata, N., Bost, C.A., and Weimerskirch, H. 2009. Scaling of soaring seabirds and implications for flight abilities of giant pterosaurs. *PLoS ONE* 4: e5400.
- Schmidt-Nelson, K. 1984. *Scaling: Why is Animal Size so Important?* New York, NY: Cambridge University Press.
- Sereno, P.C. 1991. Basal archosaurs: Phylogenetic relationships and functional implications. *Journal of Vertebrate Paleontology Memoir* 2: 1-53.
- Shea, B.T. 1985. Bivariate and multivariate growth allometry: statistical and biological considerations. *Journal of Zoology*, 206(3), 367-390.
- Small, C.G. 1996. *The Statistical Theory of Shape*. Springer. p. 4. ISBN 0-387-94729-9.
- Stecher, R. 2008. A new Triassic pterosaur from Switzerland (Central Austroalpine; Grisons), *Raeticodactylus filisurensis* gen. et sp. nov. *Swiss journal of Geosciences* 101: 185-201.
- Stein, R.S. 1975. Dynamic analysis of *Pteranodon ingens*: A reptilian adaptation to flight. *Journal of Paleontology* 49: 534-548.
- Tischlinger, H. and Frey, E. 2010. Multilayered is not enough! New soft tissue structures in the Rhamphorhynchus flight membrane. *Acta Geoscientica Sinica*, 31(Supplement 1), 64.
- Unwin, D.M. 2003. On the phylogeny and evolutionary history of pterosaurs. *Evolution and Palaeobiology of Pterosaurs*, Geological Society of London, Special Publications 217:139-190
- Unwin, D.M. 2005. *The Pterosaurs from Deep Time*. New York, Pi Press.
- Veldmeijer, A.J. 2003. "Description of *Coloborhynchus spielbergi* sp. nov. (Pterodactyloidea) from the Albian (Lower Cretaceous) of Brazil." *Scripta Geologica*, 125: 35-139.
- Wang, X., Campos, D.A., Zhou, Z., and Kellner, A.W.A. 2008. A primitive istiodactylid pterosaur (Pterodactyloidea) from the Jiufotang Formation (Early Cretaceous), northeast China. *Zootaxa* 1813: 1-18.
- Wang, X., Kellner, A.W.A., Jiang, S., Cheng, X., Meng, X., and Rodrigues, T. 2010. New long-tailed pterosaurs (Wukongopteridae) from western Liaoning, China. *Anais da Academia Brasileira de Ciências* 82.4: 1045-1062.
- Wang, X., Kellner, A.W.A., Jiang, S., Wang, Q., Ma, Y., Paidoula, Y., and Li, N. 2014. Sexually dimorphic tridimensionally preserved pterosaurs and their eggs from China. *Current Biology*, 24(12), 1323-1330.

- Wang, X., Kellner, A.W.A., Zhou, Z., and Campos, D.A. 2005. Pterosaur diversity and faunal turnover in Cretaceous terrestrial ecosystems in China. *Nature*, 437, 875–879.
- Wang, X., Kellner, A., Jiang, S., and Meng, X. 2009. An unusual long-tailed pterosaur with elongated neck from western Liaoning of China. *Anais da Academia Brasileira de Ciências* 81(4): 793-812.
- Wang, X., Zhou, Z., Zhang, F., and Xu, X. 2002. A nearly completely articulated rhamphorhynchoid pterosaur with exceptionally well-preserved wing membranes and "hairs" from Inner Mongolia, northeast China. *Chinese Science Bulletin* 47:226-230.
- Wedel, M.J. 2003. Vertebral pneumaticity, air sacs, and the physiology of sauropod dinosaurs. *Paleobiology*: June 2003, Vol. 29, No. 2, pp. 243-255.
- Wedel, M.J. 2005. Postcranial skeletal pneumaticity in sauropods and its implications for mass estimates. *The sauropods: evolution and paleobiology*. University of California Press, Berkeley, 201-228.
- Wellnhofer, P. 1970. Die Pterodactyloidea (Pterosauria) der Oberjura-Plattenkalke Süddeutschlands. *Abh Bayer Akad Wiss*, NF 141: 1–133.
- Wellnhofer, P. and Kellner, A.W.A. 1991. The skull of *Tapejara wellnhoferi* Kellner (Reptilia: Pterosauria) from the Lower Cretaceous Santana Formation of the Araripe Basin, Northeastern Brazil. *Mitt. bayer. Staatslg Paläont. hist. Geol.*31, 89–106.
- Wild, R. 1984. A new pterosaur (Reptilia, Pterosauria) from the Upper Triassic (Norian) of Friuli, Italy. *Gortania - Atti del Museo Friulano di Storia Naturale* 5:45-62.
- Wilkinson, M.T., Unwin, D.M., and Ellington, C. P. 2006. High lift function of the pteroid bone and forewing of pterosaurs. *Proceedings of the Royal Society of London B: Biological Sciences*, 273(1582), 119-126.
- Witmer, L.M., Chatterjee, S., Franzosa, J., and Rowe, T. 2003. Neuroanatomy of flying reptiles and implications for flight, posture and behavior. *Nature* 425: pp. 950-953.
- Witton, M. 2008a. A new approach to determining pterosaur body mass and its implications for pterosaur flight. *Zitteliana* B28: 143-159.
- Witton, M. 2012. "New Insights into the Skull of *Istiodactylus latidens* (Ornithocheiroidea, Pterodactyloidea)." *PLoS ONE*, 7(3): e33170. doi:10.1371/journal.pone.0033170.
- Witton, M. 2013. *Pterosaurs: Natural History, Evolution, Anatomy*. Princeton University Press.
- Witton, M. and Habib, M.B. 2010. On the Size and Flight Diversity of Giant Pterosaurs, the Use of Birds as Pterosaur Analogues and Comments on Pterosaur Flightlessness. *PLoS ONE* 5(11): e13982. doi: 10.1371/journal.pone.0013982.



Witton, M. and Naish, D. 2008. A reappraisal of azhdarchid pterosaur functional morphology and paleoecology. *PLoS One* 3.5: e2271.

Zambelli, R. 1973. *Eudimorphodon ranzii* gen. nov., sp. nov., a Triassic pterosaur. *Istituto Lombardo di Scienze e Lettere Rendiconti B Scienze Biologiche e Mediche* 107:27–32.

**APPENDIX A**  
Raw Data for All 39 Specimens Used

#	Species	Skull	M	Neck	PCRW	H	R	U	IVMc	I	II	III	IV	F	T
1	<i>P. antiquus</i>	44.5	34.7	25.9	33.3	15	19.5	19.5	14.3	19.2	17.9	16.2	15	15.4	19
2	<i>P. antiquus</i>	83.9	76	70	61.6	29.5	41.5	41.5	31.5	44	40.5	38	30	31	44
3	<i>P. antiquus</i>	86.7	83	62.7	63.7	30.5	45	45	30	48.5	41	37	31	33	47
4	<i>P. antiquus</i>	108	92	80	63	31.5	47	47	35	48.5	44.2	37	29	34.7	48
5	<i>P. antiquus</i>	140	89.8	89.8	90	43.7	60	60	44	58	57.5	50.5	39	45	59
6	<i>P. antiquus</i>	23	15.5	16	20	12.3	15.5	15.5	10.5	14.6	12.5	13.2	13	11	13
7	<i>P. antiquus</i>	25	18.2	15	23	12.8	15.7	15.7	10.2	14.8	14.3	13.2	11	10	14
8	<i>P. antiquus</i>	35	26.5	27	30	15.5	18.5	18.5	13	18	17.5	16	14	13.5	17
9	<i>P. antiquus</i>	38	27	21	27	14.5	19	19	13	17.2	16.8	16.5	10	13	16
10	<i>P. antiquus</i>	57.5	46	36	42	21.3	28.9	28.9	20	27	25.8	23.3	19	21.5	28
11	<i>P. antiquus</i>	70	57	51.4	52.2	25	32	32	22.5	30	29	27	23	23	32
12	<i>P. antiquus</i>	73.5	60.5	50	53	24	30.5	30.5	25	32.5	32.5	27.8	23	24	34
13	<i>P. antiquus</i>	74	60.5	56	57	26	36.5	36.5	28	34	32.5	27	26	26.8	34
14	<i>P. antiquus</i>	80	59.6	59.6	60.5	29	38	38	28	40	35.5	31.5	26	25	39
15	<i>P. antiquus</i>	83	66	55	55	26.5	40	40	27	35	34.3	31.8	26	29	39
16	<i>P. antiquus</i>	83	67.5	60	57	31	39	39	29	39	35.5	33.5	27	28.5	40
17	<i>P. antiquus</i>	83.5	68.5	64	63	29	38	38	27	38	37	34	26	30	39
18	<i>P. antiquus</i>	84	67	53	60	28.5	41.5	41.5	30.5	40	36.4	31.4	26	30.3	42
19	<i>P. antiquus</i>	84	69	64	69	30	43	43	30	41	39	34.5	28	32.5	42
20	<i>P. antiquus</i>	87.5	71	65	65	31.7	42.5	42.5	31.8	43	41.5	36.5	29	32	44
21	<i>P. antiquus</i>	93	78	69	67.5	32.5	41.5	41.5	34.5	44.5	41	35	29	32	45
22	<i>P. antiquus</i>	114	92.5	100	81	41	52	52	43.5	56	53	41	35	43.5	55
23	<i>P. antiquus</i>	83	65	60	63	29	39	39	27.5	38.5	36.5	32.5	27	28.5	39
24	<i>P. antiquus</i>	71	58	45	50	23	32	32	23	31	29	26	22	22	32
25	<i>A. micronyx</i>	26	16	16.5	30	14.5	19	19	17	23.2	20	15	13	15	18
26	<i>A. micronyx</i>	25.5	19	19	28	15	18.8	18.8	16.1	21.8	16	13.7	14	14	18
27	<i>A. micronyx</i>	27.5	19.5	22	30	16.5	20.5	20.5	17.5	22.5	19	15	16	15	19
28	<i>A. micronyx</i>	28	22.7	20	31	16.9	21.8	21.8	19.2	24.3	21.5	16.9	17	16.8	20
29	<i>A. micronyx</i>	32.5	23.5	25	32	18.5	25	25	19.8	28.5	24	19.8	18	18.4	24
30	<i>A. micronyx</i>	36	24	27	33	18.8	23	23	21	27	23	18	15	15	22
31	<i>A. micronyx</i>	41.5	33	25.3	37	18	25	25	24	32	25	22	19	20	27
32	<i>A. micronyx</i>	46	38	30	35	18.5	24.5	24.5	21	27.5	25	20	17	16	24
33	<i>A. micronyx</i>	45.1	33.8	30.8	44	23	30.5	30.5	30.5	41	32	24	18	26	34
34	<i>A. micronyx</i>	57	47	35	48	25	31	31	40	46	28.5	19.5	18	29	41
35	<i>A. micronyx</i>	67	56.5	44	53	26	35	35	38	48	35.5	26	23	30	44
36	<i>A. micronyx</i>	70	52	56	58	28	40	40	50	54	37	22	19	34	48
37	<i>A. micronyx</i>	46.5	39	32	38	19	23.5	23.5	23	28	25	19.5	18	16	25
38	<i>A. micronyx</i>	38.5	28.8	26.3	40	20.5	26	26	26	34	28	22	18	22	29
39	<i>A. micronyx</i>	51	40	30.3	43	23	30	30	31	38	31	23.5	21	24	33

## APPENDIX B

### Results for all 14 Principle Components

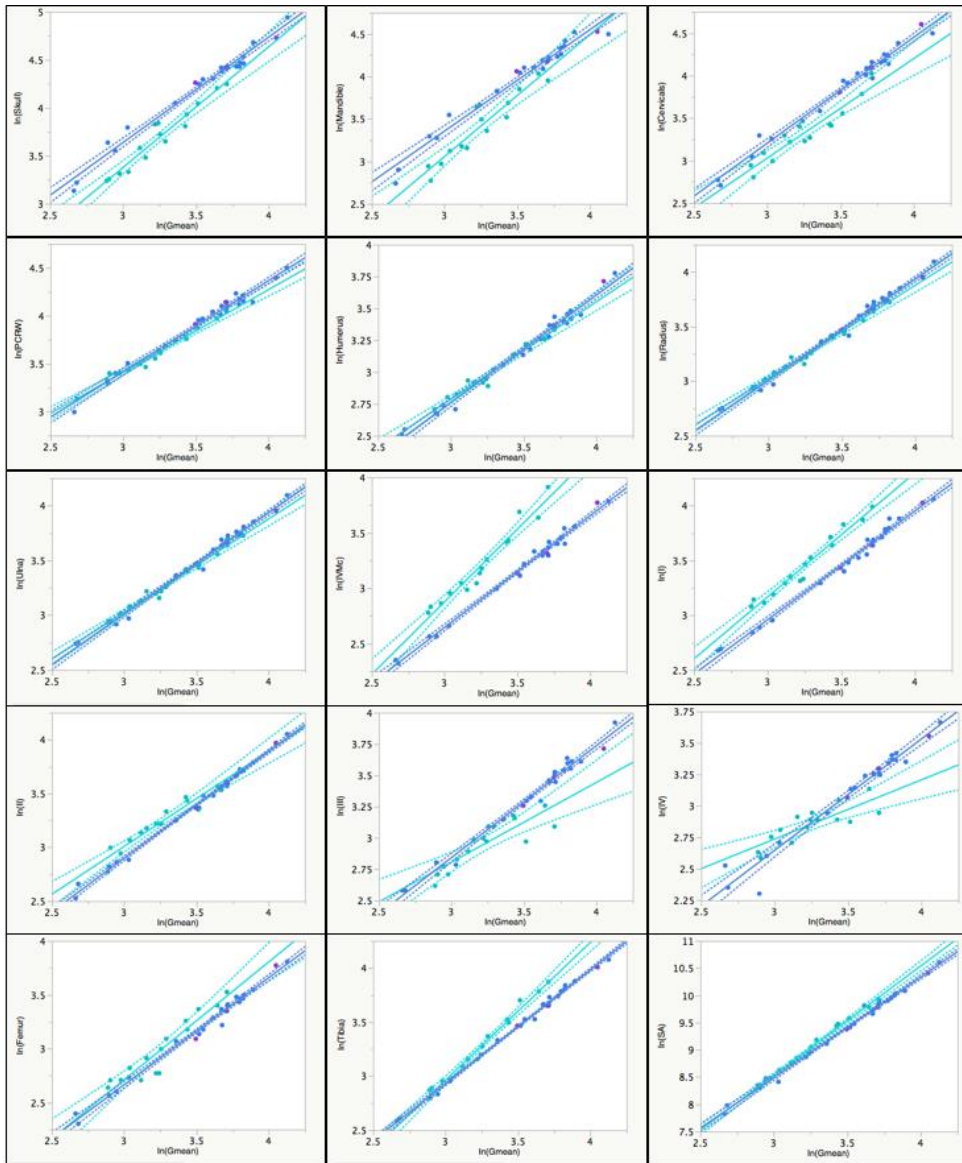
#### *Pterodactylus antiquus*

Column 1	Prin1	Prin2	Prin3	Prin4	Prin5	Prin6	Prin7	Prin8	Prin9	Prin10	Prin11	Prin12	Prin13	Prin14
1 ln(Skull)	0.29263	-0.39115	0.23816	0.27395	0.35287	-0.1275	-0.13152	-0.56550	0.04826	-0.10747	-0.37104	-0.00495	-0.01251	-0.00000
2 ln(Mandible)	0.31765	-0.67960	0.08295	-0.42739	-0.13315	0.10955	0.05978	0.15946	-0.01259	0.29529	0.17943	0.08842	0.24818	0.00000
3 ln(Cervicals)	0.33151	-0.17011	-0.65487	0.24286	-0.37395	-0.1369	-0.34204	0.04917	-0.22846	-0.15171	-0.04346	-0.02801	-0.13209	-0.00000
4 ln(PCRW)	0.25204	-0.09212	-0.17205	0.28159	0.56157	0.34406	0.26205	0.44591	-0.06893	-0.15261	0.07599	-0.28982	-0.00621	-0.00000
5 ln(Humerus)	0.22346	0.24592	-0.05412	0.38379	-0.00963	0.09178	0.06892	-0.07243	-0.03923	0.83790	-0.03980	0.11922	0.03806	0.00000
6 ln(Radius)	0.24498	0.19862	0.31130	-0.05374	0.05976	-0.1213	-0.19986	0.15054	-0.44772	-0.07017	0.04251	0.08863	0.06925	-0.70711
7 ln(Ulna)	0.24498	0.19862	0.31130	-0.05374	0.05976	-0.1213	-0.19986	0.15054	-0.44772	-0.07017	0.04251	0.08863	0.06925	0.70711
8 ln(IVMc)	0.26770	0.09435	0.00235	0.14249	-0.12024	-0.4512	0.49410	-0.26253	0.03389	-0.13491	0.52353	-0.18999	0.19608	0.00000
9 ln(I)	0.26319	0.19207	0.08111	-0.15055	-0.39727	0.18633	0.35684	0.00789	-0.03767	-0.09664	-0.61329	-0.34554	0.19590	0.00000
10 ln(II)	0.26336	0.07445	0.08024	0.21338	-0.15166	0.19516	0.18662	0.13077	0.29718	-0.30855	-0.02192	0.75802	0.03891	0.00000
11 ln(III)	0.23791	0.18676	0.17547	0.05008	-0.15314	0.46905	-0.48113	-0.17932	0.34691	-0.08983	0.34721	-0.30638	0.15900	0.00000
12 ln(IV)	0.23523	0.32806	-0.46787	-0.54102	0.39765	0.05877	-0.01204	-0.31067	0.01435	-0.00493	-0.02939	0.19157	0.17147	0.00000
13 ln(Femur)	0.26394	0.11449	0.05432	-0.10998	0.12006	-0.5301	-0.20842	0.41816	0.57147	0.10165	-0.17691	-0.12210	-0.07244	-0.00000
14 ln(Tibia)	0.27962	0.03736	0.12461	-0.23483	-0.06354	0.12534	0.16572	-0.11549	-0.01091	0.04316	0.11779	-0.04344	-0.87832	-0.00000

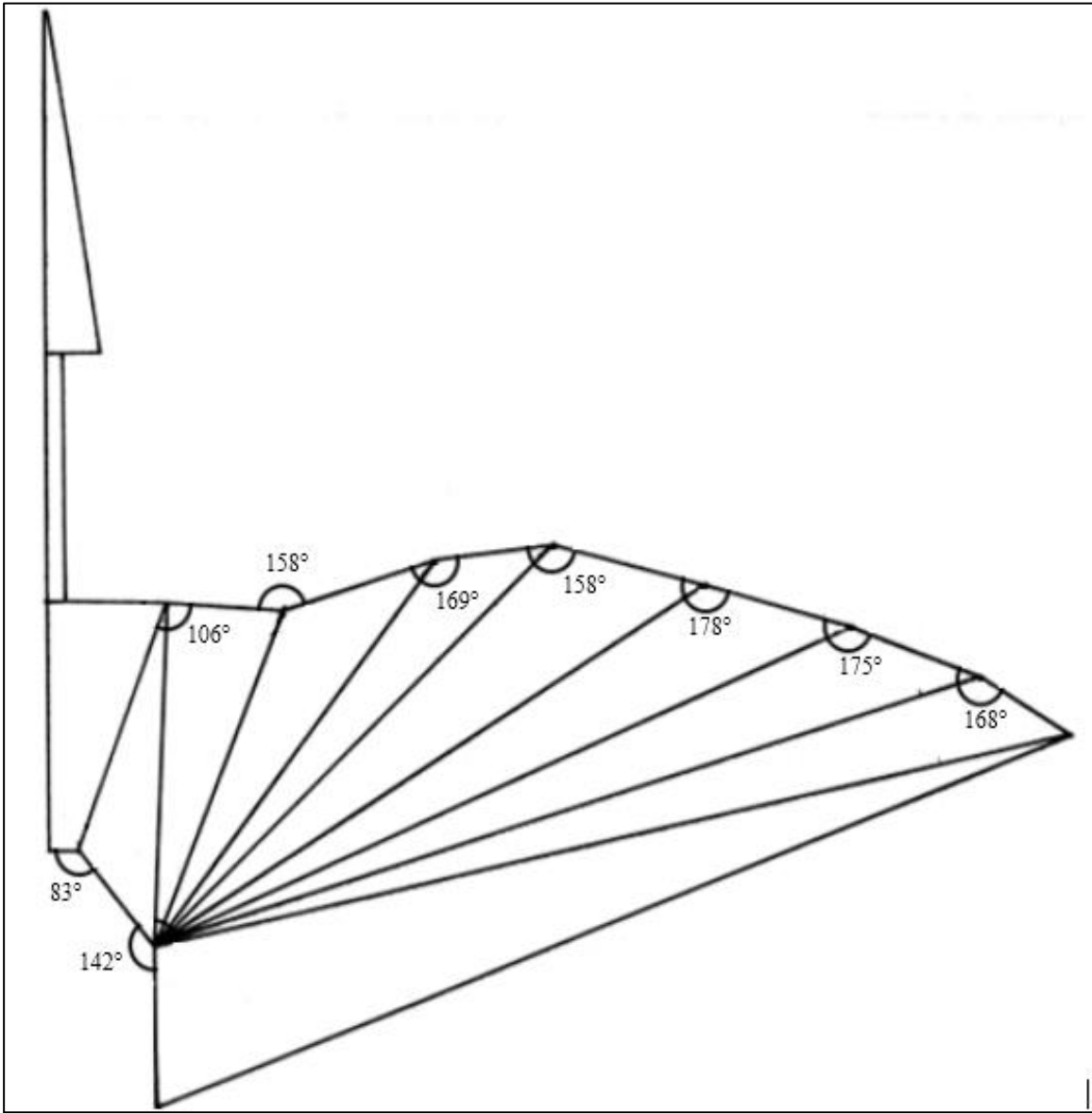
#### *Aurorazhdarcho micronyx*

Column 1	Prin1	Prin2	Prin3	Prin4	Prin5	Prin6	Prin7	Prin8	Prin9	Prin10	Prin11	Prin12	Prin13	Prin14
1 ln(Skull)	0.32643	-0.35077	-0.09200	-0.09651	-0.34571	-0.15706	-0.11028	-0.03715	0.61168	0.24748	0.12445	-0.13831	0.35339	0.00000
2 ln(Mandible)	0.37226	-0.58471	0.01701	-0.48548	0.13340	0.08380	0.20074	-0.22655	-0.36716	-0.01378	-0.07518	0.07086	-0.14646	-0.00000
3 ln(Cervicals)	0.30377	-0.29789	-0.37474	0.63514	0.22371	-0.12072	-0.25905	0.07695	-0.22895	-0.14550	-0.20196	-0.03307	0.14841	0.00000
4 ln(PCRW)	0.22226	0.07660	-0.07828	-0.06396	-0.19911	0.24450	-0.47006	0.22414	-0.28108	0.09209	0.63850	0.24909	-0.08171	-0.00000
5 ln(Humerus)	0.19743	0.07434	-0.04409	0.14645	0.10353	0.12430	0.68704	0.46697	-0.11224	0.29402	0.18258	0.05168	0.28425	0.00000
6 ln(Radius)	0.21895	0.11149	0.03630	0.23674	0.16077	-0.00418	0.17101	-0.40003	0.16765	-0.00639	0.29245	0.02432	-0.22994	-0.70711
7 ln(Ulna)	0.21895	0.11149	0.03630	0.23674	0.16077	-0.00418	0.17101	-0.40003	0.16765	-0.00639	0.29245	0.02432	-0.22994	0.70711
8 ln(IVMc)	0.33896	0.24078	-0.27763	-0.17130	-0.12026	0.41056	0.10706	0.14914	0.21930	-0.64109	-0.11413	-0.17443	-0.03798	-0.00000
9 ln(I)	0.29107	0.26940	-0.00428	-0.09619	-0.12603	-0.43145	0.04017	0.00944	0.04334	-0.10891	-0.24147	0.74524	0.04760	0.00000
10 ln(II)	0.22737	0.05599	0.33387	0.29579	-0.43222	0.48237	-0.03299	-0.13117	-0.08267	0.31144	-0.43241	0.05849	-0.11912	-0.00000
11 ln(III)	0.16173	-0.07443	0.65909	0.14833	-0.23420	-0.31477	0.05448	0.10776	-0.20192	-0.43586	0.18439	-0.24086	0.14365	0.00000
12 ln(IV)	0.11961	-0.11868	0.46133	-0.02879	0.60136	0.23989	-0.25072	0.30158	0.37440	-0.01567	-0.07800	0.19609	-0.00053	-0.00000
13 ln(Femur)	0.28076	0.46712	0.05716	-0.22981	0.27443	-0.00358	-0.20403	-0.30113	-0.23025	0.18082	-0.08275	-0.26916	0.52369	0.00000
14 ln(Tibia)	0.32821	0.19640	-0.03244	-0.11056	0.04042	-0.36665	-0.08565	0.34677	0.00651	0.28218	-0.14405	-0.38823	-0.57064	-0.00000

**APPENDIX C**  
Bivariate Plots of All 14 In-lengths vs In-Geometric Mean

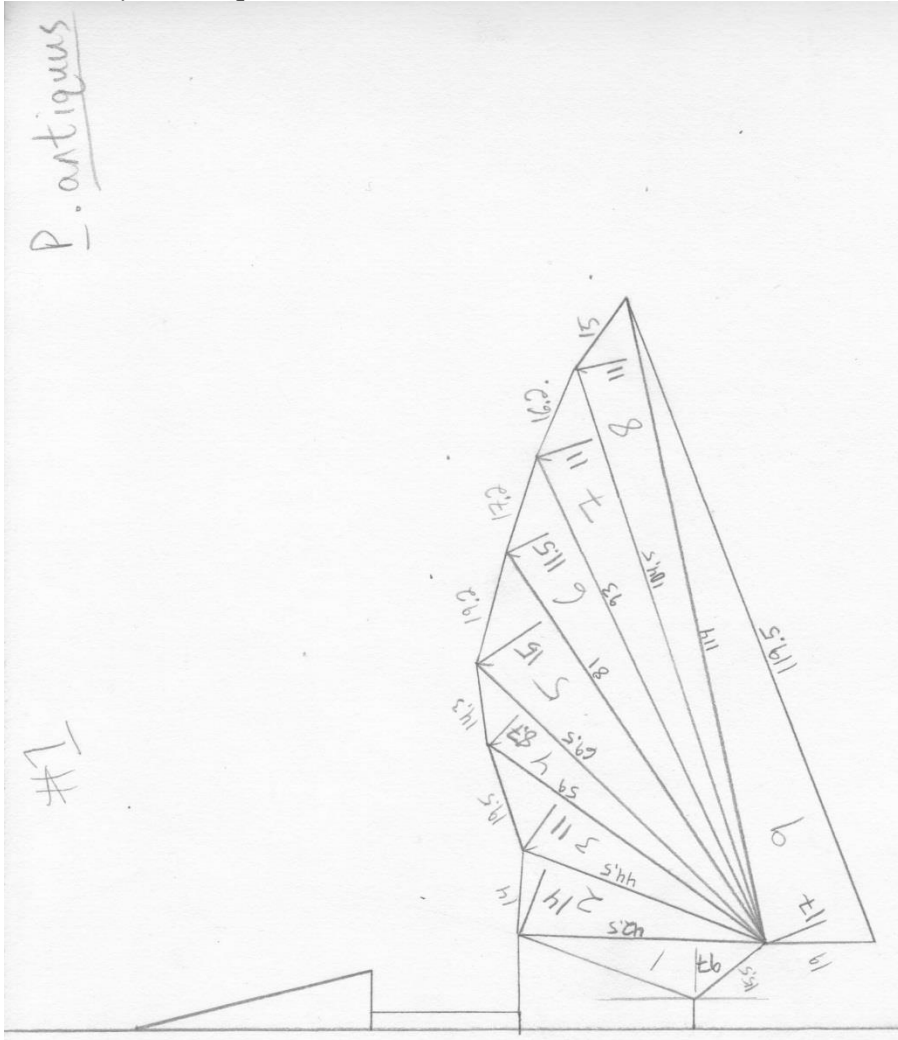


**APPENDIX D**  
Standardized Angles Used for Wing Reconstructions



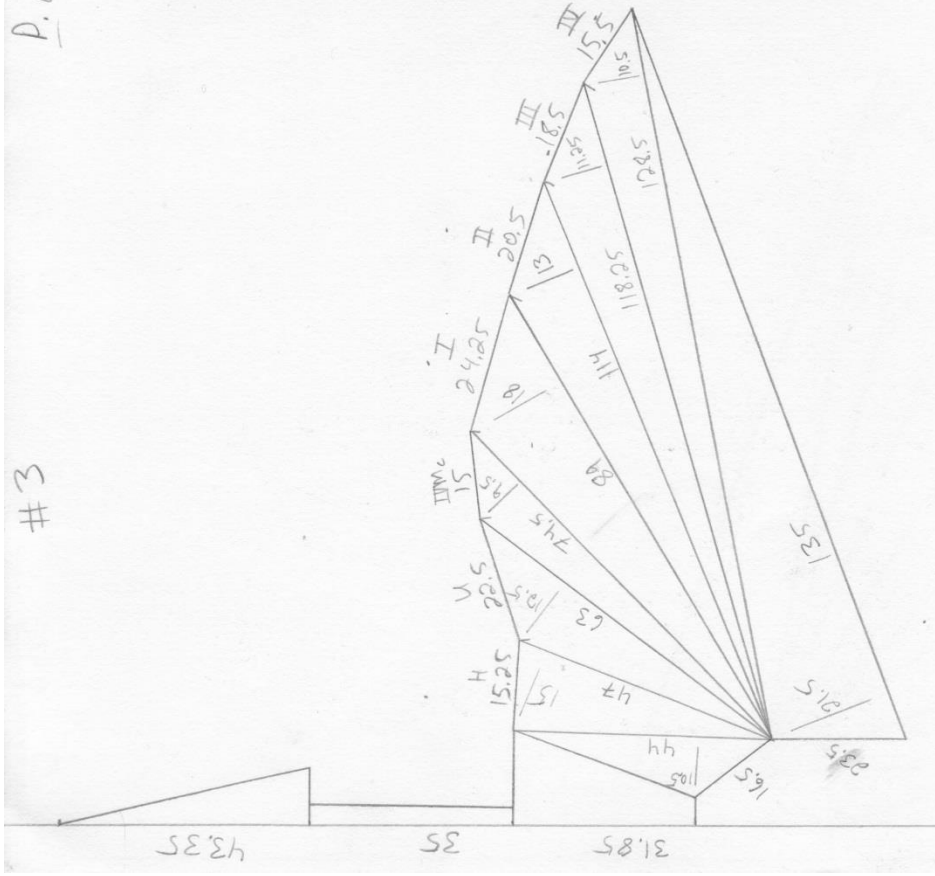
**APPENDIX E**  
All 39 Wing Reconstructions

*Pterodactylus antiquus*



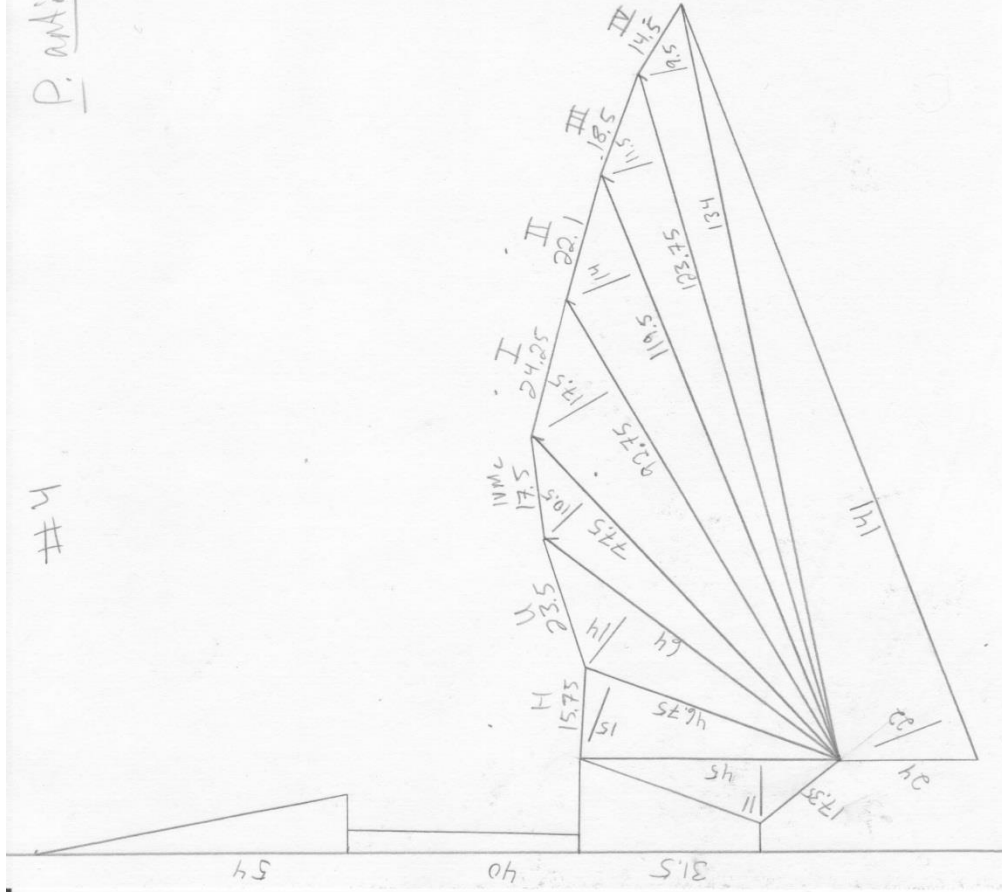
P. antiquus

#3



P. antiquus

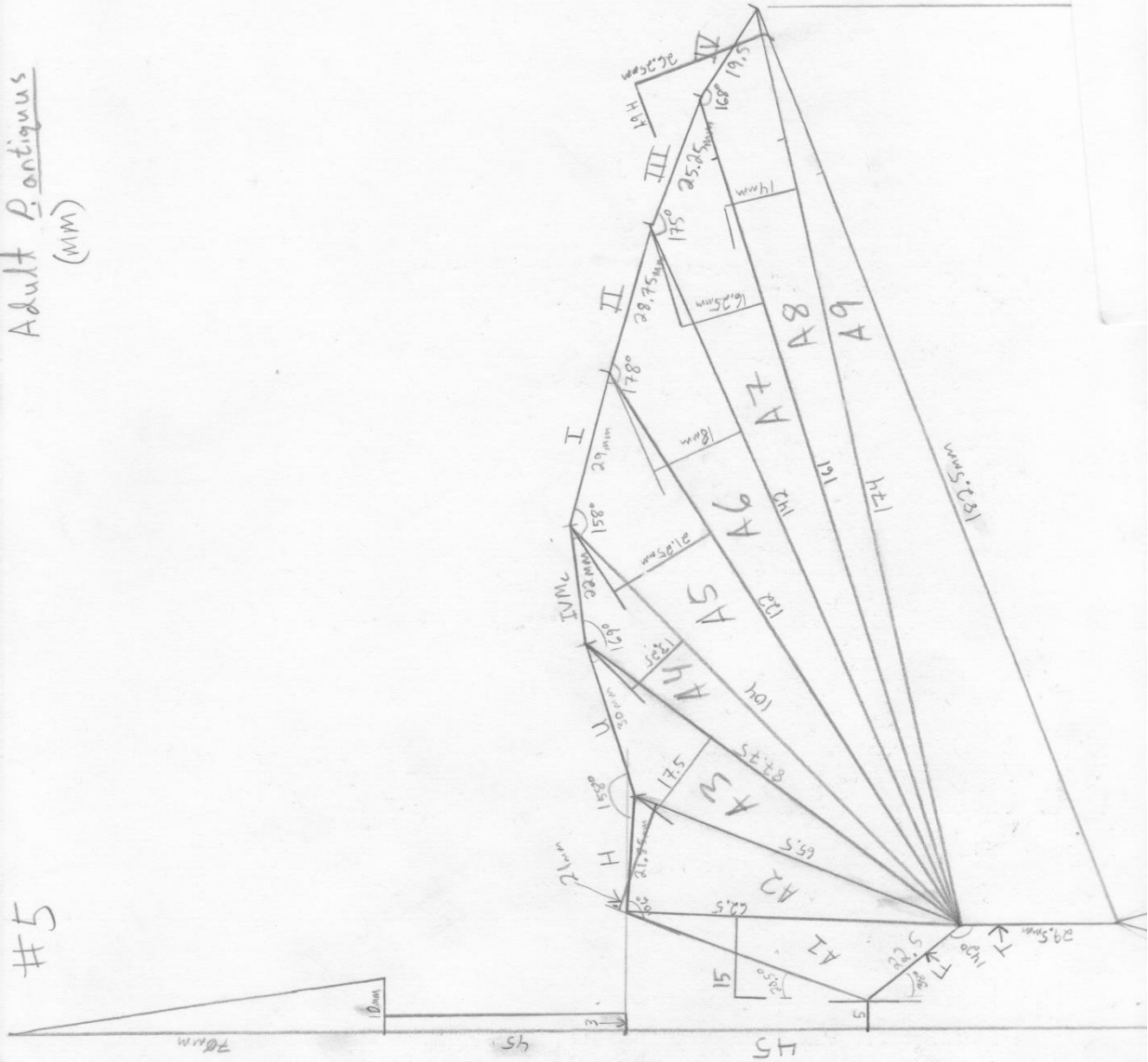
Y  
#





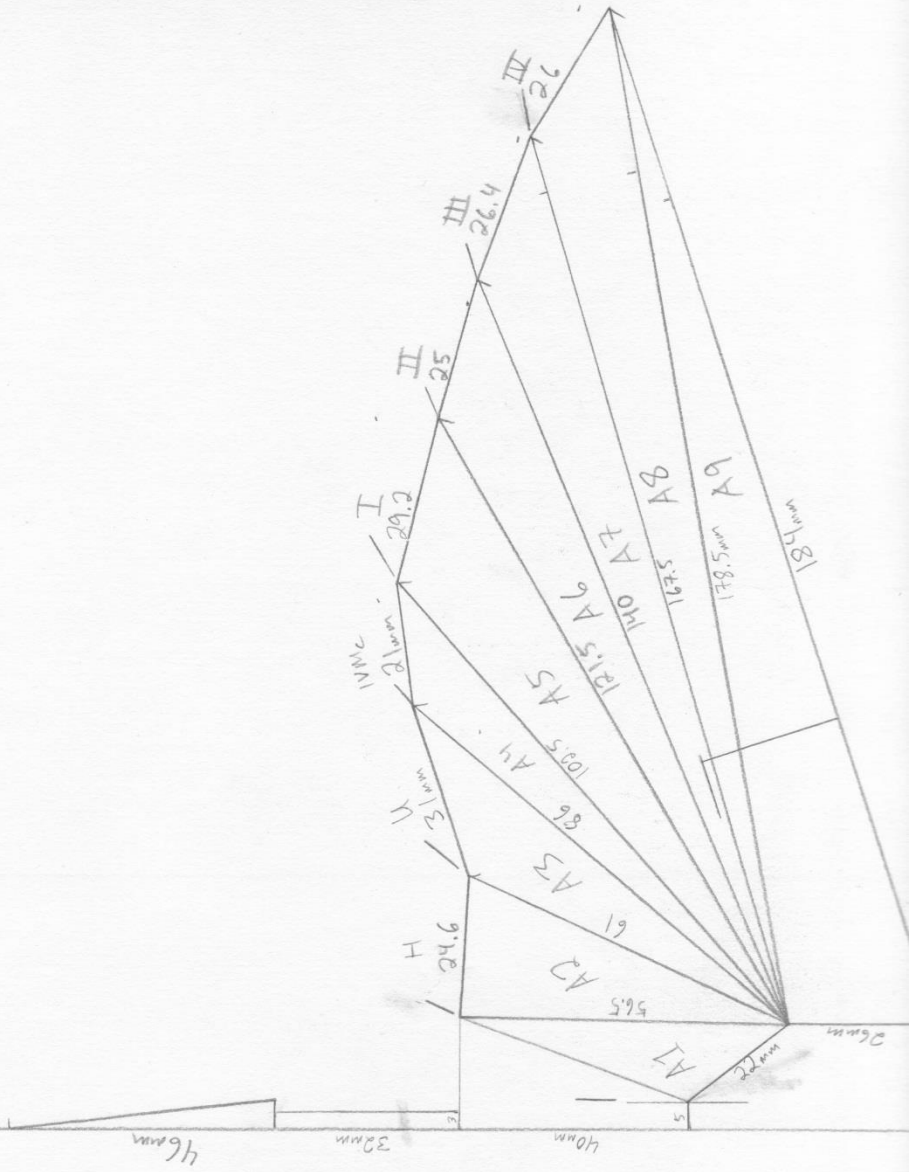
Adult Pontinus  
(MM)

#5



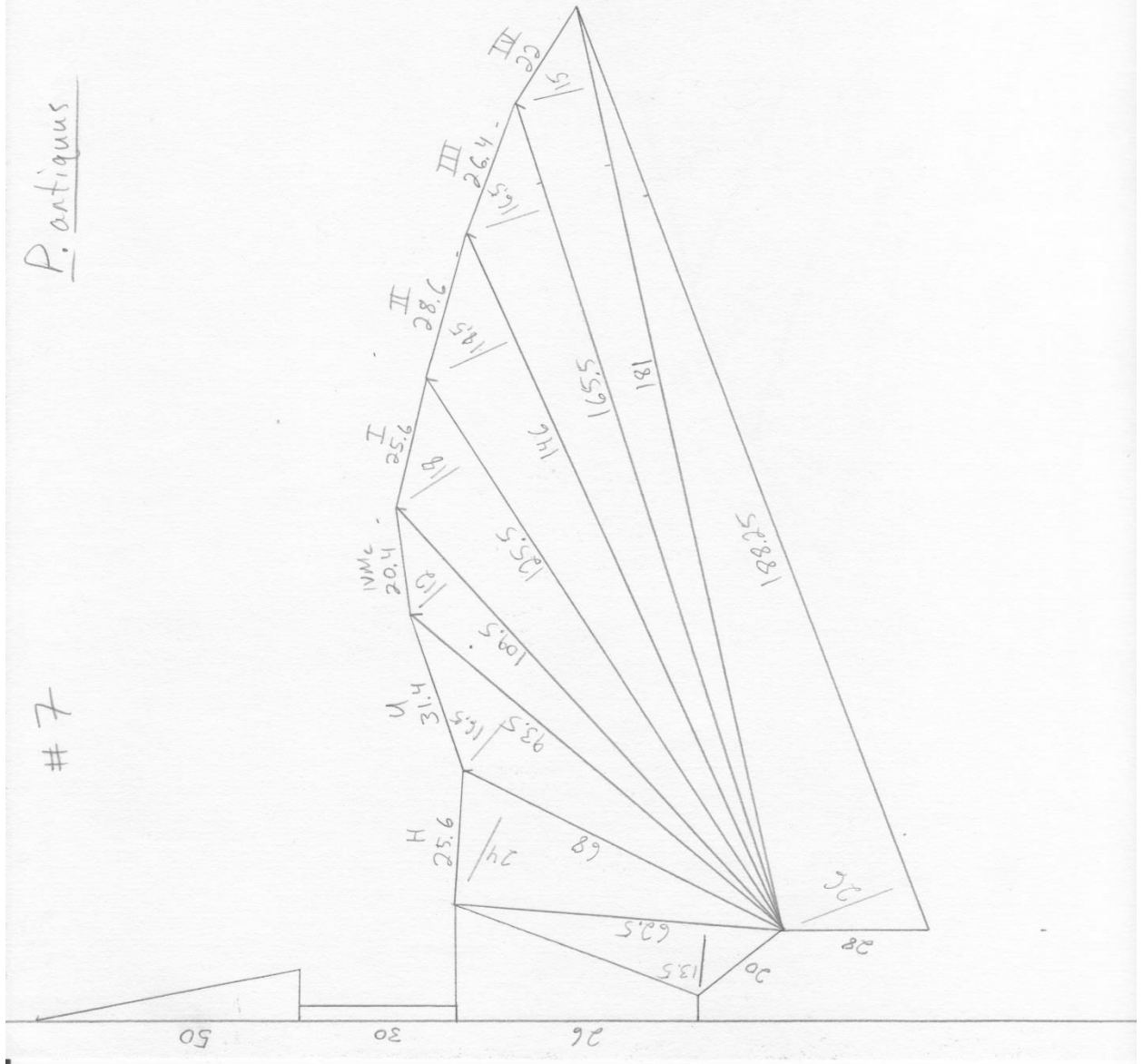
Juvenile *P. antiquus*

#6



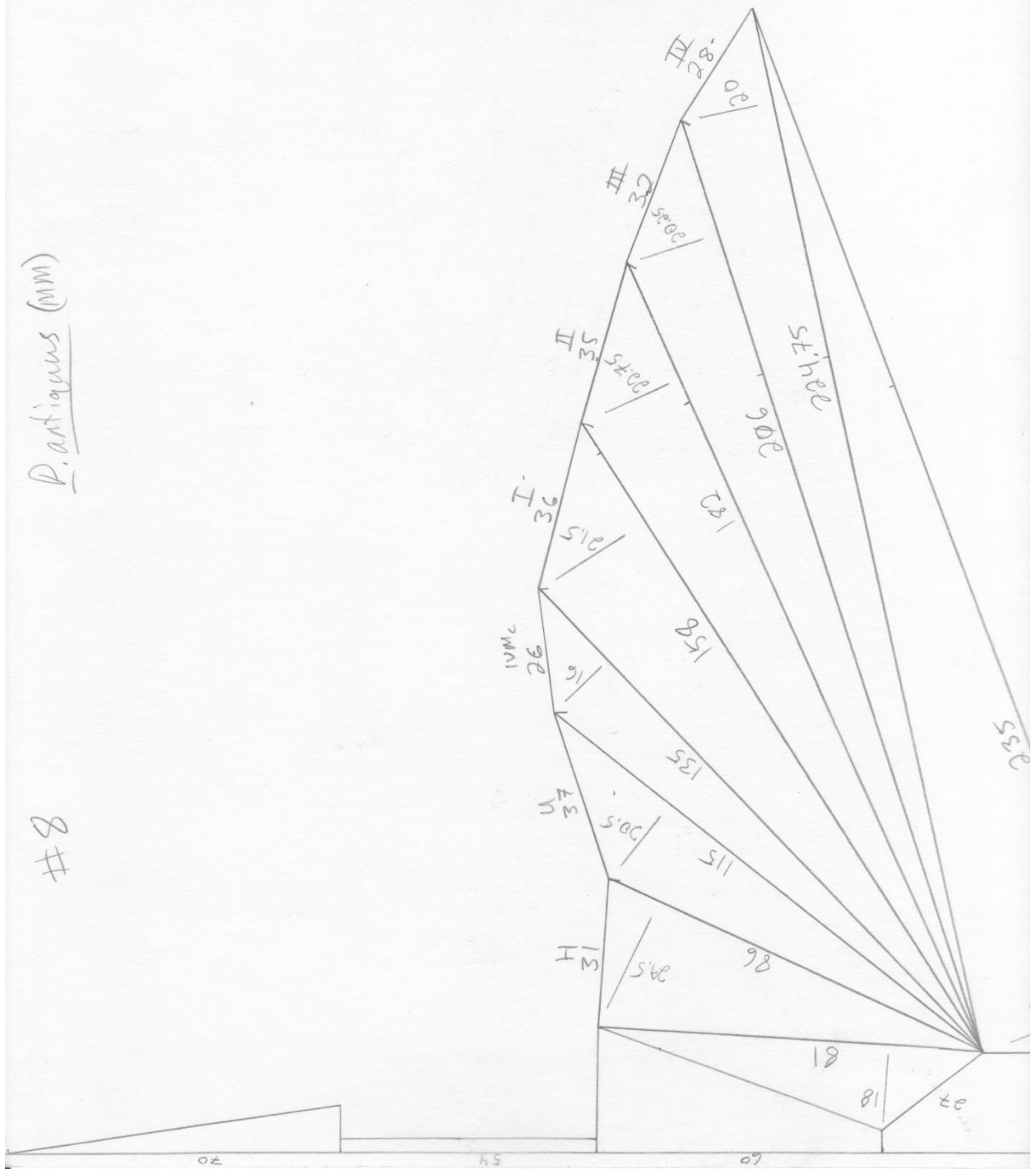
P. antiquus

# 7



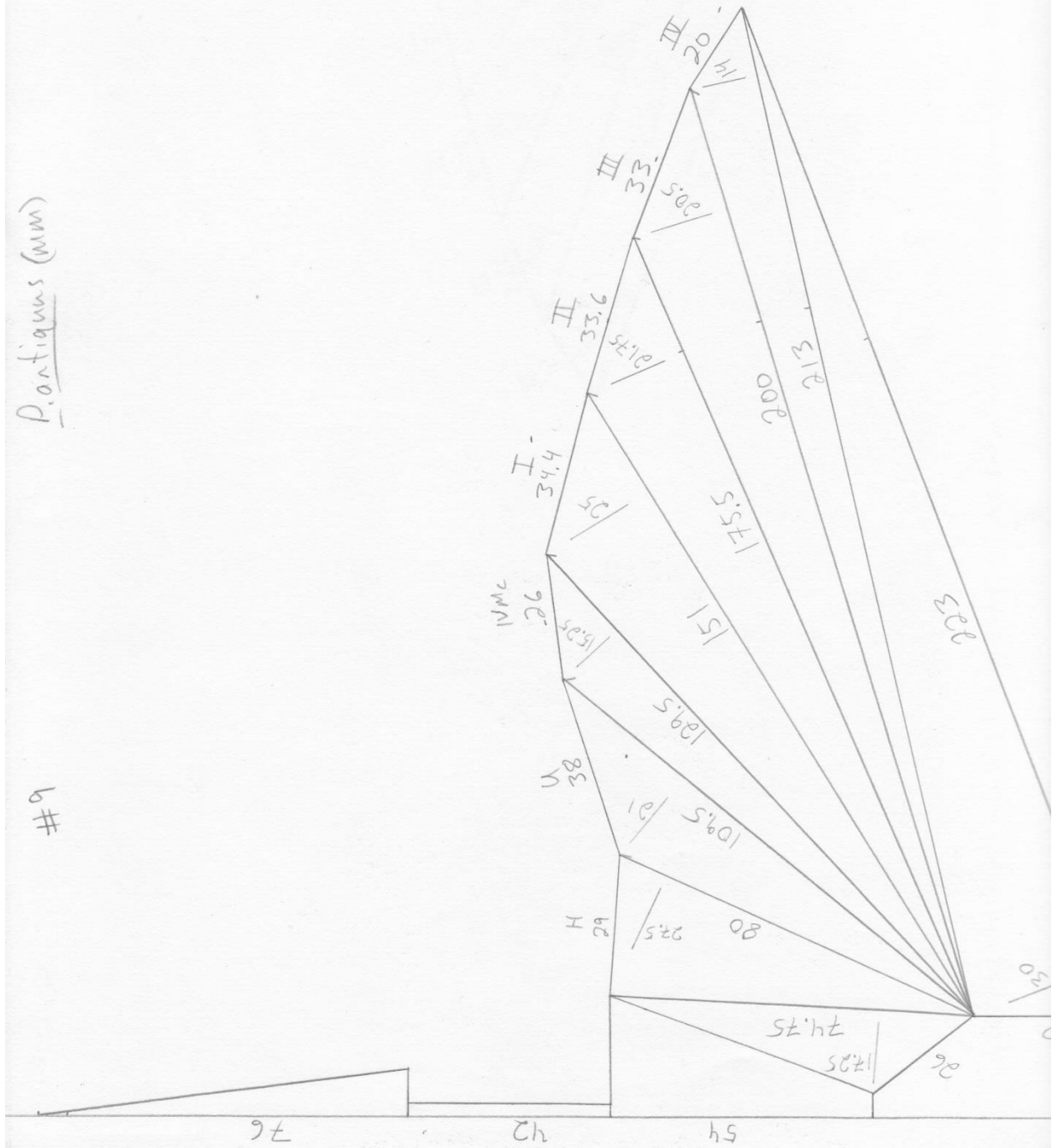
*P. antiquus* (mm)

#8



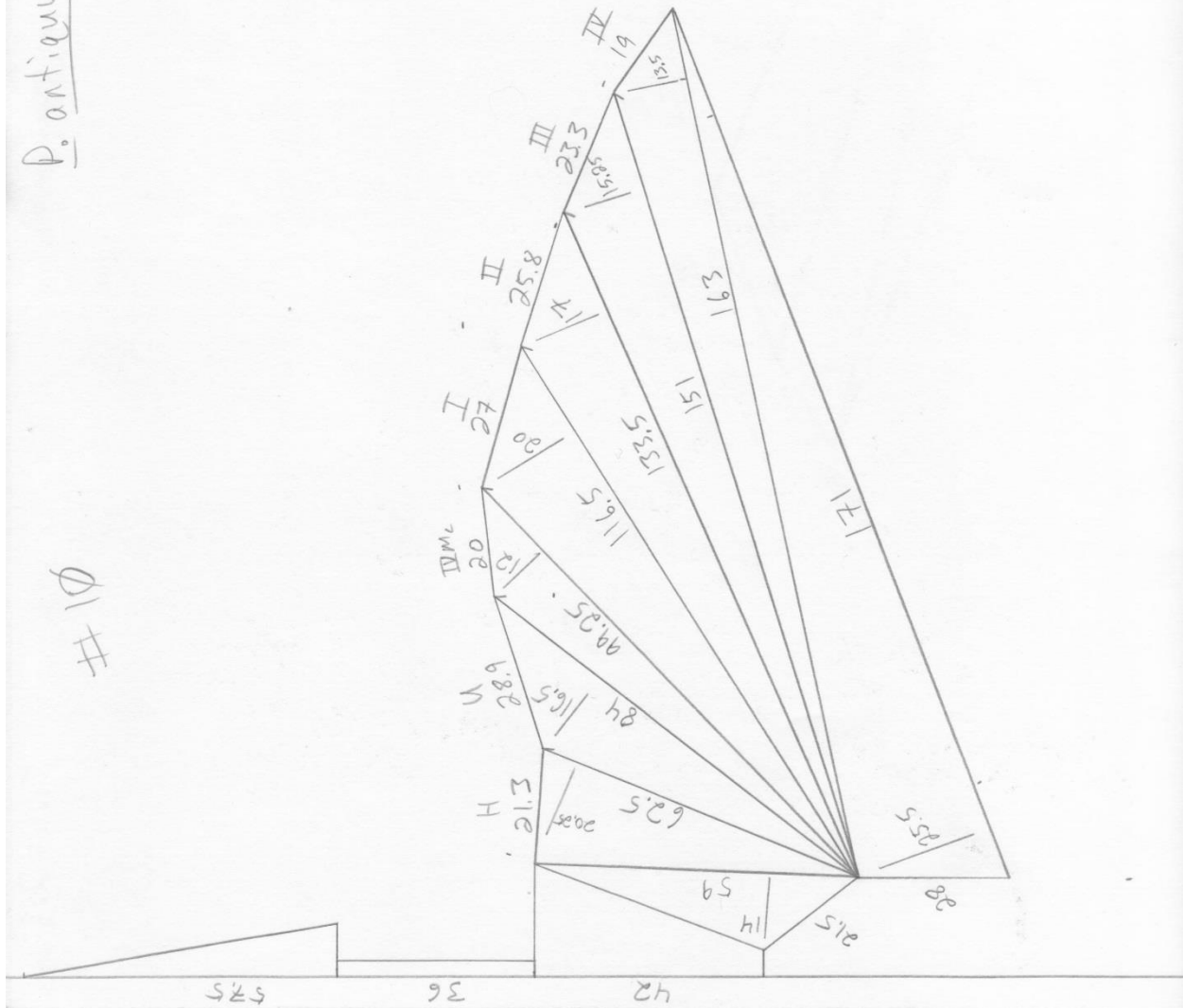
Ponticus (mm)

#9



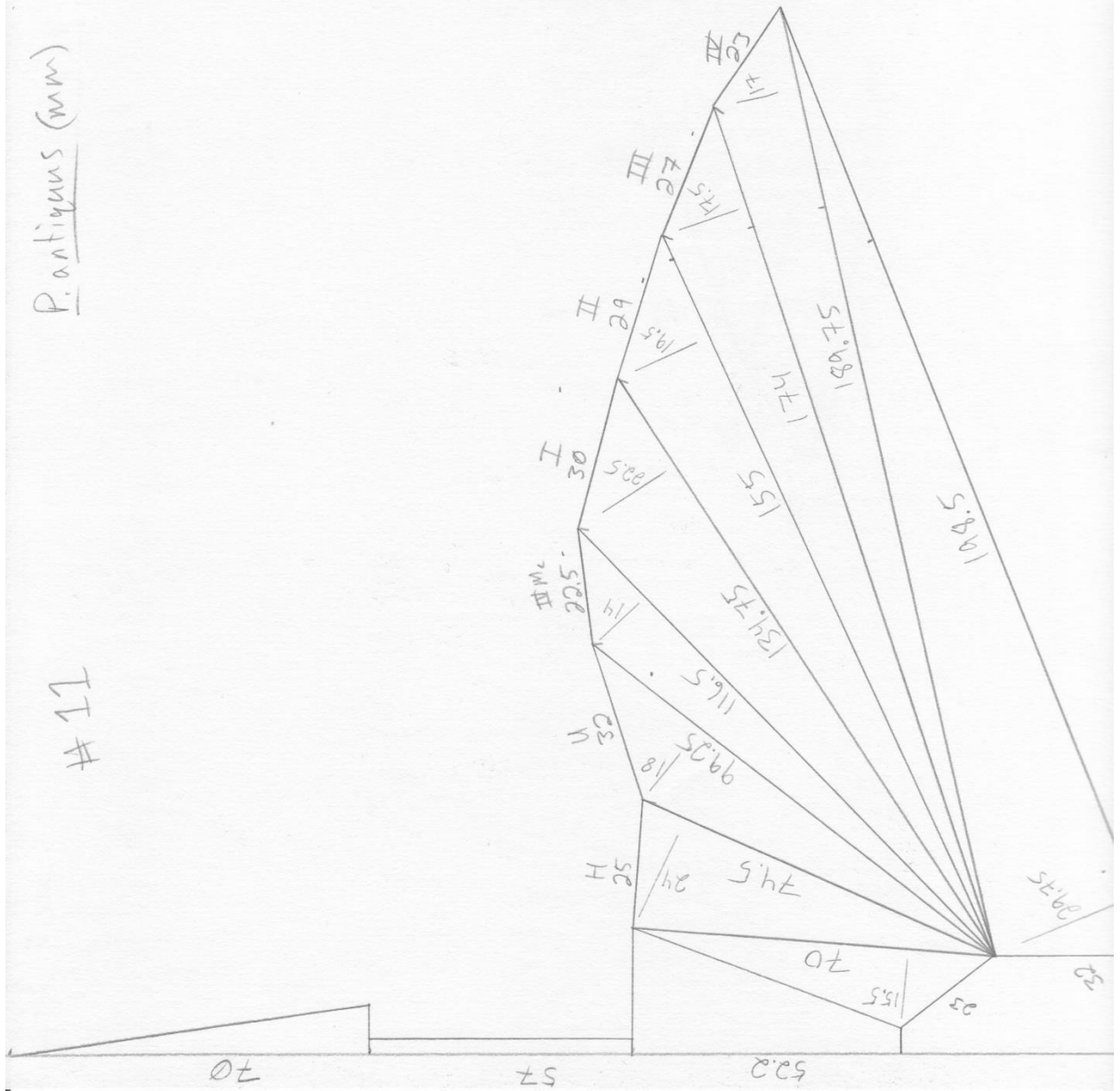
P. antiquus (mm)

# 10



P. antiquus (mm)

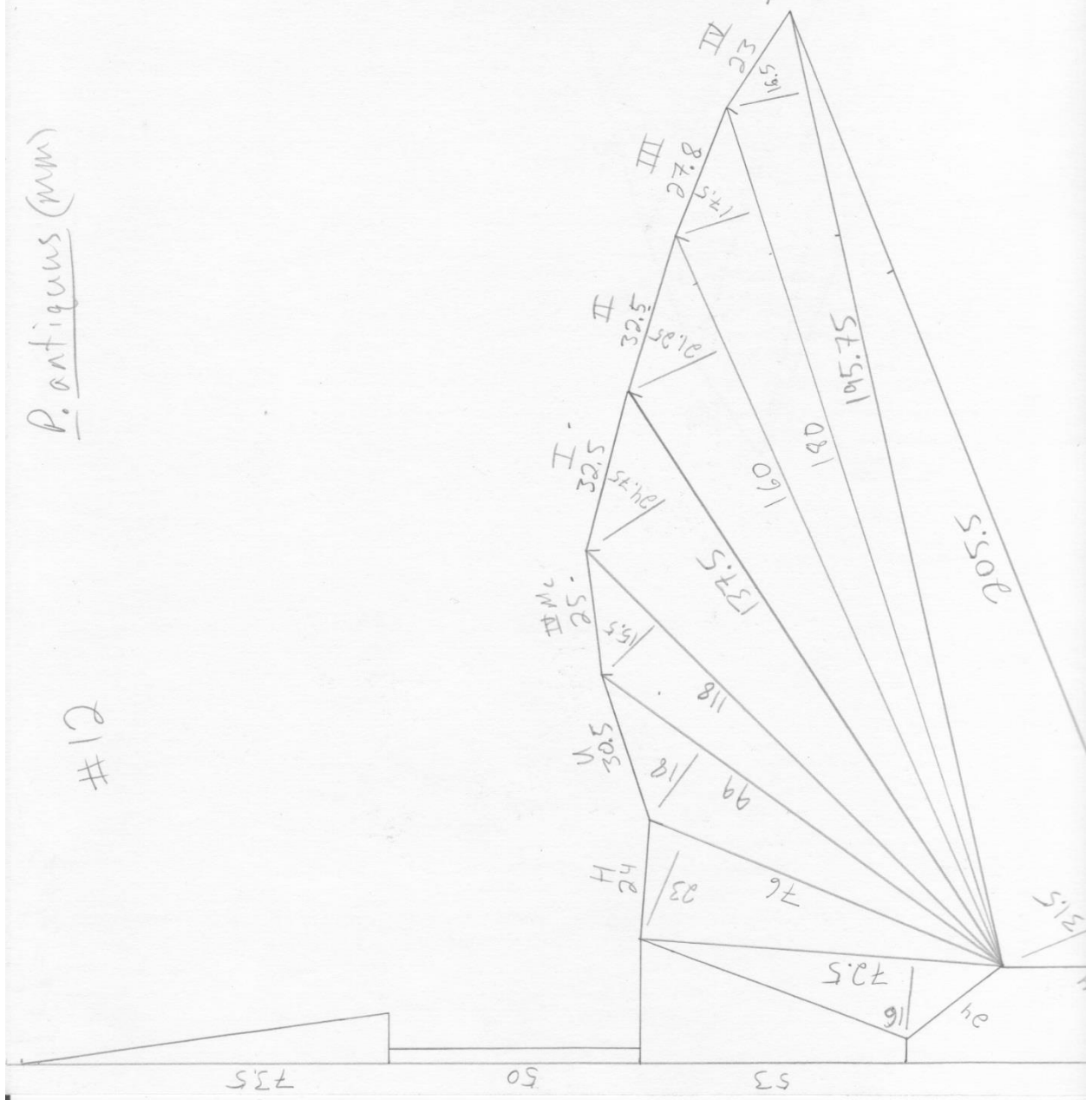
# 11





P. antiquus (mm)

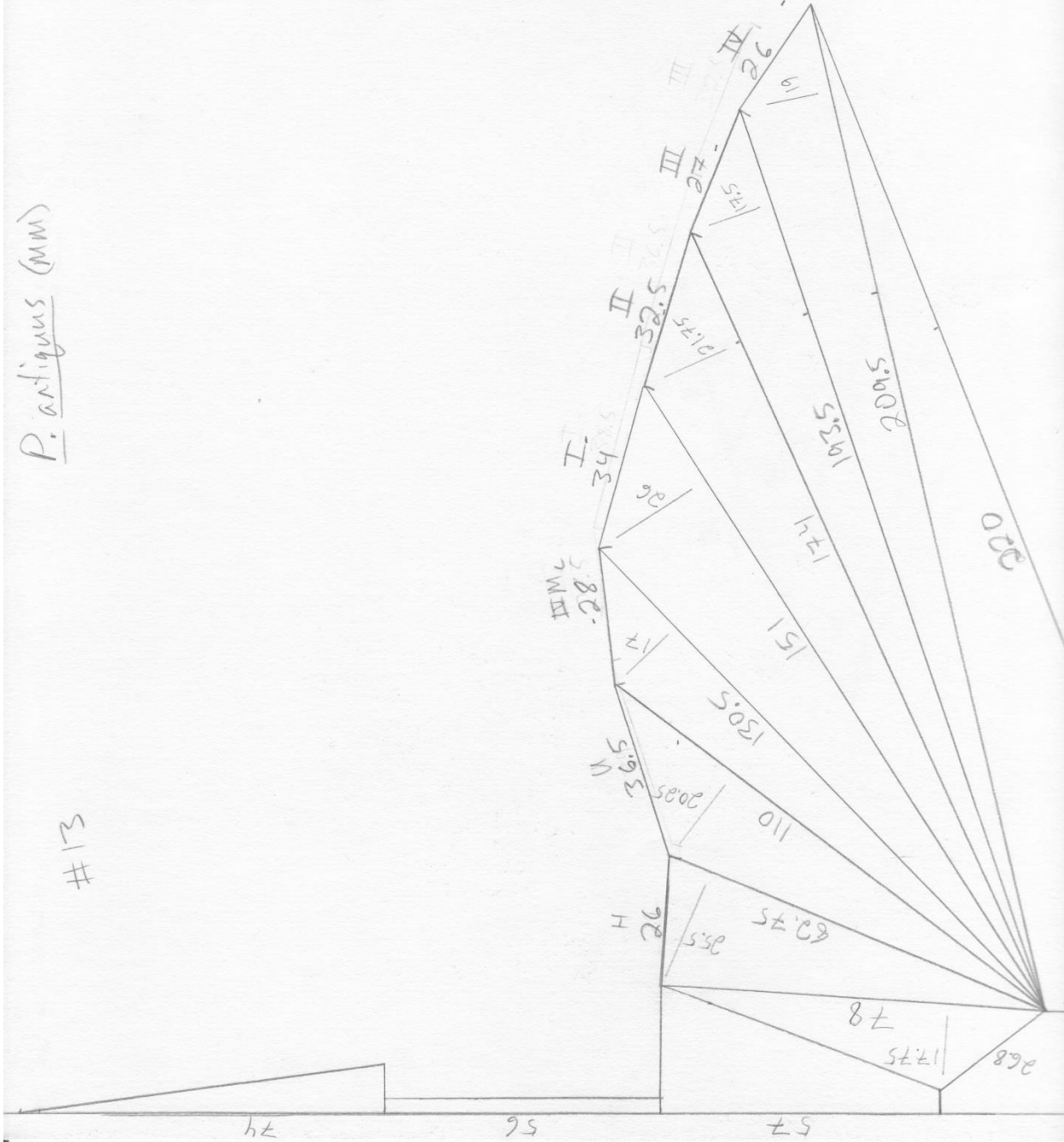
#12





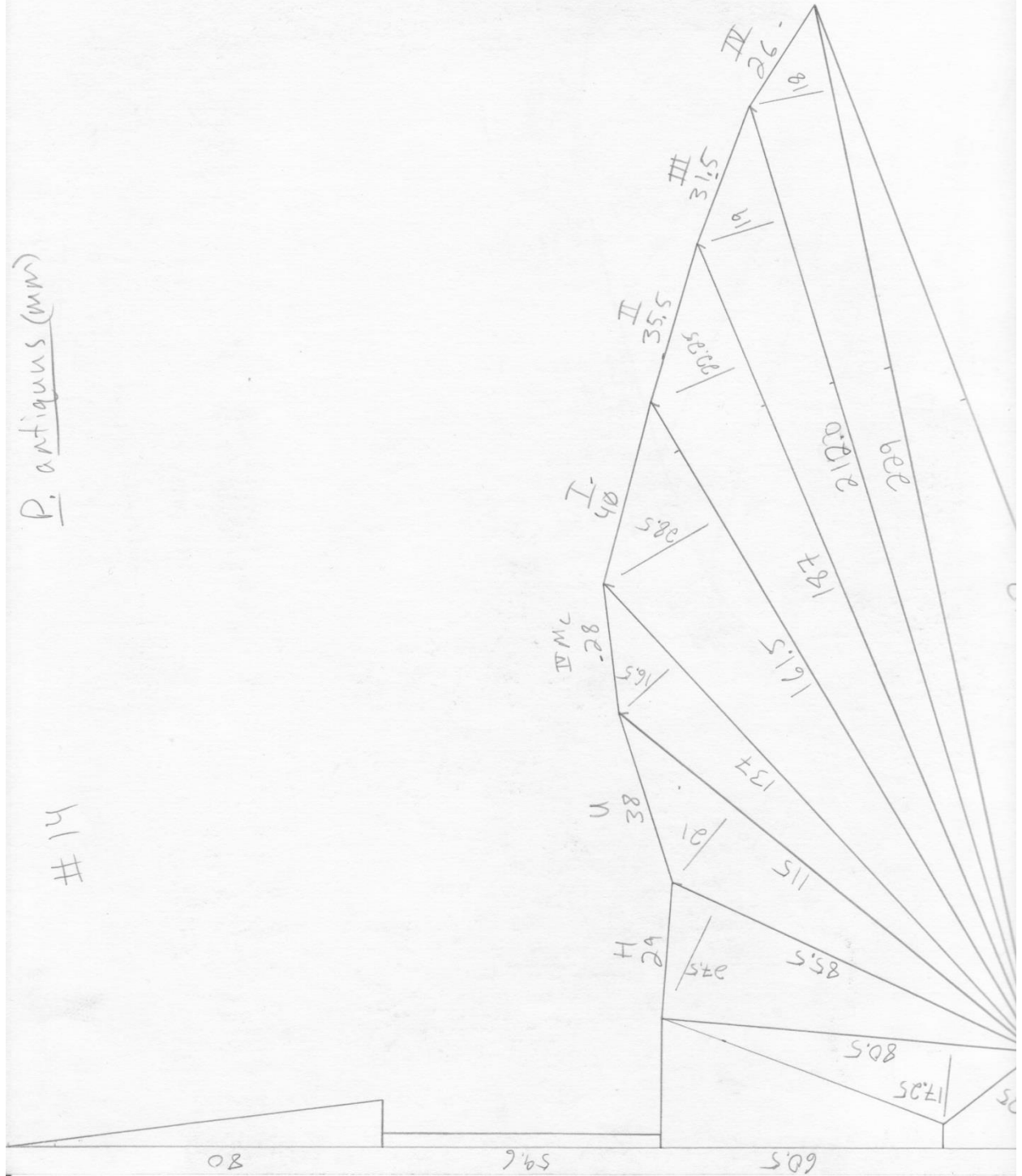
*P. antiquus* (mm)

#13



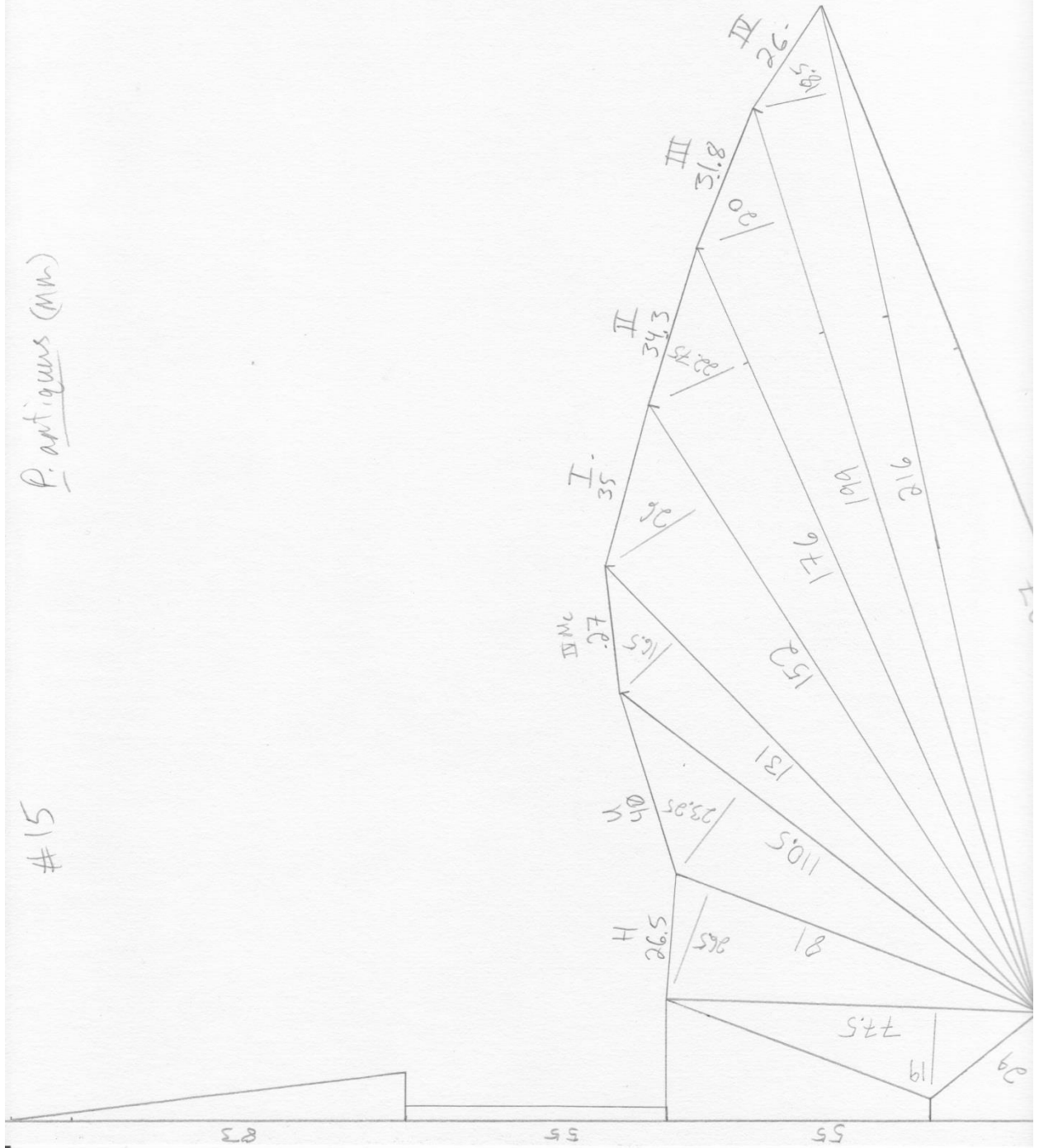
*P. antiquus* (mm)

# 14



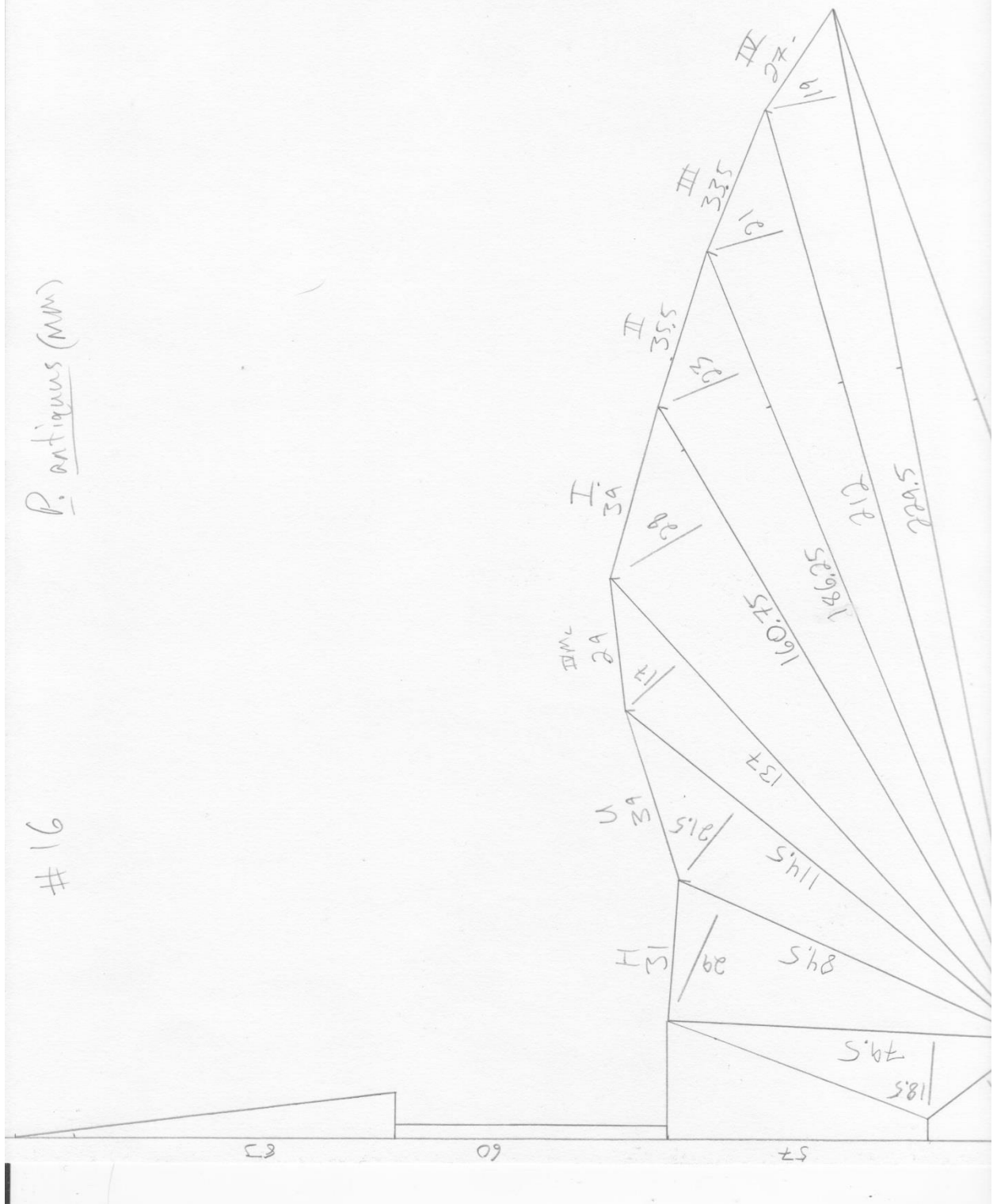
*P. antiquus* (mm)

#15



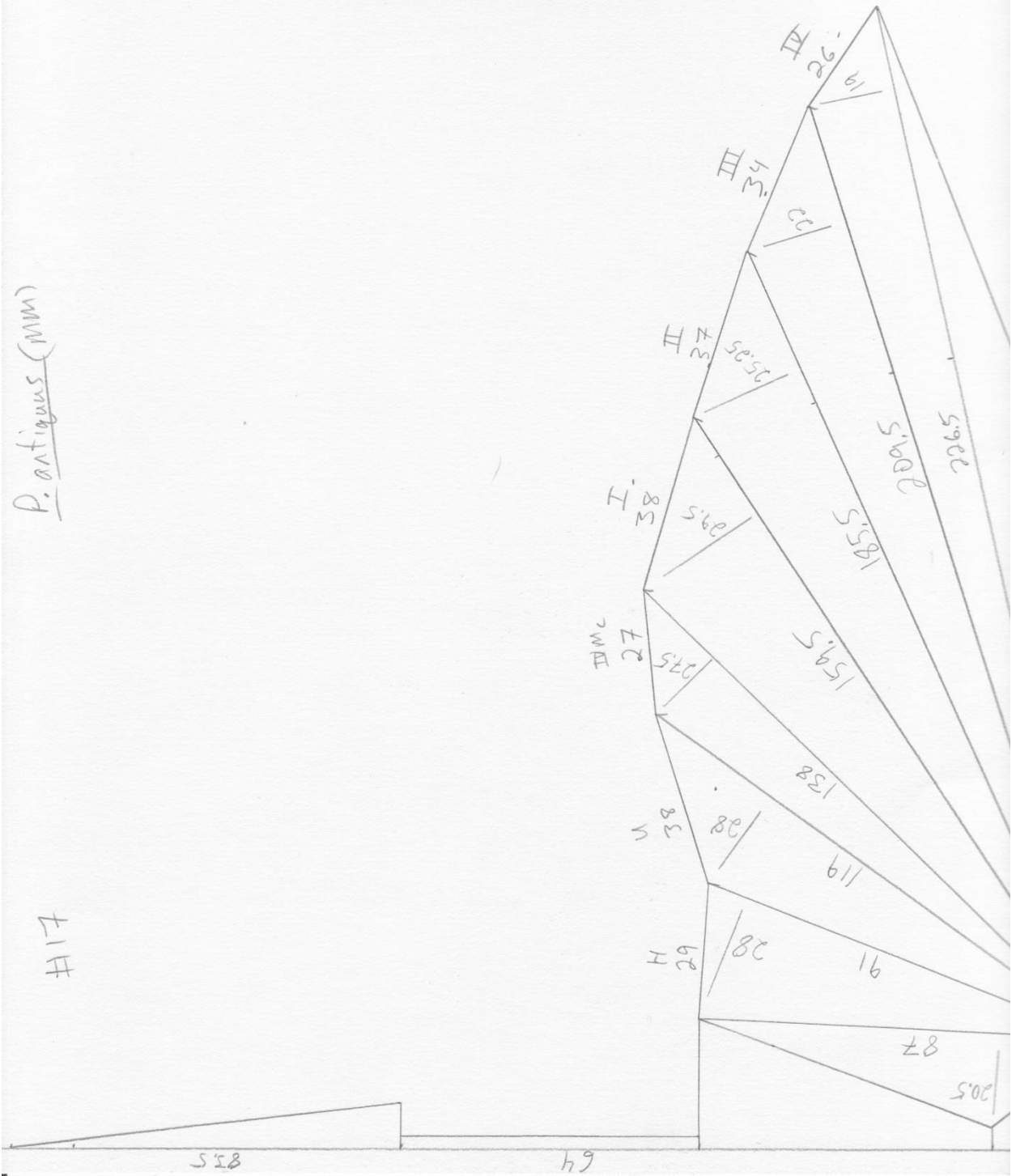
#16

*P. antiquus* (mm)



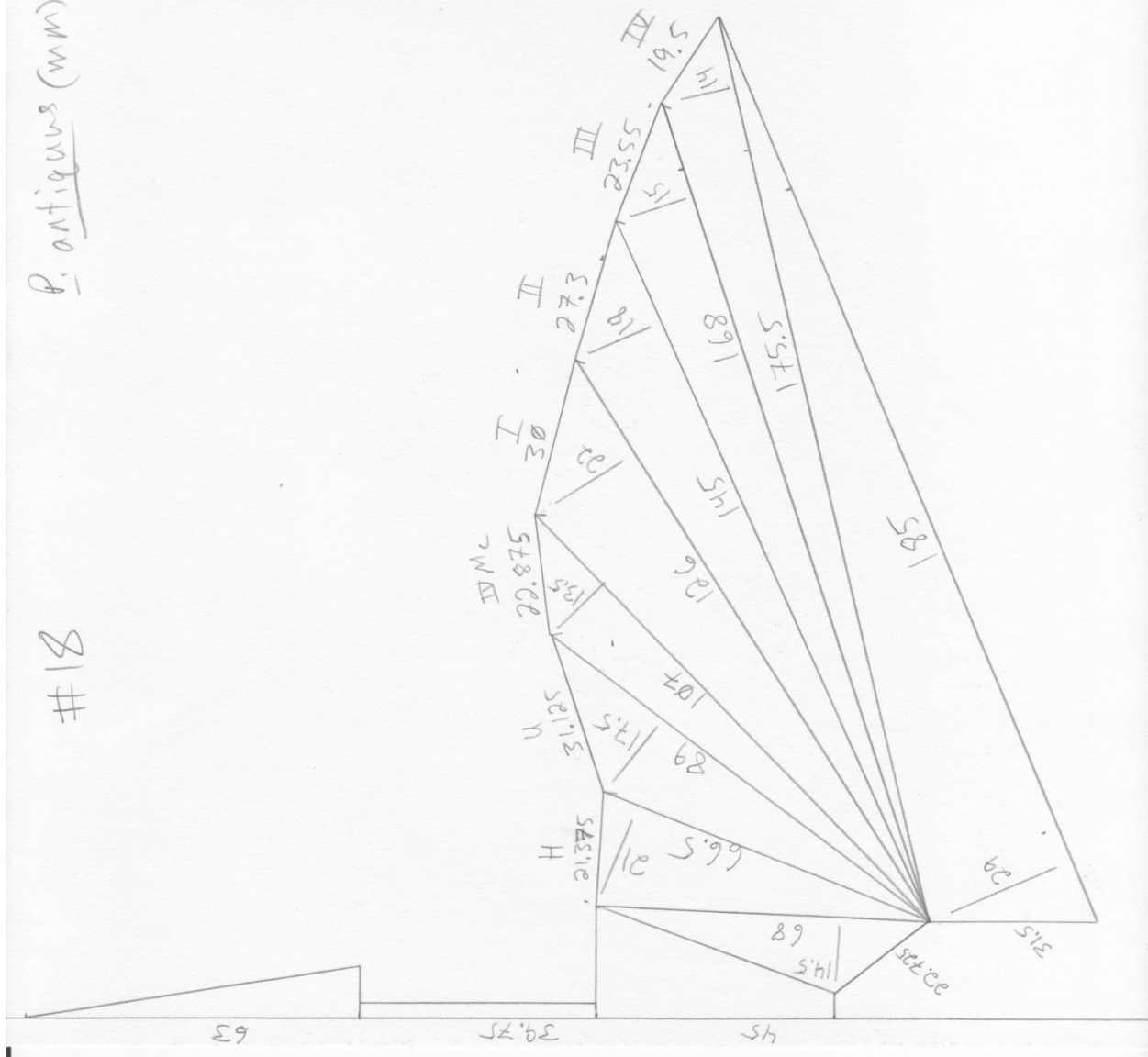
P. antiquus (mm)

F17



*P. antiquus* (mm)

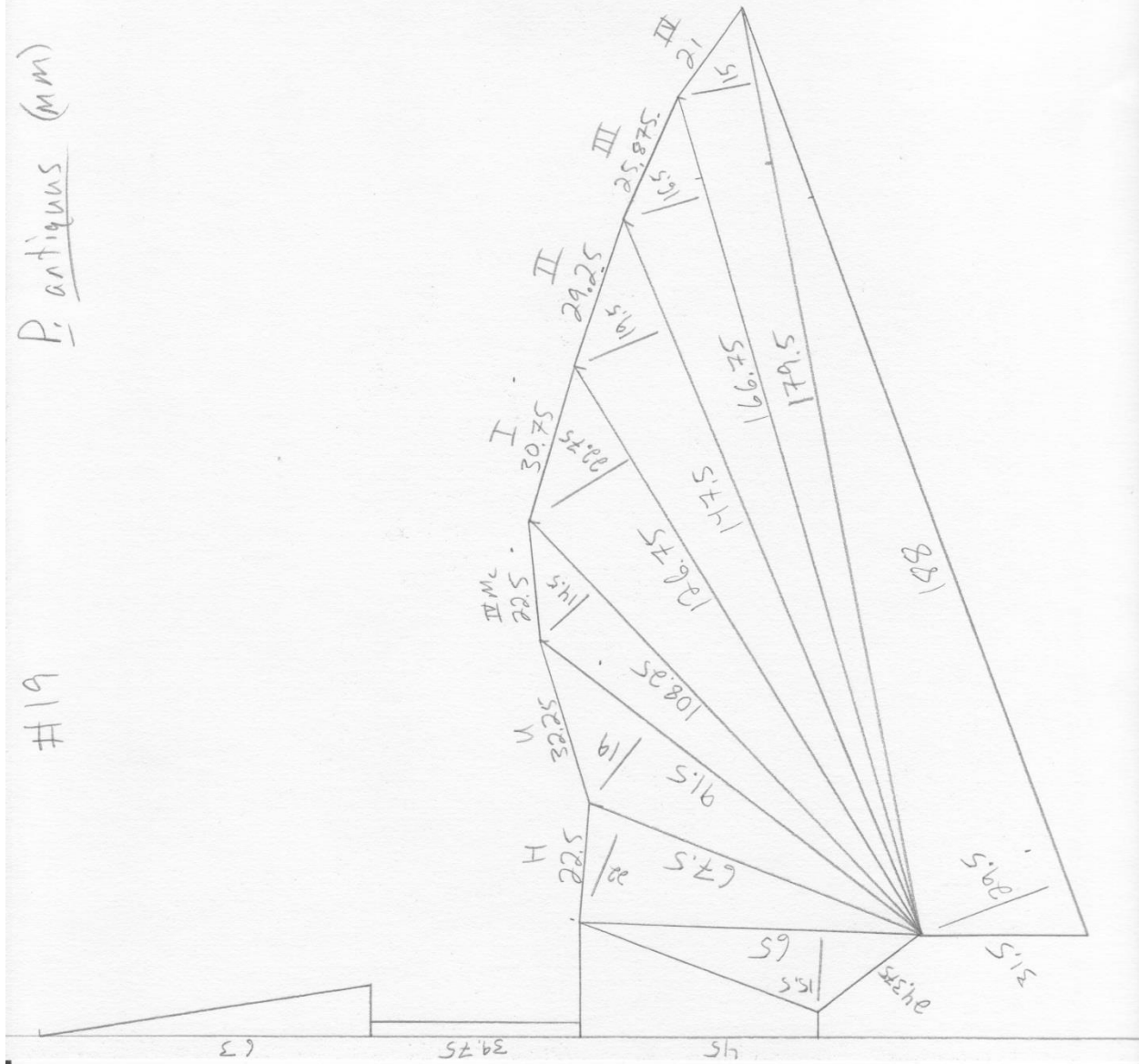
#18

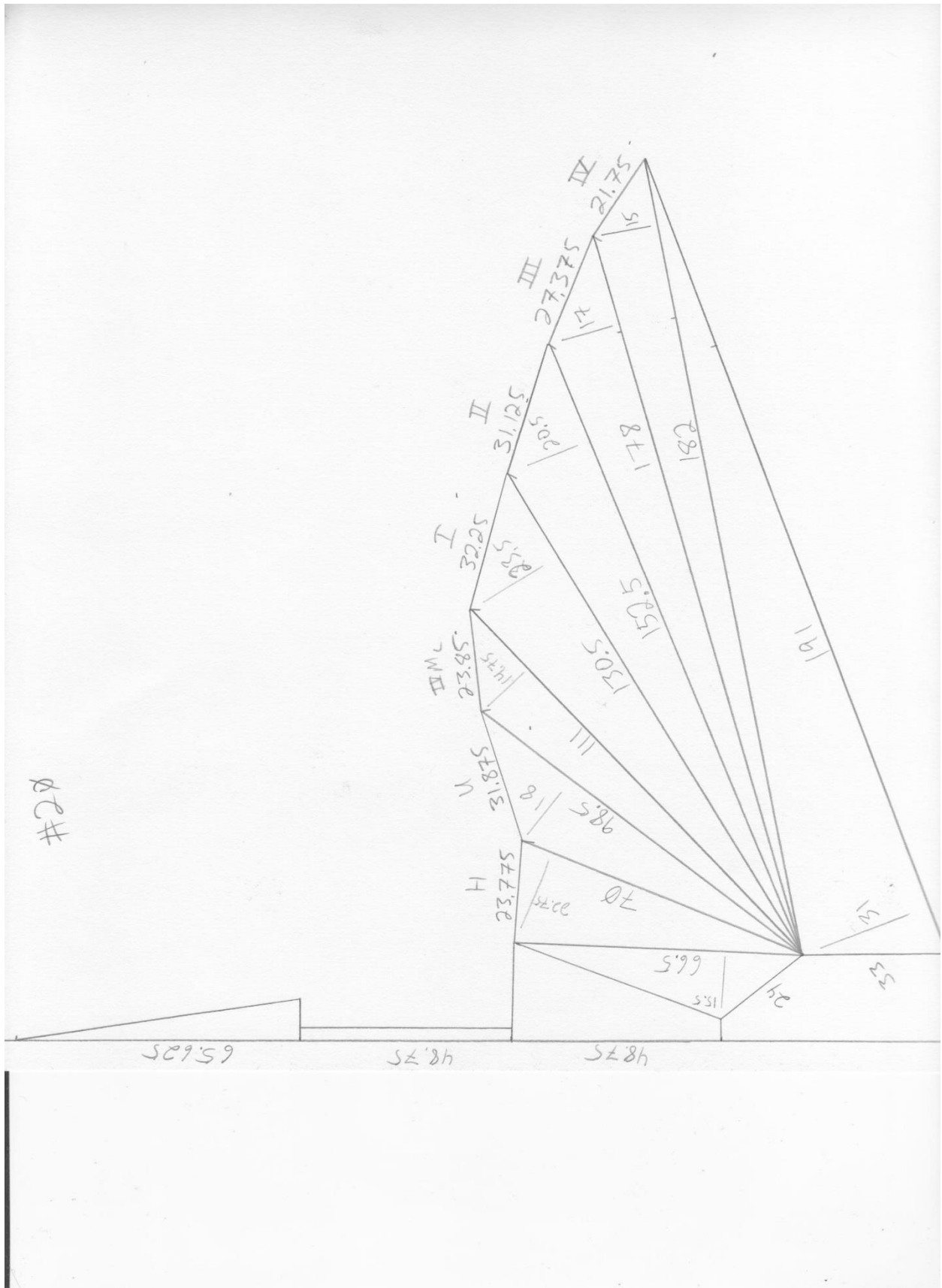




*P. antiquus* (mm)

#19

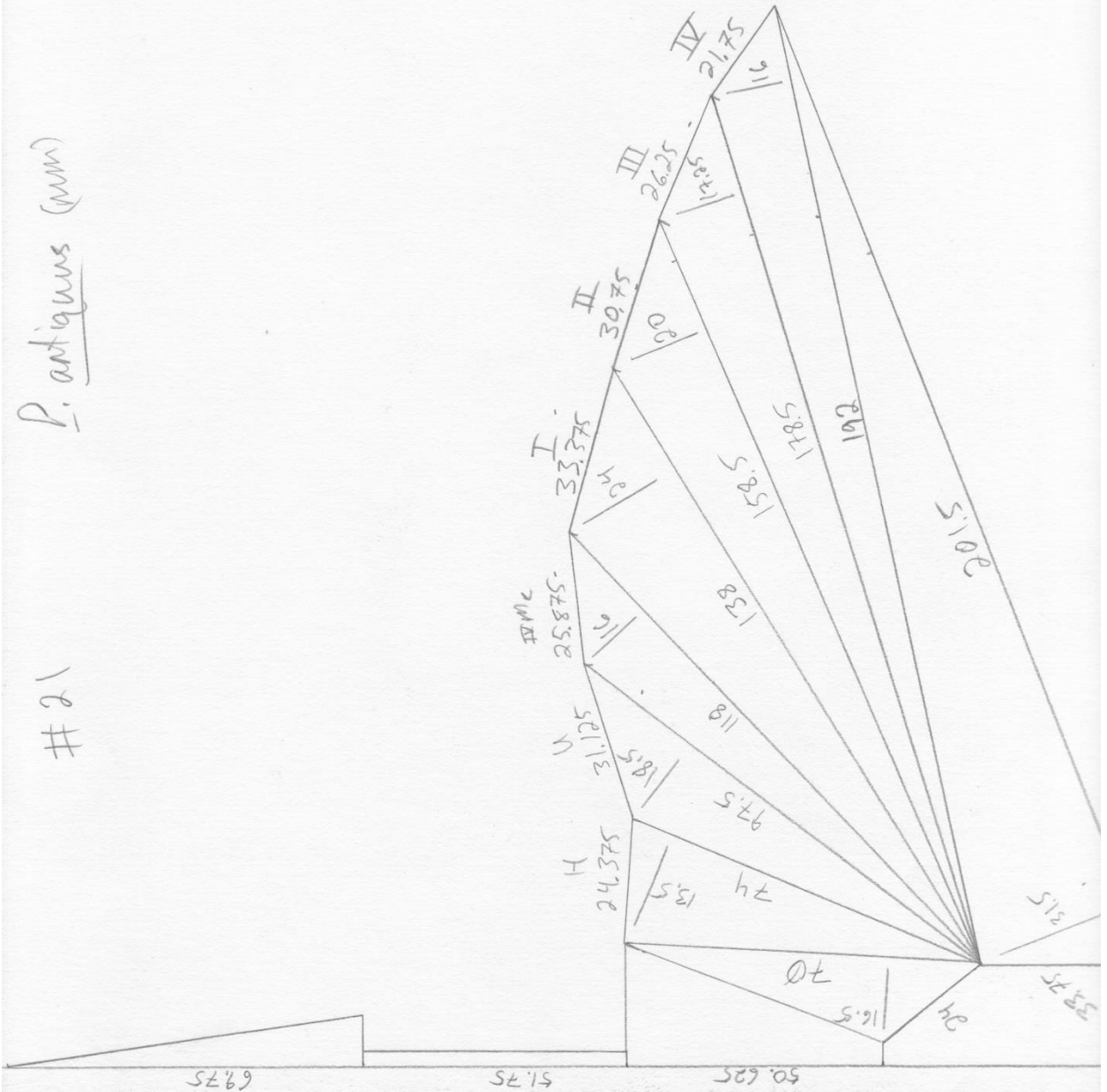






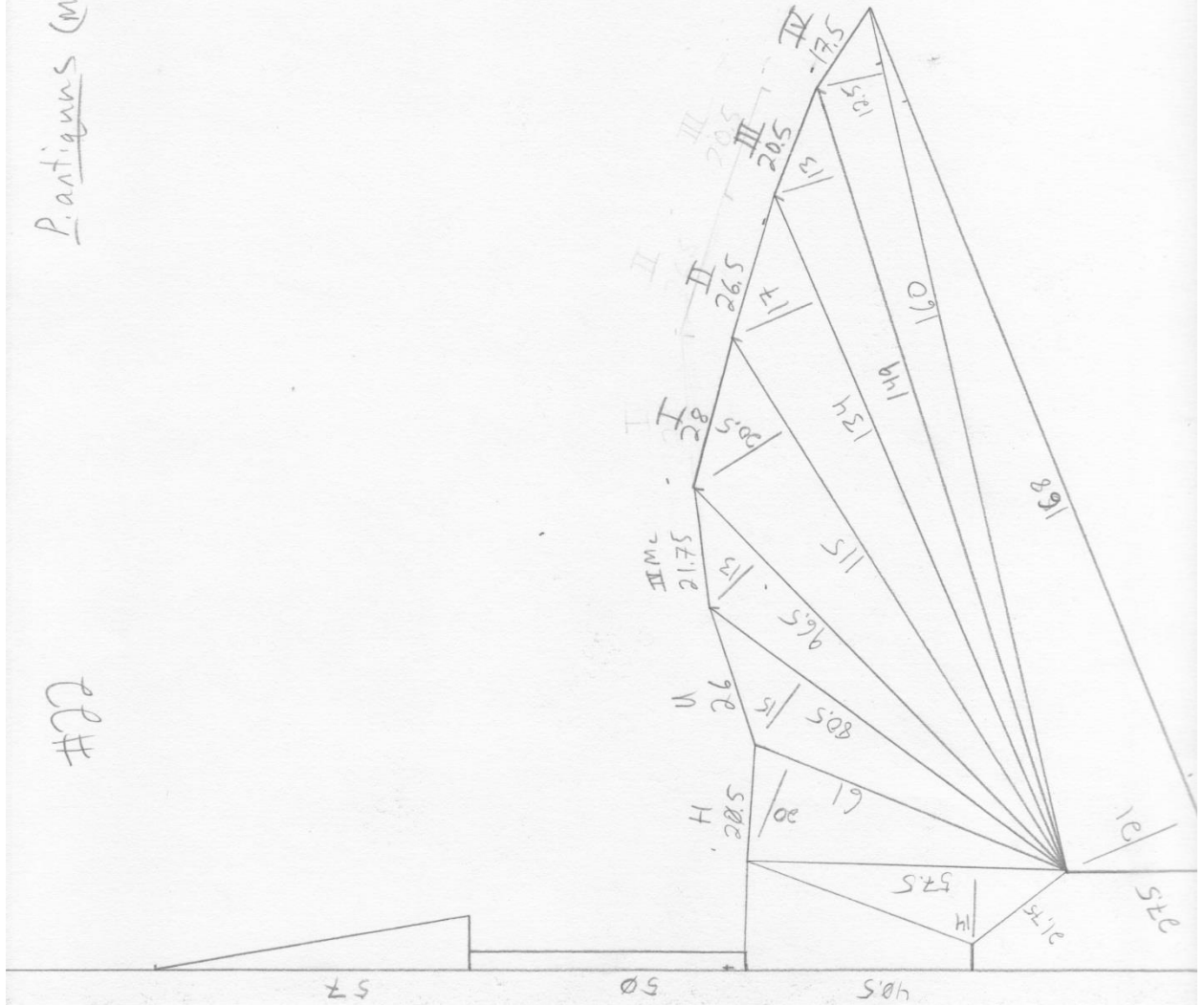
*P. antiquus* (mm)

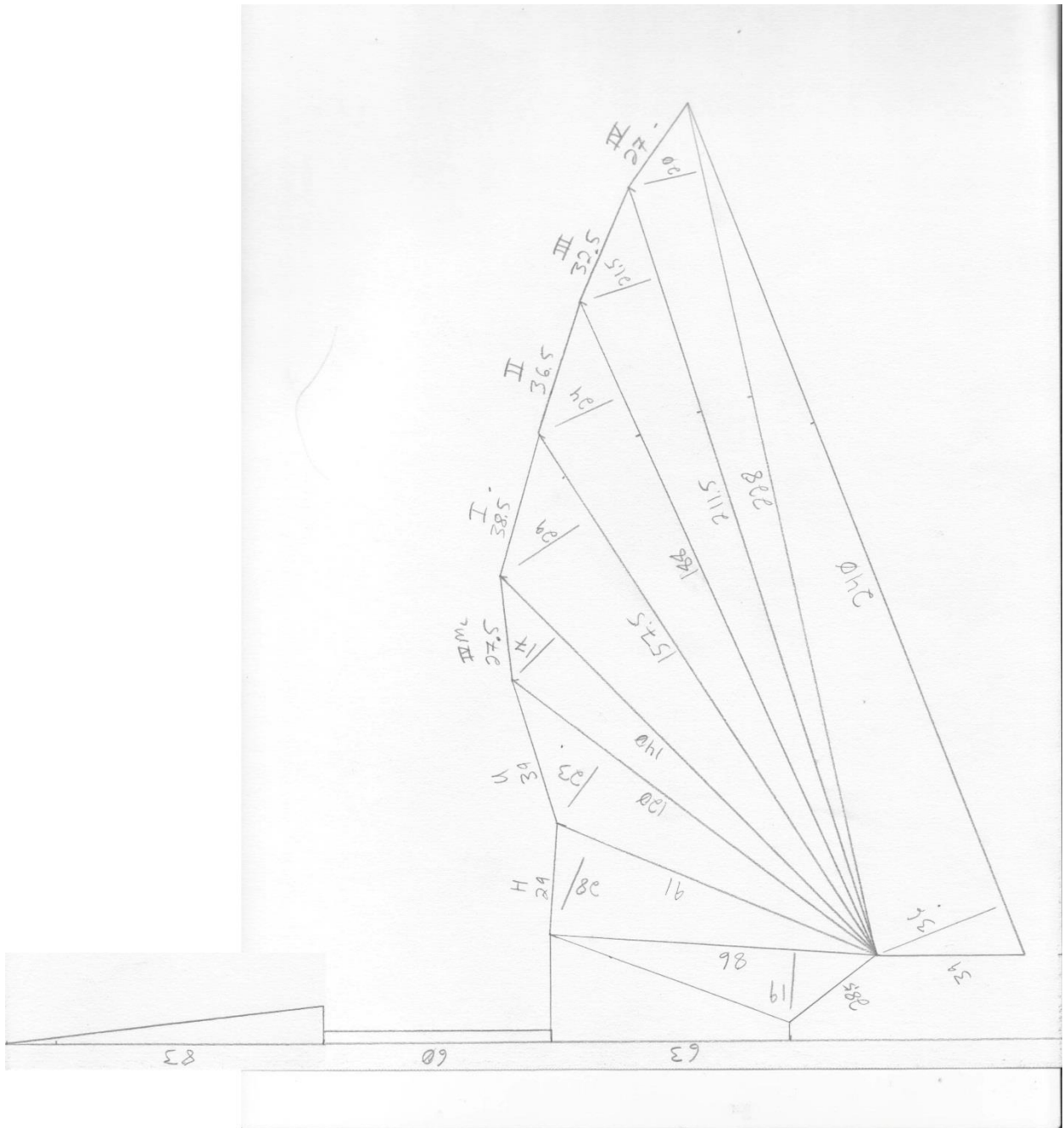
#21



P. antiquus (mm)

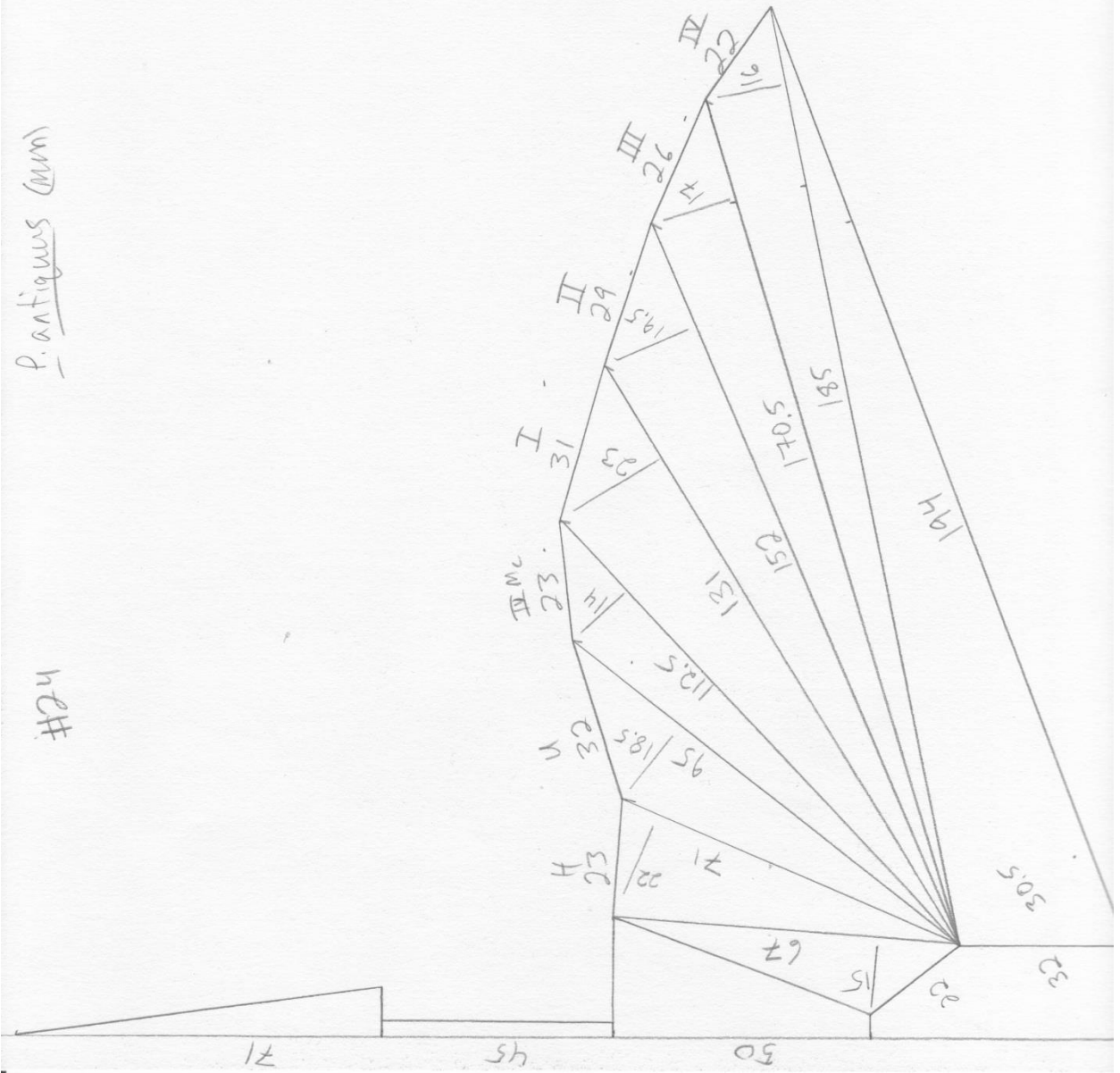
PL#

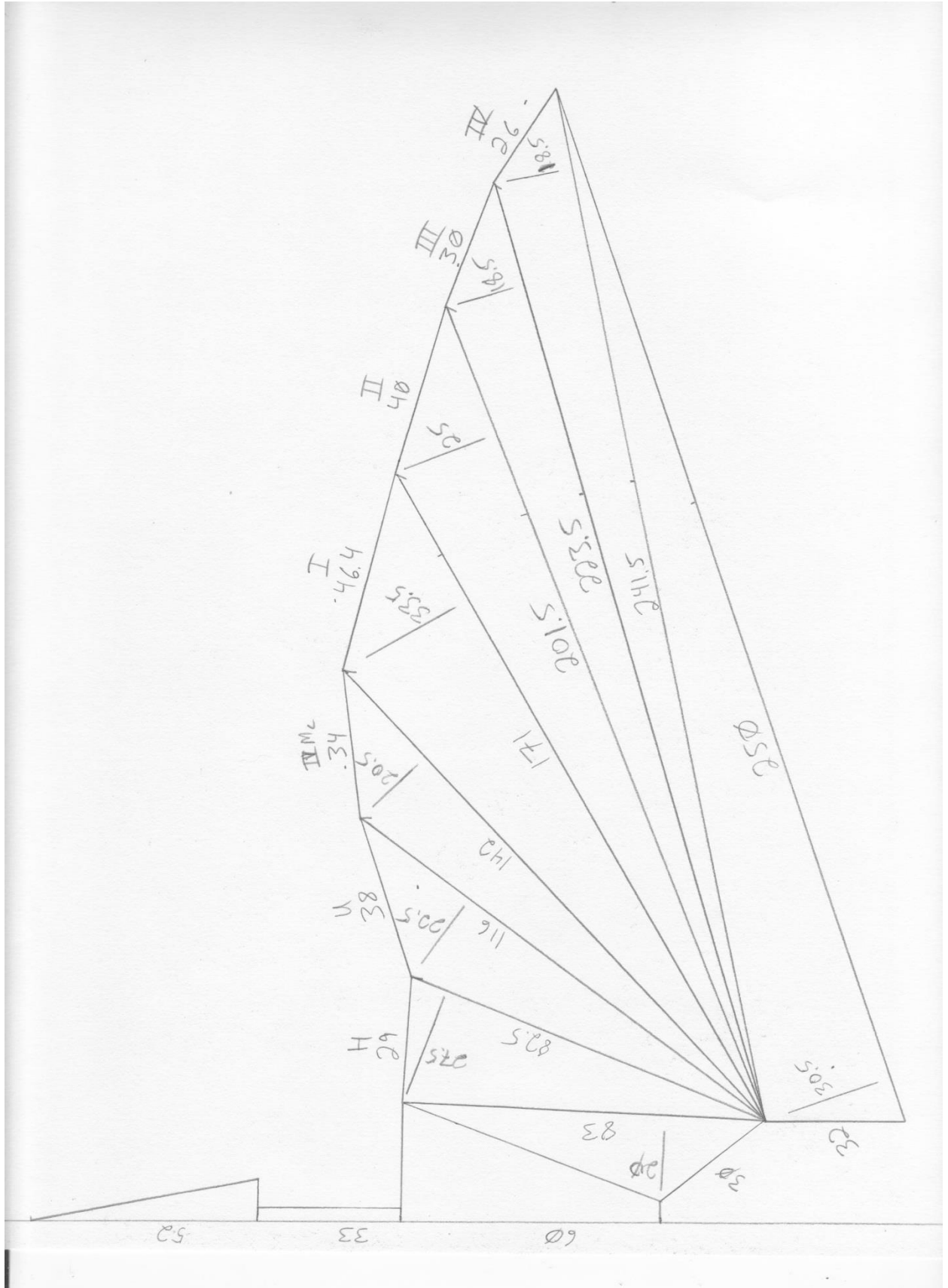




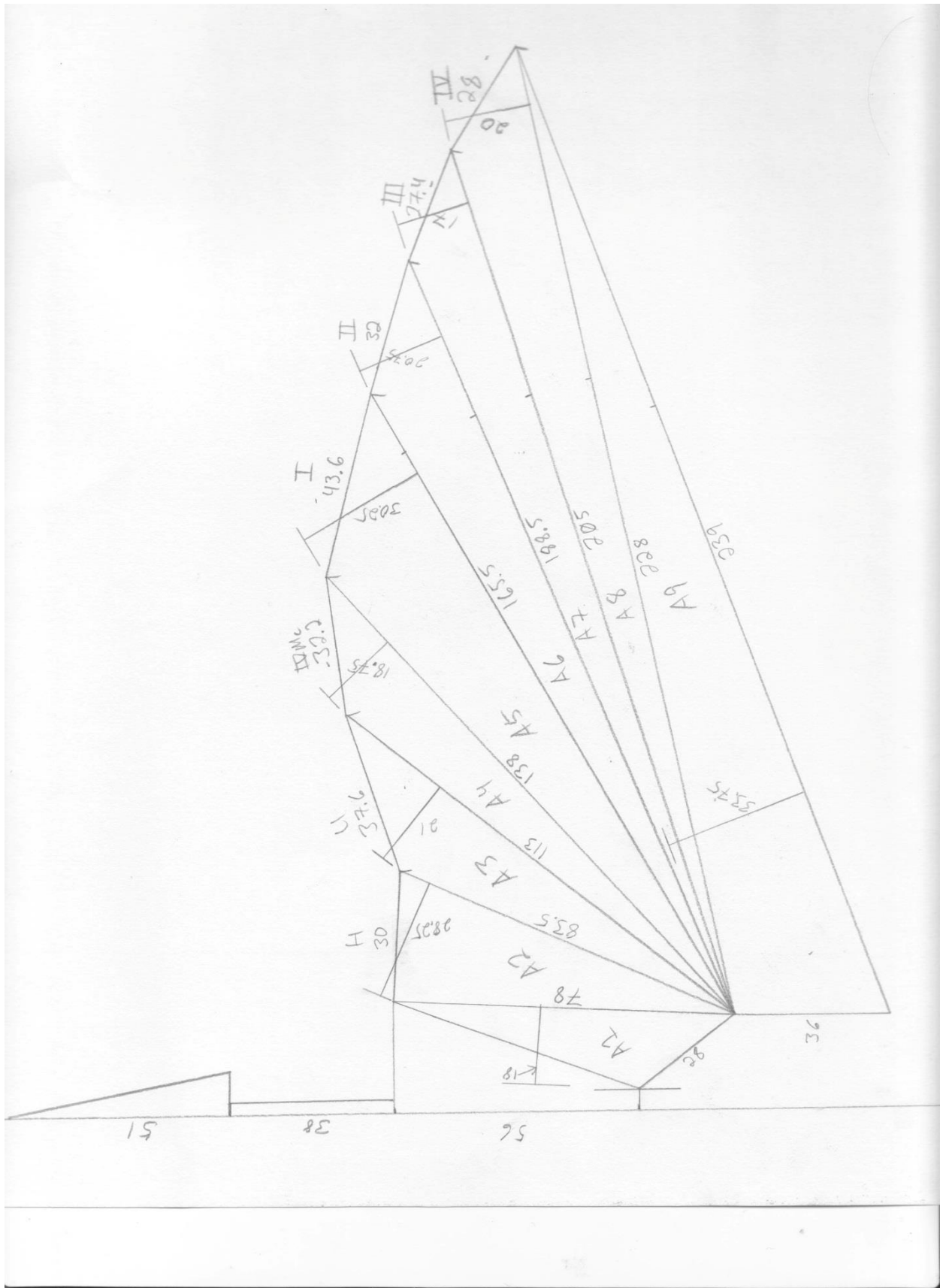
*P. antiquus* (mm)

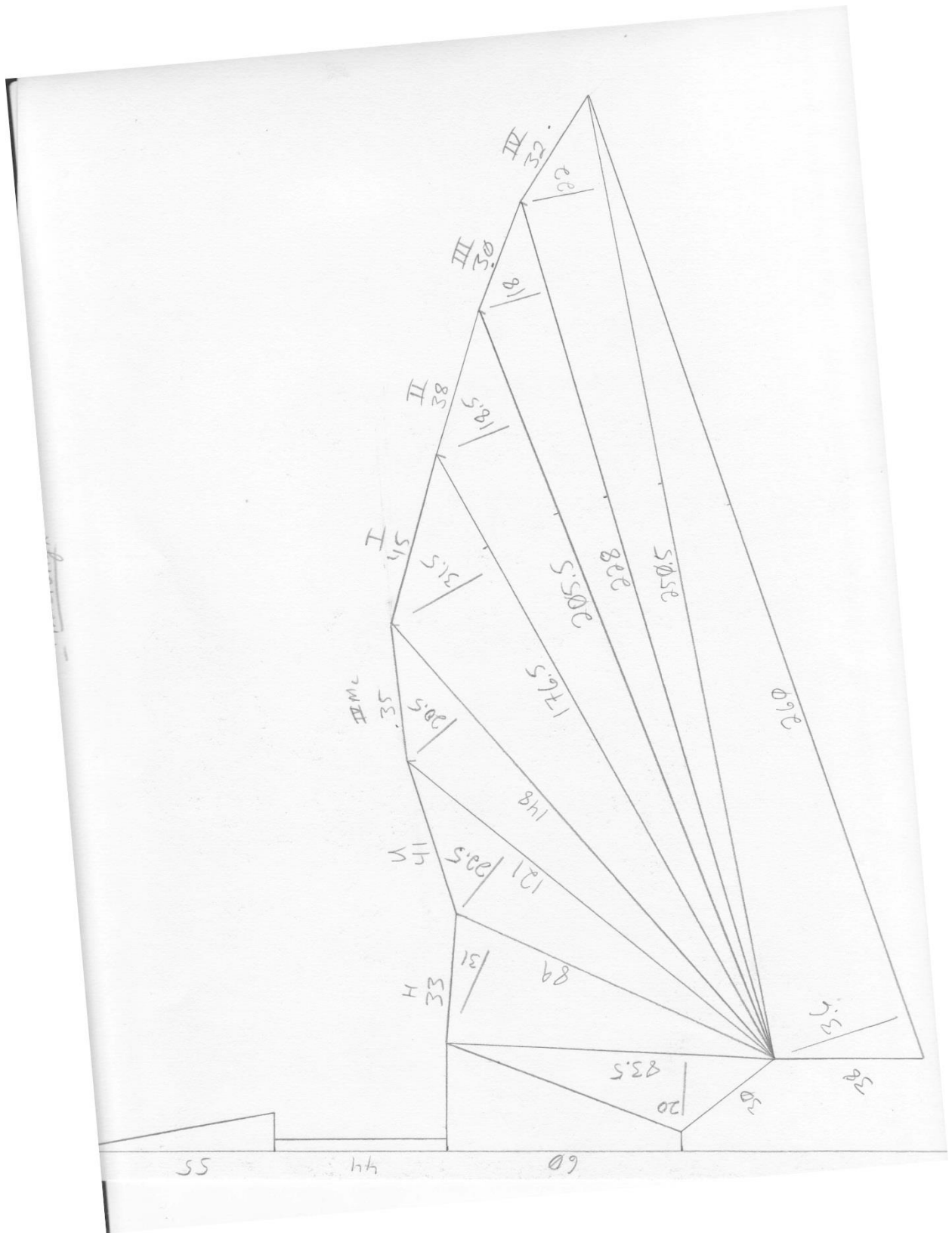
hEH











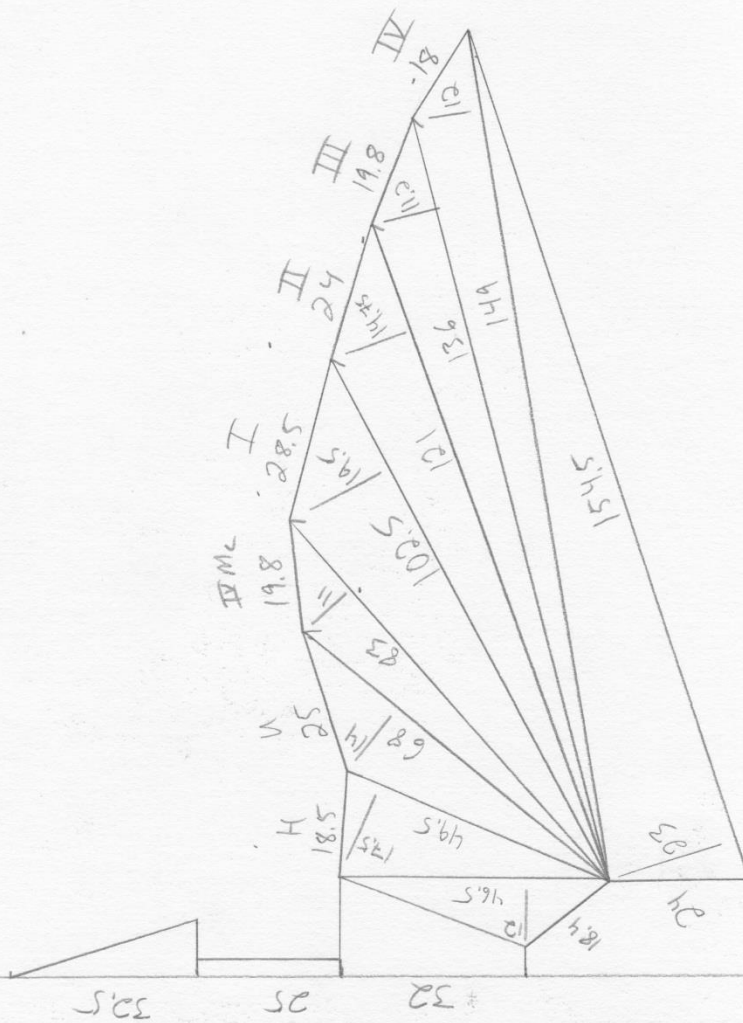
*Aurorazhdarcho micronyx*





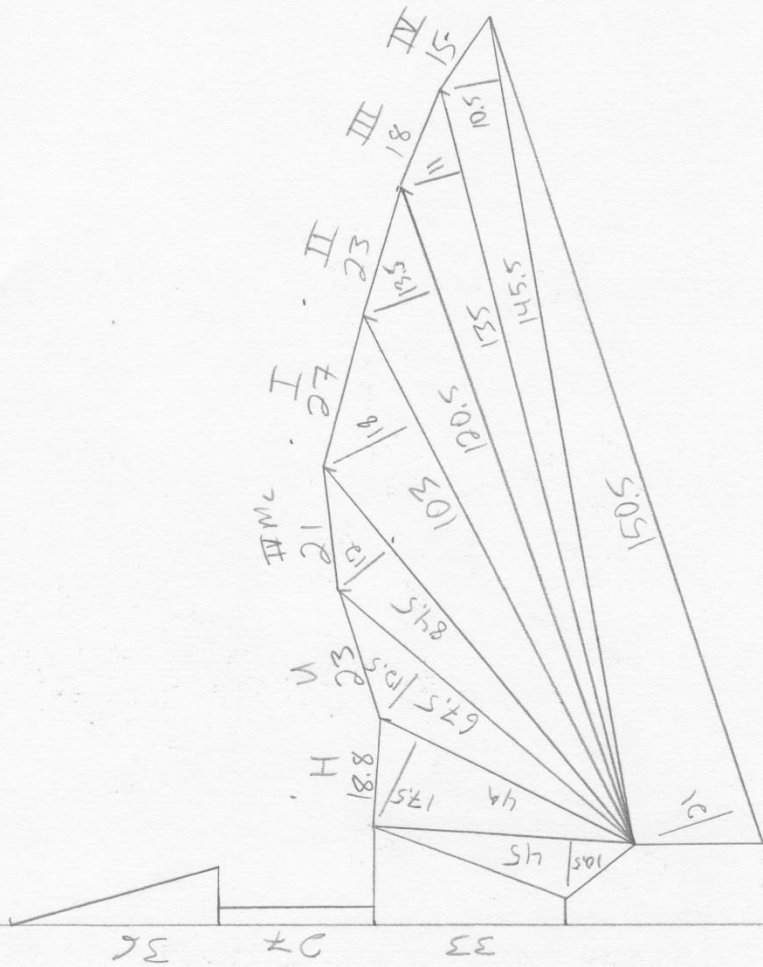
A. micranthx

#29



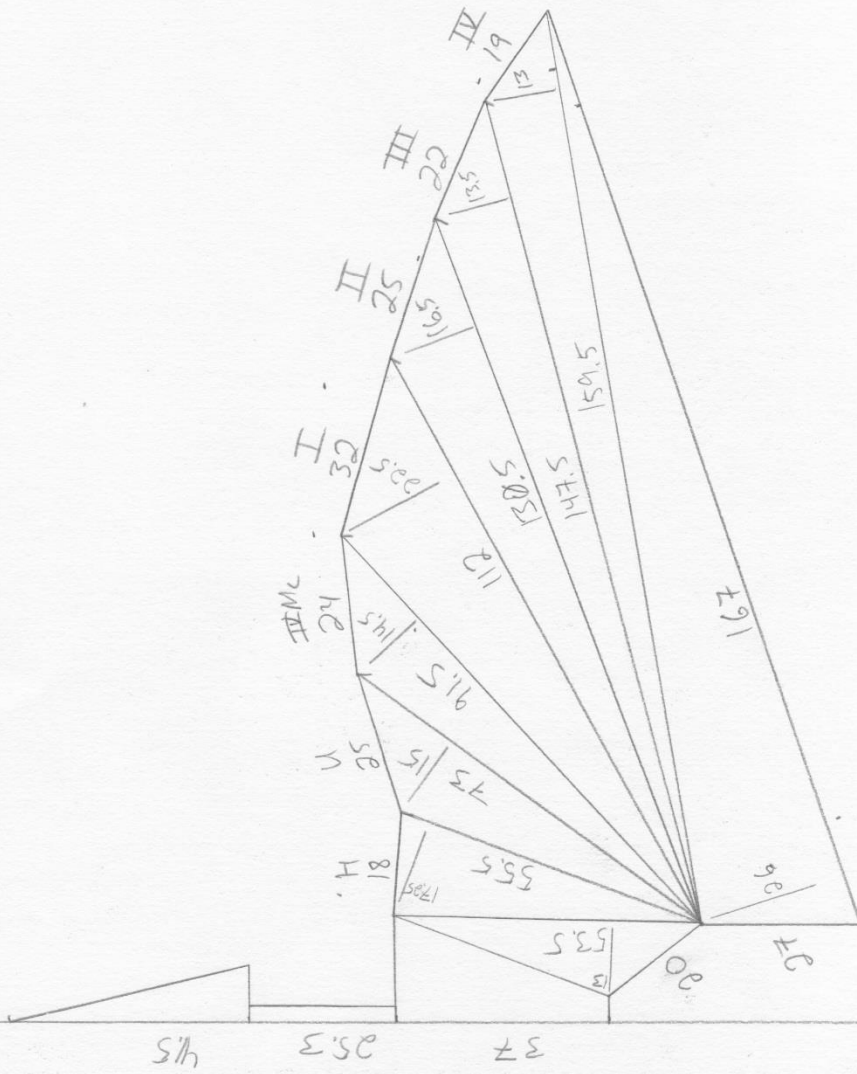
A. microonyx

#30



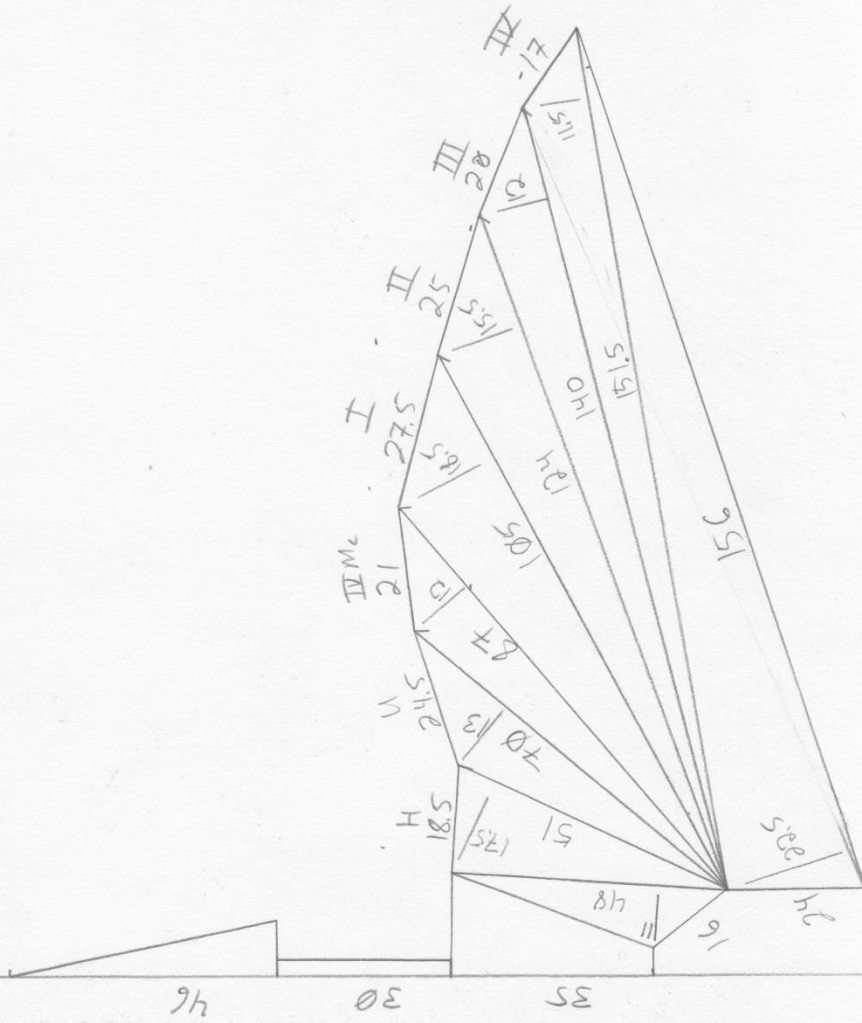
A. micronyx (mm)

#31



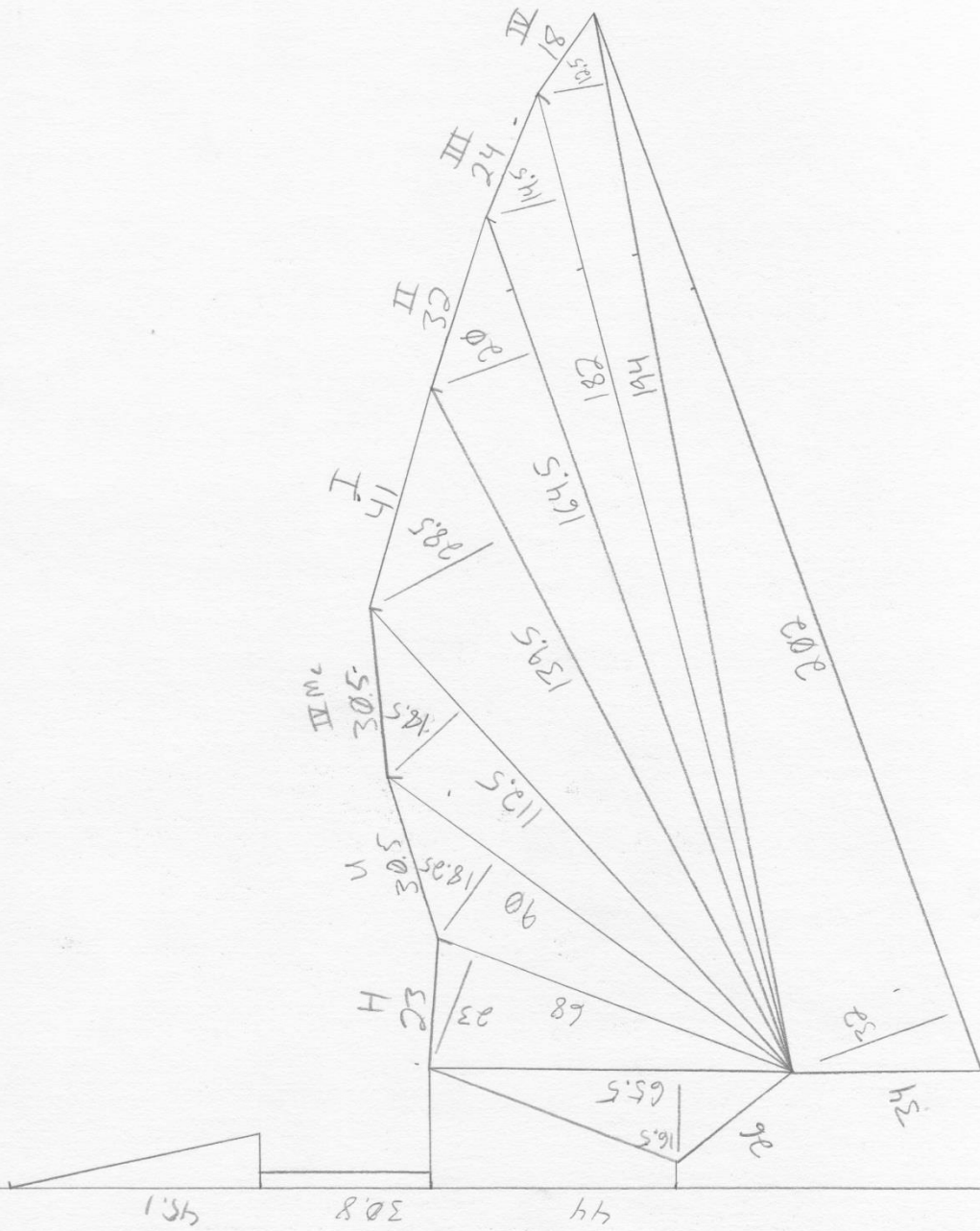
A. microrhynch (mm)

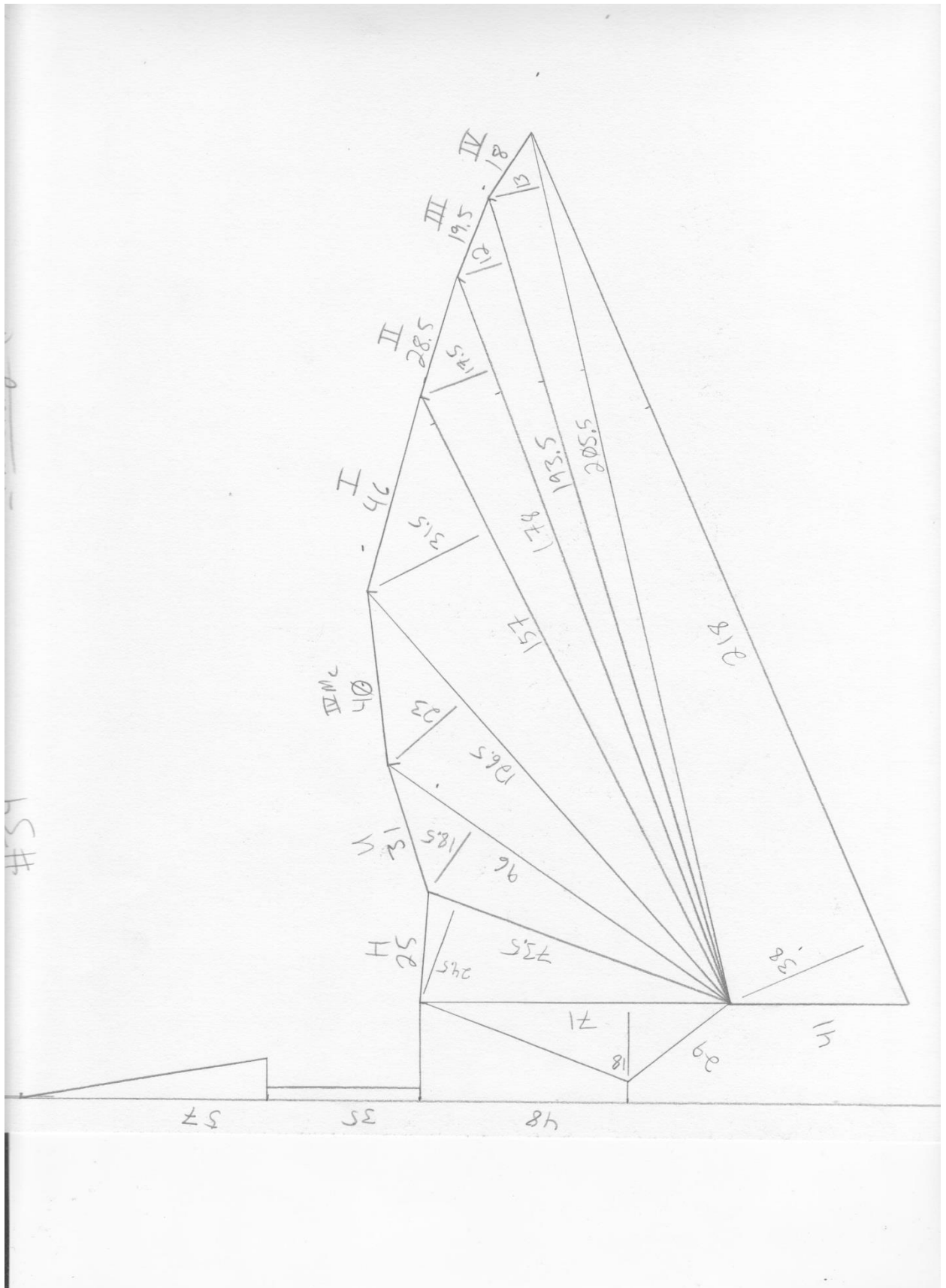
#32



A. microgynx (mm)

#33



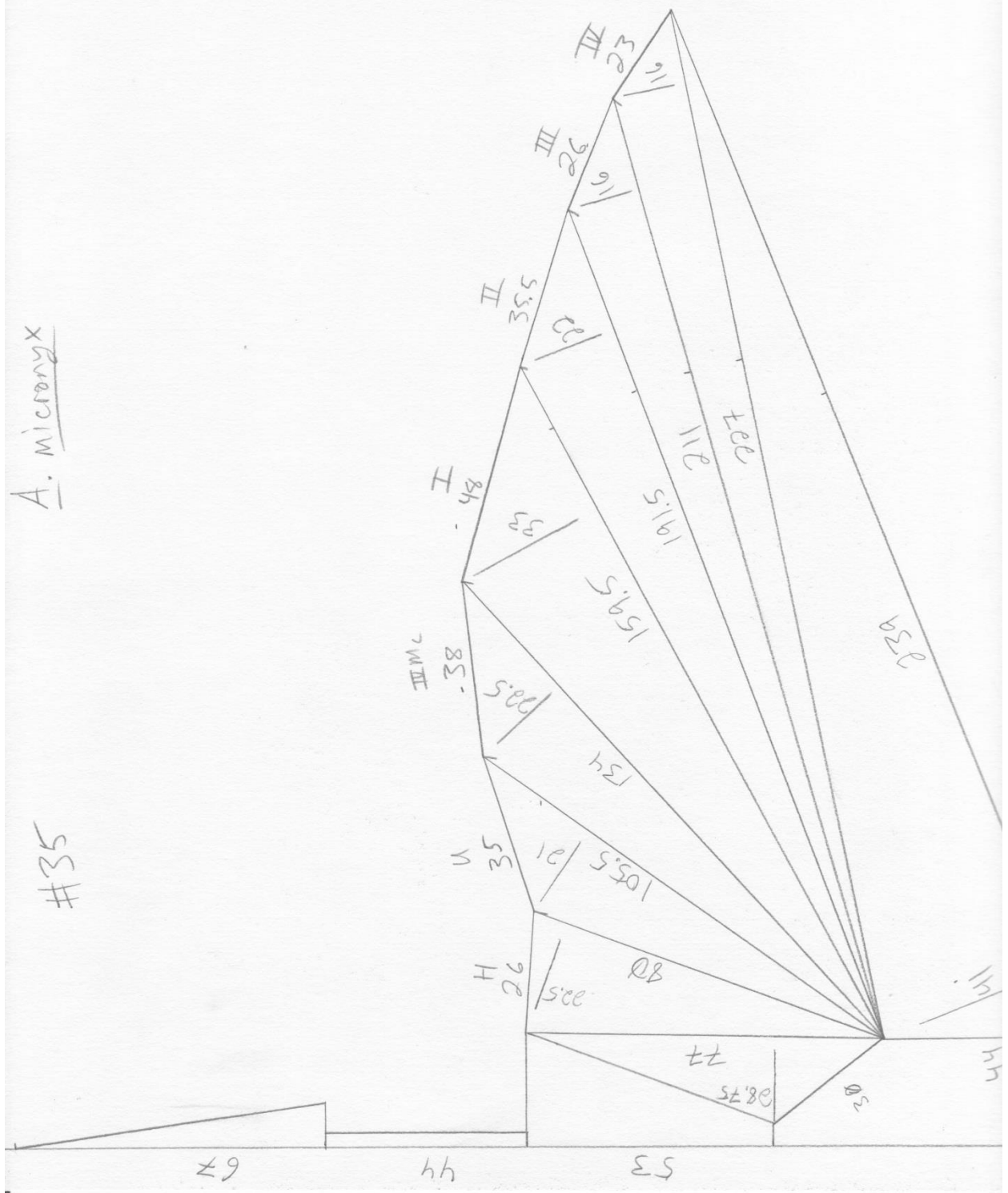




500

A. micranyx

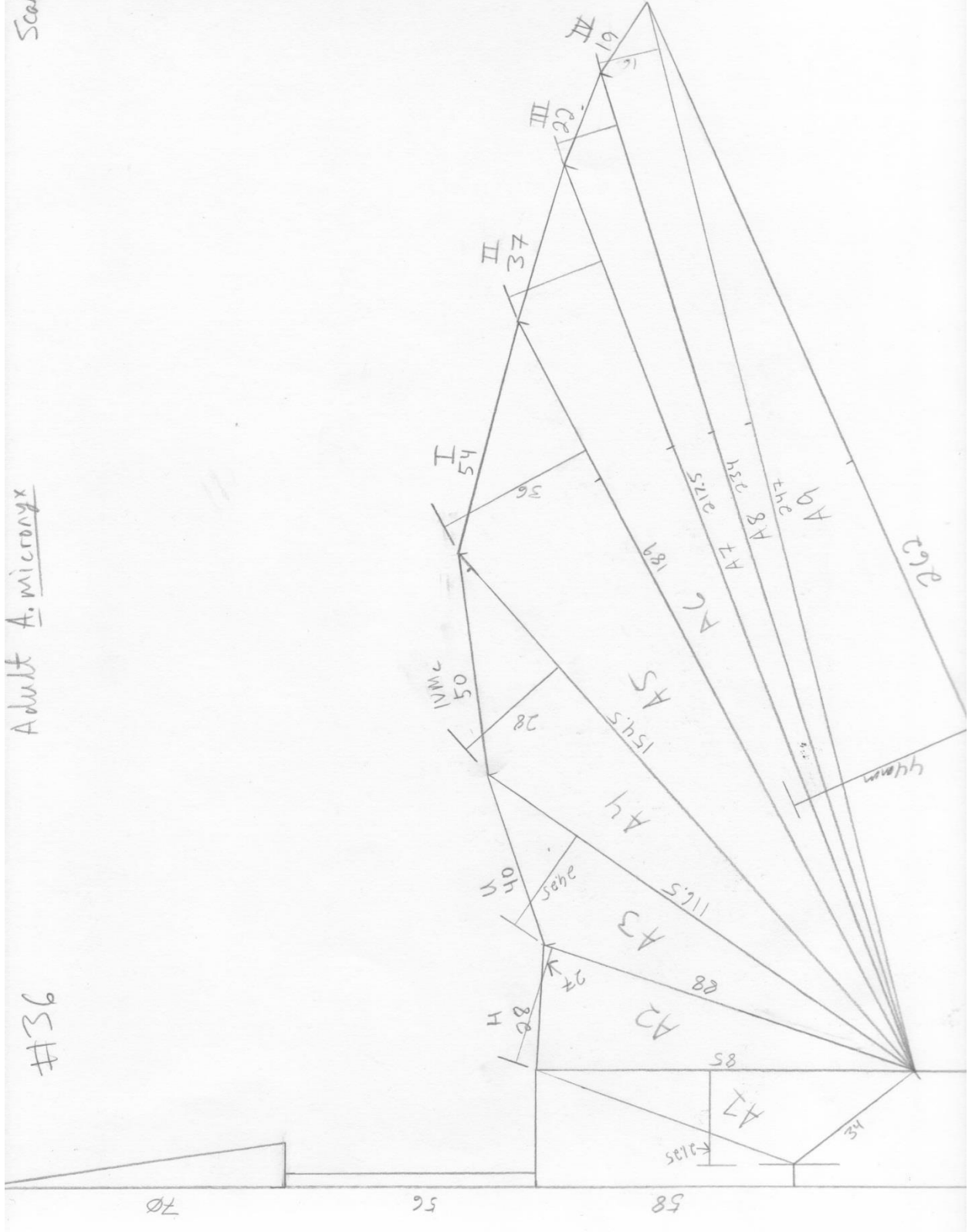
#35



Scale 1:1

Adult A. micronyx

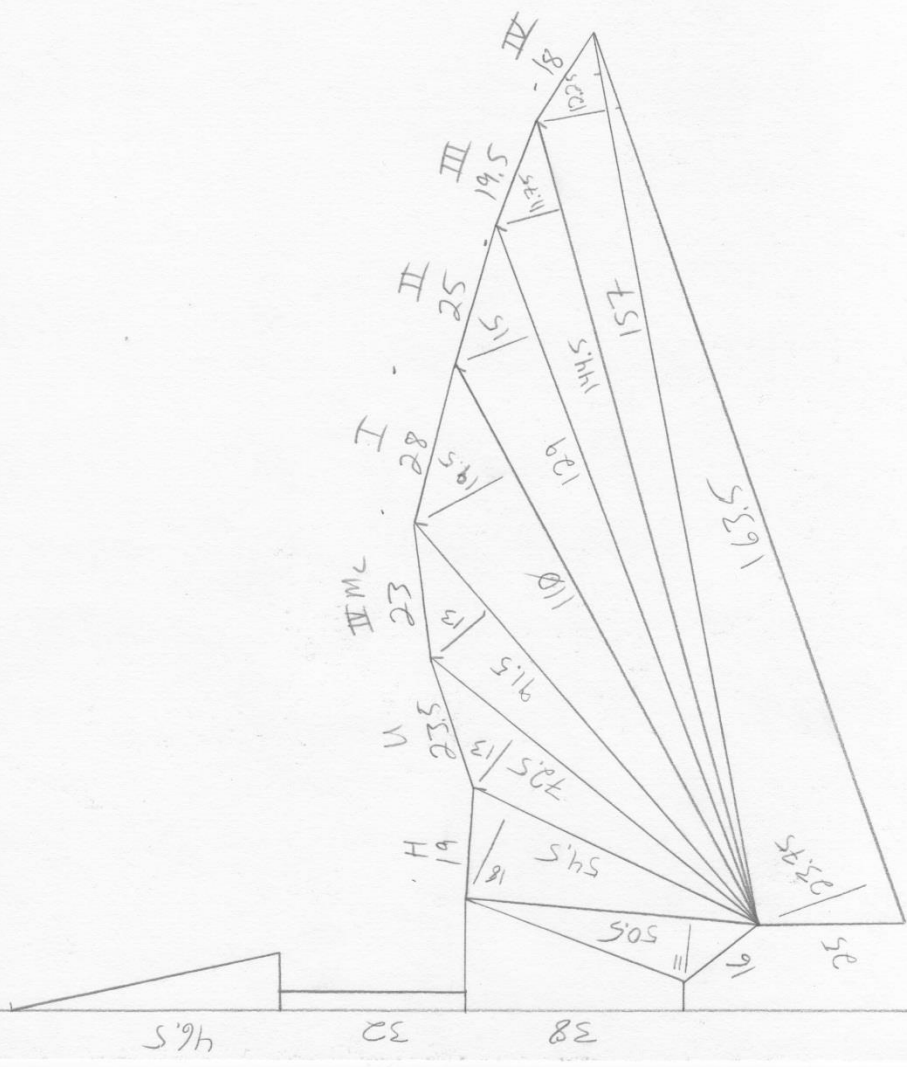
#36

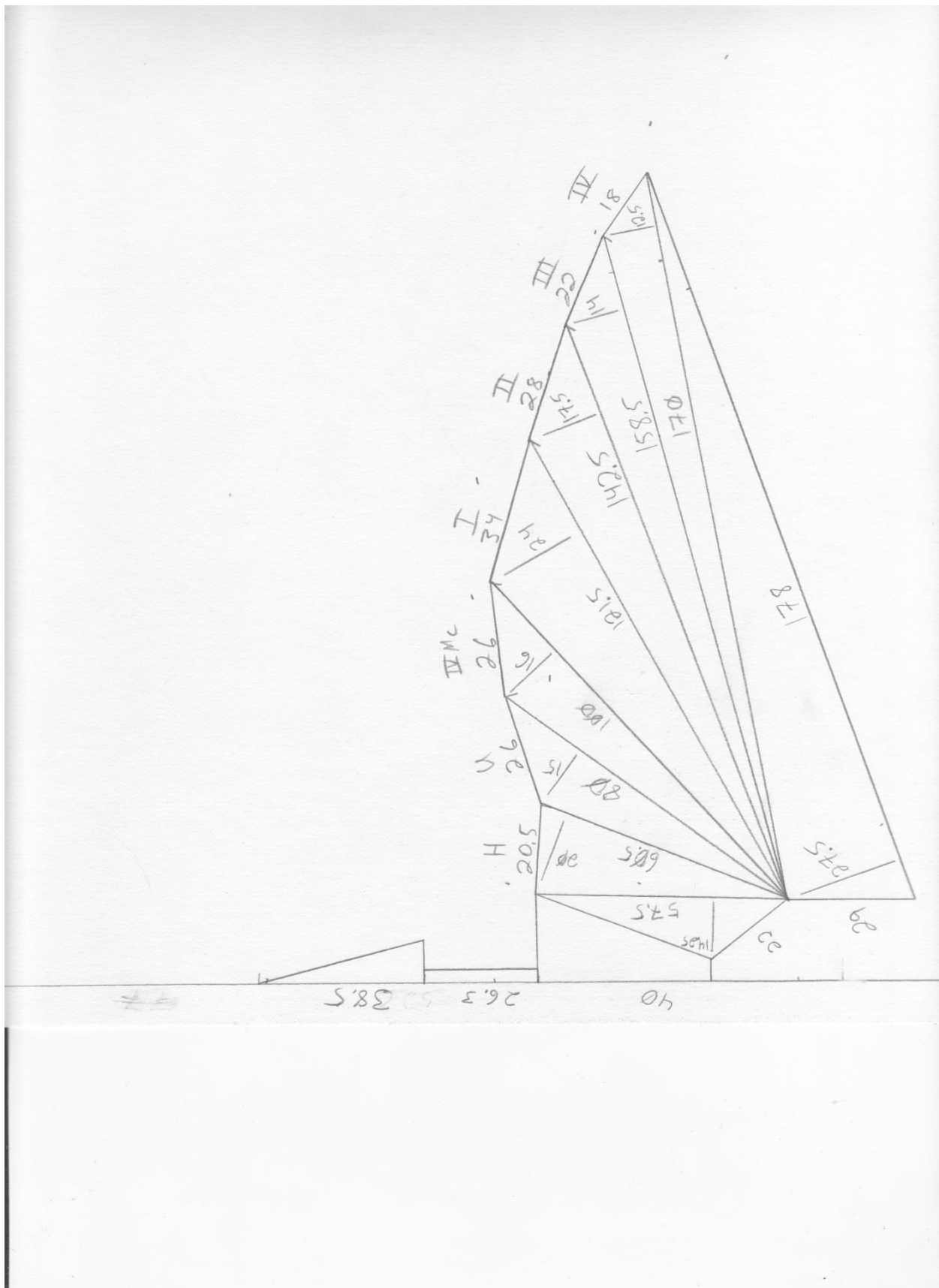




A. micromyx (mm)

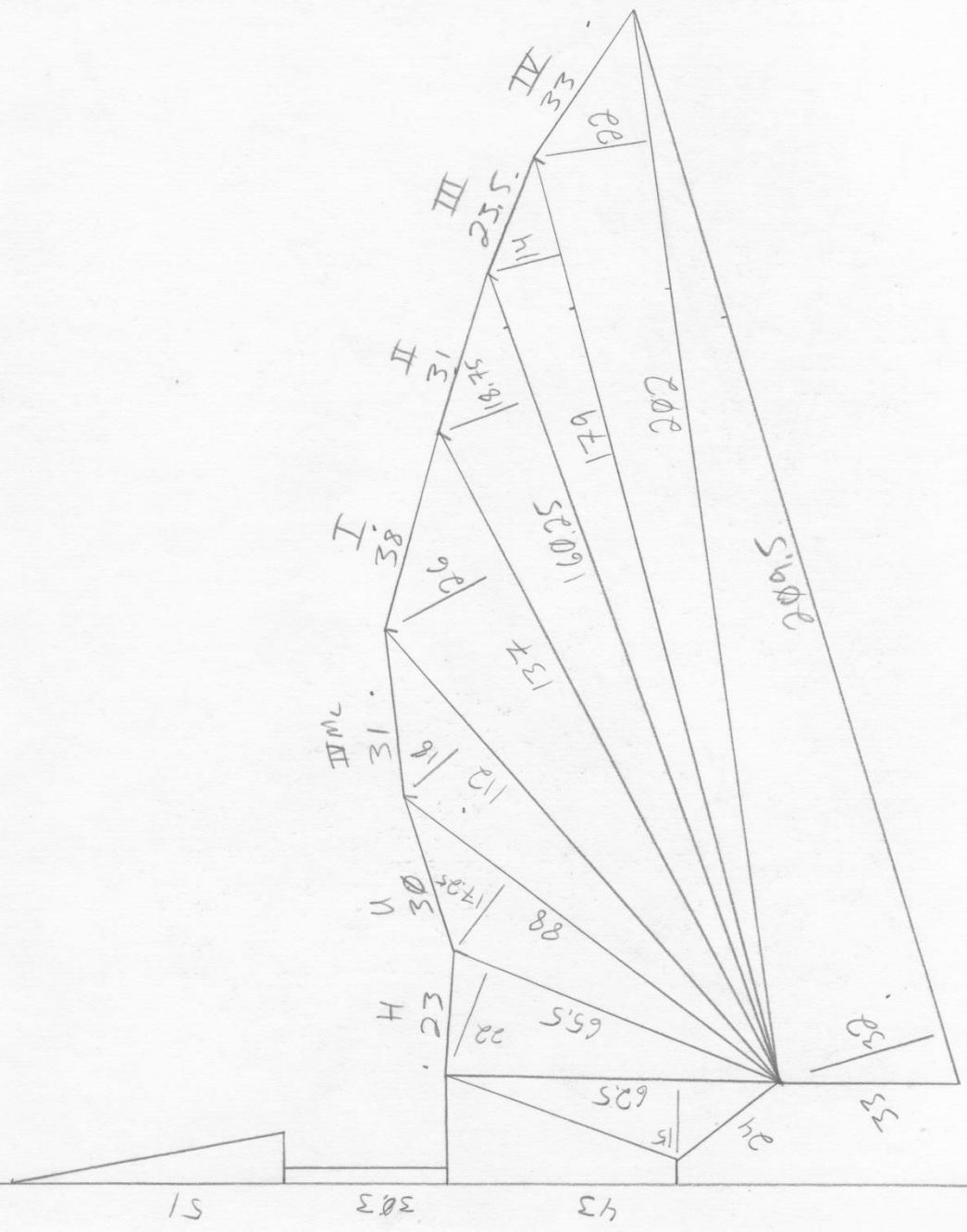
#37





A. microryx (mm)

#39



## APPENDIX F

### Letter from Institutional Research Board



Office of Research Integrity  
Institutional Review Board

April 23, 2015

Erick Anderson  
630 20th St. Apt. 5  
Huntington WV, 25703

Dear Mr. Anderson:

This letter is in response to the submitted thesis abstract entitled "*Analyzing Pterosaur Morphology with Multivariate Allometry*." After assessing the abstract it has been deemed not to be human subject research and therefore exempt from oversight of the Marshall University Institutional Review Board (IRB). The Code of Federal Regulations (45CFR46) has set forth the criteria utilized in making this determination. Since the information in this study does not involve human subjects as defined in the above referenced instruction it is not considered human subject research. If there are any changes to the abstract you provided then you would need to resubmit that information to the Office of Research Integrity for review and a determination.

I appreciate your willingness to submit the abstract for determination. Please feel free to contact the Office of Research Integrity if you have any questions regarding future protocols that may require IRB review.

Sincerely,



Bruce F. Day, ThD, CIP  
Director

**WE ARE... MARSHALL™**

401 11th Street, Suite 1300 • Huntington, West Virginia 25701 • Tel 304/696-7320 for IRB #1 or 304/696-4305 for IRB #2 • [www.marshall.edu/irb](http://www.marshall.edu/irb)  
A State University of West Virginia • An Affirmative Action/Equal Opportunity Employer